Characterisation of the Role of Brain Factor 1 in the Olfactory Neuroepithelium during Neuronal Development

Pride Linda

Submitted in fulfilment of the requirements for the degree of Master of Science
in the
Department of Molecular and Cellular Biology
University of Cape Town
South Africa
January 2003

Declaration

I hereby declare that this thesis entitled:

Characterisation of the Role of Brain Factor 1 in the Olfactory Neuroepithelium during Neuronal Development

Is my own work, and has not been previously in its entirety or in part been submitted at any university for another degree.

Signed: _____ **Date:** _____

List of Contents

Abstract

Brain Factor 1 (BF-1), a winged helix transcription factor, displays a restricted pattern of expression within the developing forebrain, playing a critical function in the regulation of neuronal progenitor cell proliferation and differentiation within the developing forebrain. The molecular mechanisms by which BF-1 carries out its function remain to be elucidated. Hence, this study aimed to investigate and characterise the molecular mechanisms by which BF-1 function is regulated during neuronal development.

Several approaches were used to determine how BF-1 is regulated. The first approach was to verify, by northern blot analysis, that a BF-1 interacting protein (BF1-IP_1), which was originally identified in a yeast two-hybrid screen, was co-expressed with BF-1 in conditionally immortalised neuroepithelial cell lines. A series of BF-1 deletions were made in order to map which domain of BF-1 interacted with BF1-IP_1. A deletion of the Histidine, Proline and Glutamine (HPQ)-rich domain, the DNA-binding domain (DBD) and the transcriptional repressor domain (TRD) (AS1.5$\Delta_{HPQ, DBD, TRD}$), as well as a deletion of the DNA-binding domain (DBD) and the transcriptional repressor domain (TRD) (AS1.5$\Delta_{DBD, TRD}$) were successful. Site-directed mutagenesis, to introduce a stop codon was successful for the AS1.5$\Delta_{HPQ, DBD, TRD}$, but not for the AS1.5$\Delta_{DBD, TRD}$ construct. The subsequent subcloning of the mutagenised AS1.5$\Delta_{HPQ, DBD, TRD}$ construct into the yeast two-hybrid vector was unsuccessful.

Western blot analysis using antibodies raised against BF-1, detected two protein products sized 62 kDa, and 95 kDa. Addition of retinoic acid, to induce differentiation of the synchronised OP27 cells, resulted in the shift of the 62 kDa protein to the 66 kDa protein product. This suggested that BF-1 might possibly undergo post-translational modification upon and during neuronal progenitor cell differentiation.

Lastly, the regulation of BF-1 by spatial localisation during neuronal development was investigated. As a first step, BF-1 fluorescent fusion proteins were generated that can be used to follow the localisation of BF-1 in live cells at different stages of the cell cycle, and at different stages of neural development. In order to show that the fusion constructs were functional, the fusion constructs were injected into *Xenopus* embryos, and observed that the fusion constructs disrupted expression of *N-tubulin* in a similar pattern to high doses of *Xenopus* BF-1 mRNA injected into *Xenopus* embryos. The BF-1 fluorescent fusion protein was found to be localised in the nucleus of both the injected *Xenopus* embryos, and the transiently transfected OP27 cells.

Acknowledgements

I wish to thank my supervisors, Assoc. Prof. Nicola Illing and Assoc. Prof. Hugh Patterton for their constant guidance and support with such a difficult project.

I would like to extend a special thank my fellow lab colleagues: Mrs Faezah Davids, Mr Aubrey Shoko, Mr Keke Tloti, Mr Michael Gardner, Dr Helen Collett and Ms Michelle Morley, for their support and congeniality throughout the years, and for all the good times shared. I would like to thank the staff at UCT who supported me throughout the years. I would also like to thank Anita Schwegmann, for helping me to set up the project and for her constant interest in my work throughout the years.

I wish to extend a special thank you to Dr Helen Collett for selflessly giving of her constructive criticism, guidance and the very long hours spent reading my drafts, without whose help my thesis would still be in disarray.

I wish to extend my sincerest gratitude to Dr Nancy Papalopulu, for offering me a place in her lab for my six month tenure in the UK to carry out a portion of my MSc with her, and for her constant help every step of the way to ensure the success of my project. I would also like to extend my appreciation to all the members of the Wellcome/CRC Institute (Cambridge, UK) who were always helpful whenever I approached them for help, as well as the media staff and those at stores. Most importantly, I wish to thank my lab mates who welcomed me and made me feel very welcome in my new environment: Andrew Chalmers, Zoe Hardcastle, Elena Fineberg, Bernard Strauss, Samantha Carruthers, Penny Day and Jana Voigt. And to Dina Mufti, thank you for welcoming me into your home.

I would also like to thank the Equity Development Programme (EDP/GOOT) Molecular Biology Scholarship (UCT) and the National Research Foundation (NRF) for financially supporting my MSc, without which, this project would never have taken root.

Most important of all, I would like to thank my grandmother, Mrs Thabitha Daisy Linda, for her unwavering love, support and faith in me, through thick and thin, and for her patience in enduring the long months far away from me.

"Seeing much, suffering much, and studying much, are the three pillars of learning."

Benjamin Disreali

Abbreviations:

^{32}[P]-dCTP	α-32-P labelled deoxycytidine 5'triphosphate
AmpR	ampicillin resistance
ATG	transcription initiation codon
bBF-1	Branchiostoma Brain Factor 1
BF-1	Brain Factor 1
BF1-IP	Brain Factor 1 interacting protein
BMP	bone morphogenetic protein
bp	base pairs
BrdU	5-bromo-2-deoxyuridine
cBF-1	chick Brain Factor 1
cDNA	clonal DNA
CMV	cytomegalovirus
CN-4B	cyanogen bromide activated Sepharose 4B
CNS	central nervous system
CO_2	carbon dioxide
C-terminal	carboxy-terminal
DBD	DNA-binding domain
DEAE	diethylaminoethyl
DEPC	diethyl pyrocarbonate
DMEM	Dulbecco's modified eagle medium
DMEM/F12	Dulbecco's modified eagle medium/Ham's F-12
DMSO	dimethlysulphoxide
DNA	deoxyribonucleic acid
DNAse	deoxyribonuclease
dNTP	deoxyribonucleotides
DTT	Dithiothreitol
E10	embryonic day 10
EDTA	ethylene diamine tetraacetic acid
EGTA	ethylene glycol tetra acetic acid
FAST2	forkhead activin signal transducer 2
FCS	foetal bovine serum
FGF	fibroblast growth factor
FKH	forkhead homologue
Fox	forkhead containing box
FREAC-3	forkhead-related transcription factor 3
GST	glutathione S-transferase
hBF-1	human Brain Factor 1
HCl	hydrogen chloride (hydrochloric acid)
Hes	hairy and enhancer of split
HNF-3	hepatocyte nuclear factor 3
HPQ	histidine, proline and glutamine
KanR/NeoR	kanamycin resistance/neomycin resistance
kb	kilo base
KCl	potassium chloride
kDa	kilodalton
Ltd	limited
M	molar concentration (moles/litre or grams/mole)
MAP2	microtubule associated protein 2

mBF-1	mouse Brain Factor 1
MBS	modified bovine serum
MF-1	myogenic factor 1
mg	milligram
$MgCl_2$	magnesium chloride
$MgSO_4$	magnesium sulphate
ml	millilitres
mM	millimolar
MOPS	3-(N-morpholino) propanesulfonic acid
Mv1Lu	Mink lung epithelial-like cell line
Na_2HPO_4	di-sodium hydrogen phosphate
NaCl	sodium chloride
NBT/BCIP	nitroblue tetrazolium chloride/ 5-bromo-4-chloro-3-indolyl-phosphate
NEB	New England Biolabs
ng	nano grams
nl	nano litre
NP-40	Nonidet P-40
N-terminal	amino-terminal
OP	olfactory placode
PBS	phosphate buffered saline
PCR	polymerase chain reaction
PMSF	phenylmethyl sulfonylfluoride
RA	retinoic acid
rBF-1	rat Brain Factor 1
RNA	ribonucleic acid
SDS	sodium dodecyl sulphate
SDS-PAGE	sodium dodecyl sulphate-polyacrylamide gel electrophoresis
shh	sonic hedgehog
slp	*sloppy paired*
Smad	similar to mothers against decapentaplegic homologue
SSC	sodium chloride/sodium citrate
STE	sodium chloride, tris-HCl and EDTA
SV40 Poly A	simian virus 40 poly adenylation signal
TAE	tris-acetate electrophoresis buffer
TBS	tris buffered saline
TGF-β	transforming growth factor-beta
TLE	transducin-like enhancer of split
TNT	tris-sodium chloride-triton X-100
TRD	transcriptional repressor domain
Tris	tris (hydroxymethyl) aminomethane
TTR	transthyretin
UTP	uridine triphosphate
V	volt
*X*BF-1	*Xenopus* homologue of the mouse brain factor 1/*Xenopus* Brain Factor 1
X-gal	5-bromo-4-chloro-3-indolyl-beta-D-galactoside
XSox3	*Xenopus* neural specific transcription factor
zBF-1	Zebrafish Brain Factor 1
µg	micrograms

List of Figures		Page
Figure 1.1	Phylogenetic analysis of mouse Forkhead box genes	7
Figure 1.2	Phylogenetic analysis of vertebrate Brain Factors	11
Figure 1.3	Protein sequence alignment of vertebrate Brain Factors	13
Figure 2.1	Northern blot analysis of OP6, OP27, OP47 and OP55	46
Figure 2.2	Use of recombinant GST-BF-1 and GST to test specificity of antibodies	47
Figure 2.3	Western blot analysis of endogenous BF-1 extracted from OP27 cell line	49
Figure 3.1	Flow diagram to illustrate PCR-mediated site-directed mutagenesis protocol	62
Figure 3.2	Diagrammatic representation of the domains of BF-1	67
Figure 3.3	Restriction enzyme digest of AS1.5 to generate deletion constructs	68
Figure 3.4	*Hind III* restriction digest of putative positive transformants	69
Figure 3.5	PCR-mediated site-directed mutagenesis amplification of $AS\Delta_{HPQ, DBD, TRD}$ to introduce stop codon	72
Figure 3.6	Full-length amplification of mutagenesis fragment	72
Figure 3.7	T7 and SP6 sequenced $AS1.5\Delta_{HPQ, DBD, TRD}$ mutagenesis fragment in pGEM-T Easy alignment	73
Figure 3.8	Subcloning of $AS1.5\Delta_{HPQ, DBD, TRD}$ mutagenesis fragment from pGEM-T Easy	75
Figure 3.9	Restriction digest of AS1.5 using *BsrG I* and *NgoM IV*	76
Figure 3.10	Digestion of putative positive subcloning transformants using *Xho I* and *Pst I*	77
Figure 3.11	PCR amplification of $AS1.5\Delta_{HPQ, DBD, TRD}$ deletion construct to optimise PCR conditions	78
Figure 3.12	PCR amplification of $AS1.5\Delta_{HPQ, DBD, TRD}$ transformants to screen for putative positives	79
Figure 4.1	Amplified mBF-1 open reading frame	97

1 Introduction

One of the most remarkable evolutionary events of mammalian development is the enlargement of the anterior neural tube to give rise to the enlarged cerebral hemispheres. Enlargement of the cerebral hemispheres is due to the extensive growth and proliferation of the neuronal progenitor cells of the telencephalic neuroepithelium (Xuan *et al.*, 1995). The attainment of superior intellect or empirical comprehension by mammals, especially primates, arose as a result of the enlargement of the cerebral hemispheres (Allman, 2000; Clark *et al.*, 2001). The development of the vertebrate embryonic forebrain has, therefore, been the focus of avid research over the past two to three decades. Studies are thus being carried out in an attempt to elucidate the molecular mechanisms that govern the complex morphological changes that result in the patterning and subdivisions of the central nervous system during development (Shimamura *et al.*, 1995; Furuta *et al.*, 1997).

The neuroepithelium, comprised of a homogeneous layer of cells, folds to give rise to the neural tube, from which all the cells of the central nervous system (CNS) are derived (Keynes *et al.*, 1990; Xuan *et al.*, 1995). During the development of the CNS, morphological changes occur that necessitate the patterning of and the regional diversity along the neural tube at the molecular level (Hatini *et al.*, 1994; Li *et al.*, 1996). The growth and patterning of the vertebrate forebrain is dependent upon the interaction of signals and the expression of genes and transcription factors within restricted domains of the developing embryonic brain (Guillemot *et al.*, 1993; Wilson *et al.*, 2000; Schuurmans *et al.*, 2002). This restricted pattern of expression has highlighted the importance of these genes and transcription factors in the regulation of the proliferation and differentiation of the CNS (Hatini *et al.*, 1994; Li *et al.*, 1996; Yao *et al.*, 2001). Brain Factor 1 (BF-1; renamed Fox G1), a winged helix transcription factor, is characterised by a restricted pattern of expression within the telencephalic epithelium (Tao *et al.*, 1992). BF-1 has been implicated in the control of proliferation and neurogenesis of the neuronal progenitor cells, thus playing a vital

role in the development of the vertebrate embryonic forebrain (Tao *et al.*, 1992; Xuan *et al.*, 1995; Hanashima *et al.*, 2002). However, due to the complex nature of the vertebrate forebrain, little is known about the molecular mechanisms by which BF-1 function is regulated or how BF-1 regulates neuronal development during embryonic forebrain development. Hence, the aim of this study was to investigate how BF-1 function was regulated, and where BF-1 was localised, spatially in an attempt to characterise how BF-1 regulated embryonic neuronal progenitor cell development in the olfactory neuroepithelium.

1.1 Brief overview of the development of the vertebrate embryonic brain

During gastrulation the body plan of the embryo is laid down, with cells migrating to the region that give rise to the specific organs of the body later in development. The early embryo is comprised of three germ layers generated at gastrulation. The endoderm, that later forms the inner layer, gives rise to the gut and respiratory system; the mesoderm, that forms the middle layer, generates the muscle (including the heart), bones and connective tissue, while the ectoderm forms the outer layer and gives rise to the epidermis and the nervous system, including the brain (Gilbert, 2000).

The development of the central nervous system begins with the neural induction of the early embryo. Neural induction occurs at gastrulation and is induced by signals located in the mesoderm underlying the ectoderm (Wolpert *et al.*, 1998; Sanes *et al.*, 2000). These signals induce the ectoderm to differentiate into the neuroectoderm, rather than to form the epidermis (Doniach, 1993; Papalopulu *et al.*, 1996; Puelles *et al.*, 1993; Filosa *et al.*, 1997, Shimamura *et al.*, 1997, Rubenstein *et al.*, 1998).

1.1.1 Brief overview of the developing olfactory epithelium in the vertebrate embryo

The olfactory placodes are two epithelial thickenings that originate at the end (outer layer of the anterior neural ridge) of the gastrula stage embryo, and continue to develop until the neurula stage embryo. The olfactory placodes are cranial placodes that form at the border of the head surface ectoderm and the neural plate (Sanes *et al.*, 2000, Baker *et al.*, 2001). They occur on either side of the longitudinal axis, separated by the nasal septum.

The olfactory placodes, amongst other types of cells, give rise to two types of nerves:

1. the olfactory nerve, a bipolar structure with axons that project into the brain via the olfactory bulb, and dendrites that are in constant contact with the exterior environment and chemical stimuli, and
2. the terminal nerve (Baker *et al.*, 2001), cranial nerves that innervate the nasal septum; and also project into the retina of ray-finned fish (Butler *et al.*, 1996).

The olfactory nerves, together with the secretory supporting cells, give rise to the olfactory epithelium (OE; Sanes *et al.*, 2000).

The olfactory epithelium is made up of three main cell compartments:

1. the apical layer which is adjacent to the nasal cavity and contains a single layer of sustentacular cells,
2. the middle layer in which the olfactory receptor neurons (ORN) are found, and
3. the basal layer which comprises two types of cells:
    - horizontal basal cells (HBC) that lie adjacent to the basal lamina and express keratin
    - globose basal cells (GBC) that lie above the HBC and are the intermediate neuronal precursors that give rise to the only type of neuron found in the olfactory epithelium, the ORN.

The olfactory epithelium is structurally similar to the rest of the CNS neuroepithelium, except that it is able to regenerate ORN throughout life, especially after injury, and that it only produces one type of major neuron, the ORN (Schwob, 2002).

1.2 Spatial and temporal patterning of the embryonic neuroectoderm

During development, the most fundamental event of the mammalian central nervous system is the establishment of positional identity and regionalisation of the neural tube (Tao *et al.*, 1992; Shimamura *et al.*, 1997; Hentges *et al.*, 1999). A gradient of signals from the underlying mesoderm induce the patterning of the neuralised ectoderm (neuroectoderm) into the anterior-posterior and the dorsal-ventral domains (Papalopulu *et al.*, 1996; Filosa *et al.*, 1997; Shimamura *et al.*, 1997; Rubenstein *et al.*, 1998; Wolpert *et al.*, 1998). As the neural plate folds to form the neural tube, the lateral surface of the head ectoderm develops in a rostral (nose) to caudal (tail/feet) direction. Anterior-posterior patterning of the neural tube occurs first (Papalopulu *et al.*, 1996), generating the forebrain, midbrain, hindbrain and spinal cord domains (Filosa *et al.*, 1997; Rubenstein *et al.*, 1998). Dorsal-ventral patterning, that organises the neural tube into symmetrical halves on either side of the longitudinal axis, occurs later in development (Shimamura *et al.*, 1995; Papalopulu *et al.*, 1996; Filosa *et al.*, 1997; Rubenstein *et al.*, 1998). The forebrain further subdivides to give rise to the telencephalon and diencephalon (Tao *et al.*, 1992).

The establishment of positional identity and regionalisation of the neural tube is also characterised by the activation and expression of regulatory genes along the neural tube, in distinct spatially and temporally regulated domains (Shimamura *et al.*, 1995; Filosa *et al.*, 1997; Rubenstein *et al.*, 1998; Hardcastle *et al.*, 2000). A considerable number of genes and transcription factors have been identified and shown to be involved in the development and patterning of the posterior central nervous system. These include the *Hox* and *Krox-20* genes that are important in the specification of the genes involved in hindbrain development (Hatini *et al.*, 1994). However, due to

the highly complex nature of the forebrain anatomical structure, the molecular mechanisms that pattern the forebrain remain largely unknown (Tao *et al.*, 1992; Shimamura *et al.*, 1995; Shimamura *et al.*, 1997; Hentges *et al.*, 1999).

1.3 The forkhead box-containing proteins or winged-helix (Fox genes) transcription factors

The *forkhead*/HNF-3 family of transcription factors comprises a constantly increasing group of members. The *forkhead* transcription factors were initially identified in *Drosophila* as a distinct group of proteins shown to play a critical role in the normal development of the fly (Tao *et al.*, 1992; Kaufmann *et al.*, 1996).

To date, more than 70 different *forkhead* box- or winged helix-containing genes (renamed Fox genes) have been identified in mice (Figure 1.1). The function of many of these proteins remains largely unknown (Mariani *et al.*, 1998). However, the few genes that have been described encode proteins identified as potential transcription factors with a diversity of functions. These functions range from embryonic and adult organogenesis (such as HNF-3 β and Fox L2) to proteins associated with various leukaemias (such as mesoderm/mesenchyme forkhead 1 (MF-1) or FREAC-3), as well as proteins involved in the development of the central nervous system (such as BF-1).

Phylogenetic analysis showed that BF-1 was more closely related to the Fox L1, Fox L2, Fox I1 (or FKH 10), Fox C1 and Fox C2 proteins (Figure 1.1). Fox C1 and Fox C2, previously known as *fkh1/Mf1* and *fkh1/Mfh1*, respectively, display a restricted pattern of expression within the mesoderm (Hiemisch *et al.*, 1998; Kume *et al.*, 2000). Fox C1 and Fox C2 regulate the proliferation and differentiation of the paraxial mesoderm, somites and kidneys of the developing mouse embryo (Hiemisch *et al.*, 1998; Kume *et al.*, 2000). The forkhead homologue 10 (Fkh 10 or Fox I1) is required for the development of the vertebrate inner ear, which is derived from the cranial

placodes (Hulander *et al.*, 1998), while the pituitary forkhead factor is required for the development of the pituitary gland (Treier *et al.*, 1998). These proteins are mainly derived from or induce the development of tissues in the mesoderm. However, BF-1 is a transcription factor that displays a restricted pattern of expression within the developing telencephalon (Tao *et al.*, 1992), a neuroectoderm-derived tissue. Further analysis showed that the remainder of the BF-1 protein sequence was highly divergent from the other winged helix proteins including the HNF-3 proteins.

Figure 1.1: Phylogenetic analysis of more than 70 protein sequences (September 2002) of the mouse forkhead-box or winged-helix domain proteins currently available on the PUBMED protein sequence database (http://www.ncbi.nlm.nih.gov). BF-1 (highlighted in red) is shown located with proteins that have their Histidine-, Proline-, Glutamine-rich region at the N-terminal end of the protein (highlighted in green).

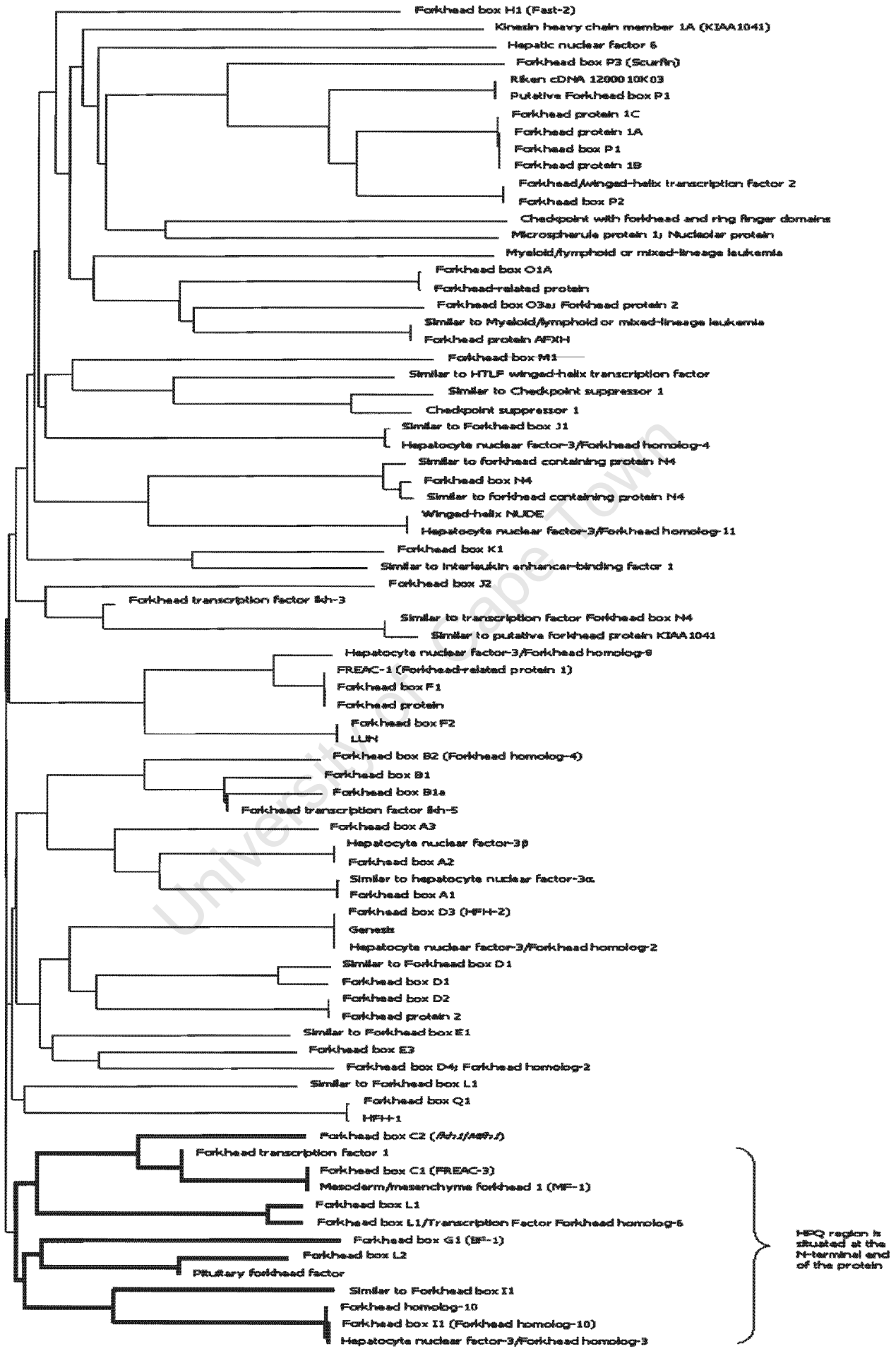

1.4 The isolation and expression patterns of Brain Factor 1

Studies into the early development of animals showed that in most animals, the gut and brain developed within close proximity of each other, that is either the brain was lying above the gut or the brain surrounded the gut or oesophagus (Allman, 2000). It was also found that there were genes common to the regulation of the development of both of these structures.

It has previously been found that the HNF-3/forkhead family of genes in *Drosophila* encoded proteins that were responsible for the development of the gut structures of the fly (Allman, 2000). Mammalian homologues of the HNF-3 proteins, first identified in *Drosophila*, HNF-3 α, HNF-3 β and HNF-3 γ, were shown to be required for the specification and activation of liver genes during development (Hacker *et al.*, 1992; Tao *et al.*, 1992; Clevidence *et al.* 1993). However, mutations in the *Drosophila* HNF-3/forkhead gene resulted in the elimination of the gut structures, and in their place was the formation of peculiar head-like structures (Allman, 2000). Hence Tao *et al* (1992) proposed that there might be further members of the HNF-3 family, in vertebrates, that were also required for the development of the vertebrate central nervous system, in this case the mammalian forebrain specifically.

To investigate this, a 327 bp probe, spanning the DNA-binding domain of HNF-3α was used to identify a 2.9 kb RNA transcript, when rat whole brain tissue was screened, and to isolate a 2.8 kb cDNA clone from the library generated from the rat whole brain (Tao *et al.*, 1992). The 2.8 kb cDNA clone, named Brain Factor 1 (BF-1), was shown to have a 480 amino acid open reading frame. BF-1 was only found expressed in the newborn and embryonic day 14 (E14) and E17 brain, but not in any other adult or foetal tissue examined by northern blot analysis (Tao *et al*, 1992). Northern blot analysis also showed that BF-1 was expressed at moderate levels at E14, with a peak in levels at E17 in the brain, while expression was greatly reduced in the neonate and adult brain (Tao *et al*, 1992). Xuan *et al.* (1995) too, found that the expression of BF-1 in the developing

neuroepithelium was restricted to the olfactory bulb, the retina and optic stalk, and the telencephalon of the developing mouse embryo. In the adult, BF-1 expression was localised in the caudate putamen, the frontal cortex, the occipital cortex, the olfactory bulb, the olfactory neuroepithelium and the hippocampus (Tao *et al.*, 1992)

1.5 The primary structure of Brain Factor 1: the three domains of BF-1

All members of the *forkhead*/HNF-3 family contained a common 100 to 110 amino-acid DNA-binding domain with a three-dimensional motif, termed the winged helix domain (Tao *et al.*, 1992; Wiese *et al.*, 1995; Kaufmann *et al.*, 1996; Gomez-Skarmeta *et al.*, 1999).

Analysis and characterisation of the BF-1 cDNA and protein by sequence homology showed that BF-1 was comprised of three domains, the Histidine (H), Proline (P) and Glutamine (Q)-rich N-terminal domain, the DNA-binding domain (DBD), and the transcriptional repressor domain (TRD), Figure 1.3; Figure 3.2 A. Multiple protein sequence alignment of the forkhead box- or winged helix-containing proteins (Figure 1.1) showed BF-1 was clustered with proteins that have proline-rich N-terminal domains, such as the mesoderm/mesenchyme forkhead 1 (MF-1) and the Forkhead box I1 (Fox I1).

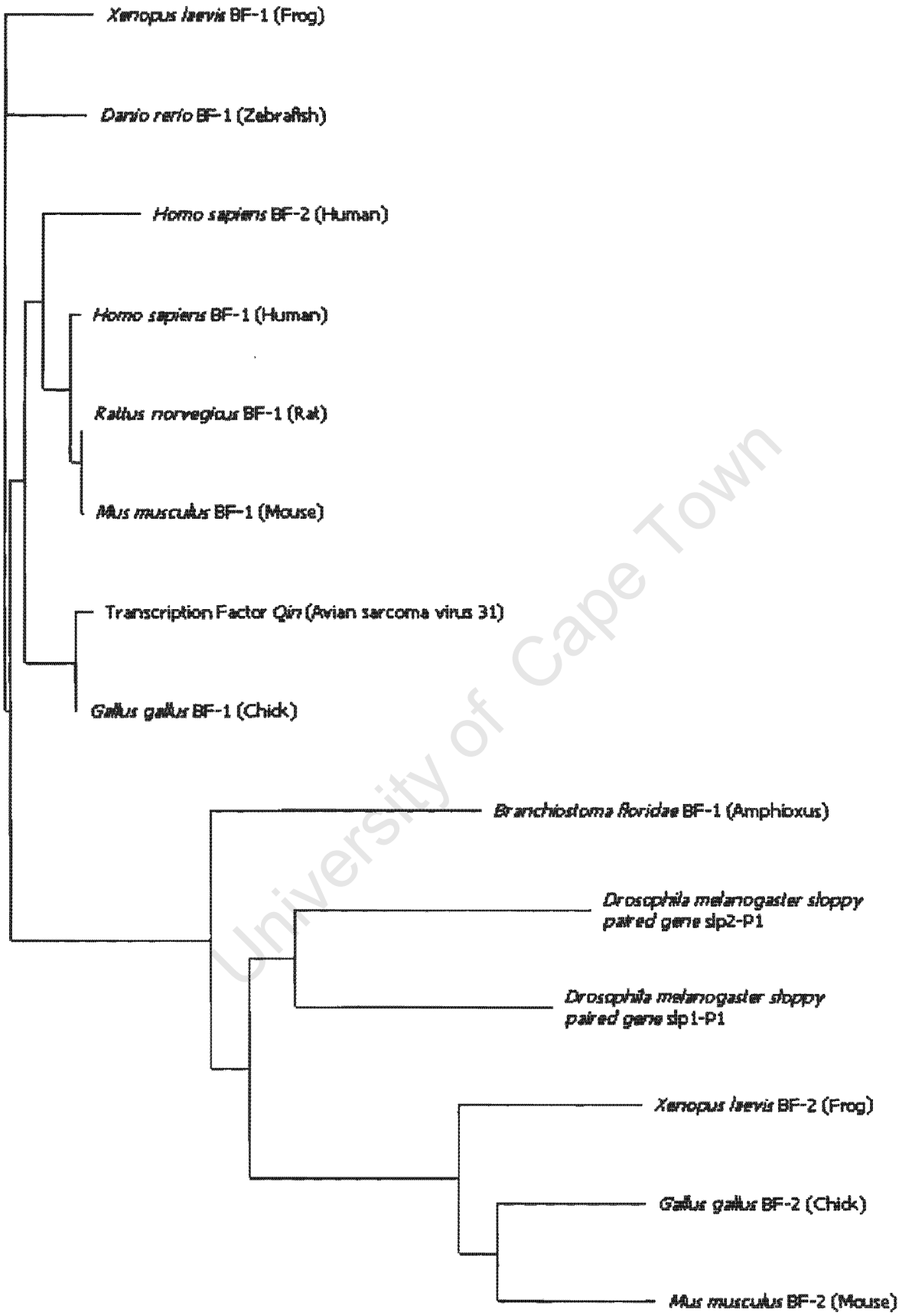

Figure 1.2: Phylogenetic analysis of the protein sequences of the vertebrate winged-helix transcription factors Brain Factor (BF), as well as the protein sequences of the *Drosophila melanogaster sloppy paired* genes that were shown to share sequence similarities to short sequences of the Brain Factor transcription factors, thereby inferring the importance of these regions

1.5.1 The histidine, proline and glutamine-rich domain

Homologues of BF-1 have been identified in the protochordate *Branchiostoma floridae*, and in several other vertebrate species as well (Figure 1.2). Analysis of the sequence alignment of these transcription factors showed that mouse BF-1 exhibits high sequence similarity to the rat BF-1, 99% (Li *et al.*, 1996), the *Xenopus* BF-1 (*X*BF-1) was closely related to the chick BF-1 (*Qin*), 70% homologous (Bourguignon *et al.*, 1998), while the human Brain Factor transcription factors 1 and 2 (hBF-1 and hBF-2) were 84% homologous to each other (Wiese *et al.*, 1995). All the BF-1 transcription factors: mBF-1, rBF-1, hBF-1, cBF-1, *Qin*, xBF-1 and zBF-1, with the exception of the BF-1 of the *Branchiostoma* species (bBF-1), have the H, P, Q-rich region located at the N-terminal end of the protein.

The *Drosophila* segmentation proteins, encoded by the *sloppy paired 1-P1* and *sloppy paired 2-P1* genes, show homology to the brain factors across the length of the forkhead or winged helix domain (Figure 1.3). These were initially identified as homologues to the mouse BF-1 due to sequence homology via the short H, P, Q-rich region, that is located at the N-terminal end of *sloppy paired* (*slp*) proteins, and the DNA binding domain. Bourguignon *et al* (1998) also identified an N-terminal region, upstream of the H, P, Q-rich region of *slp2* that was homologous to the N-terminal region of *X*BF-1 that suggested an important role of this region in the functioning of the protein.

The H, P, Q-rich region of BF-1 displayed sequence length variability between the different species (Figure 1.3). However, the function of this region remains largely unknown. The presence of the H, P, Q-rich region at the amino-terminal end suggested that BF-1 might also act as transcriptional activator (Tao *et al.*, 1992).

Figure 1.3: Protein sequence alignment of the vertebrate Brain Factor transcription factors, as well as the protein sequences of the *Drosophila melanogaster sloppy-paired* genes, to show only the Histidine-, Proline- and Glutamine-rich region (H,P,Q; pink), the DNA-binding or winged-helix domain (DBD; light blue) and the transcriptional repressor domain (TRD; light green). The highly conserved N-terminal region that had been identified by Bourguignon *et al* (1998) in the *Xenopus* BF-1 and *Drosophila* slp2 proteins, is highlighted in yellow.

1.5.2 The DNA-binding domain

Sequence comparison with HNF-3 proteins showed that Brain Factor 1 (BF-1) was not homologous along its entire DNA-binding domain with the HNF-3 protein forkhead domain. The HNF-3 proteins shared 85% sequence identity within the forkhead box, while BF-1 displayed only 74% identity to the HNF-3 proteins in this region (Tao *et al*, 1992). From this slight divergence in sequence homology, Tao *et al* (1992) also proposed that BF-1 had different binding specificity to its target DNA sequences. This was confirmed when BF-1 bound weakly to the TTR (transthyretin) promoter region, to which the HNF-3 proteins bound readily with high affinity (Tao *et al*, 1992).

BF-1 was also shown to diverge significantly along its carboxy-terminal third of the DNA-binding region when this domain was compared with other members of the HNF-3 family of transcription factors (Tao *et al.*, 1992). This sequence divergence was correlated to the definite binding specificity of BF-1 to its target sequence (Tao *et al.*, 1992).

1.5.3 The transcriptional repressor domain

Qin, encoded by the avian sarcoma virus 31 gene *qin*, was isolated from adult chickens and shown to be homologous to the *Drosophila forkhead* box proteins (Li *et al.*, 1993), and the mammalian BF-1 (Li *et al.*, 1997). Using chicken embryo fibroblasts, Li *et al* (1995) transiently co-transfected these with the RSV (rous sarcoma virus long terminal repeat promoter)-driven *qin* and the CMV (cytomegalovirus immediate-early promoter)-driven luciferase reporter gene that did or did not contain the six synthetic BF-1 (or *Qin*) binding sites upstream of the CMV promoter, that is pB6luc or pCMX, respectively. Observation of these chicken embryo fibroblasts showed that the expression of the luciferase reporter gene was greatly reduced when the BF-1 (or *Qin*) binding sites were present, and only slightly reduced when the sites were absent (Li *et al.*, 1995; Li *et al.*, 1997). This suggested that *Qin* played a

role in the repression of the reporter gene, and more importantly, in the transcriptional repression of its target genes in a DNA-sequence specific manner (Li *et al.*, 1995). Analysis of the domain deletion constructs of *Qin* showed that the domain responsible for transcriptional repression activity of *Qin* was located at the carboxy terminal end of *Qin* (Li *et al.*, 1995). Comparison of the amino acid sequence of BF-1 with *Qin* showed that BF-1 and *Qin* were highly homologous along their carboxy terminal ends (Li *et al.*, 1995). Thus this high sequence homology between *Qin* and BF-1 along the carboxy terminal region, suggested that BF-1 might also act as a transcriptional repressor in a sequence specific manner (Li *et al.*, 1995).

1.6 Deciphering the role of BF-1

BF-1 has been implicated in the control of the proliferation and differentiation of the neuronal progenitor cells of the telencephalic neuroepithelium.

1.6.1 Use of transgenic mouse knockouts to study BF-1 function in forebrain development

Targeted disruption of BF-1 in developing mice embryos has lead to the developmental defects that have aided in the elucidation of the function of BF-1 within the developing embryo.

Heterozygous BF-1 $^{(+/-)}$ mice appeared and functioned normally, whilst embryonic and newborn BF-1 $^{(-/-)}$ mice were phenotypically normal before E8.5, with defects readily distinguishable as development progressed. These BF-1 $^{(-/-)}$ mice survived to term, but died within minutes after birth. The BF-1 null mutants had cerebral hemispheres that were up to 95% reduced in mass (Xuan *et al.*, 1995). The growth defects were more severe in the ventral than in the dorsal telencephalon, affecting the basal ganglia that form in this region (Huh *et al.*,

1999). The BF-1 null mutant transgenic mice showed a reduction in the proliferation of the telencephalic progenitor cells, with the onset of differentiation of the telencephalic progenitor cells occurring prematurely (Xuan *et al.*, 1995; Huh *et al.*, 1999). In the wild type mice, the cerebral hemispheres normally expand and surround the diencephalon, resulting in the smooth and uniform appearance of the cerebral hemispheres. However, the progenitor cells of BF-$1^{(-/-)}$ mice fail to proliferate and expand the telencephalic neuroepithelium, giving rise to the small, irregular shaped dorso-lateral surface of the diencephalon by embryonic day 9.5 (E9.5) (Xuan *et al.*, 1995). Xuan *et al* (1995) noted too that the olfactory bulbs were significantly reduced in size at E9.5, with an irregular, variable-sized neuroepithelium resulting from the crumpling of the cerebral cortex and the non-uniform thickness of the cortical tissue.

Failure of the telencephalon to grow normally in the BF-$1^{(-/-)}$ mutant mice may be due to the decrease in proliferation of the neuronal progenitor cells (Xuan *et al.*, 1995). Hence a BrdU (bromodeoxyuridine) incorporation assay was used to determine the role and/or effect of BF-1 on neuronal progenitor cell proliferation. Xuan and colleagues (1995) found that in E9.5 mice, no significant differences in cell proliferation could be detected between the null mutant and the wild type E9.5 mice. Also, the number of cells leaving the cell cycle to enter differentiation versus the number of cells that remain in the cell-cycle and continue to proliferate could not be distinguished between the BF-$1^{(-/-)}$ mutant and the wild type mice. However, a 79% reduction of cell-proliferation was observed from E10.5 onwards, a stage at which the expansion of the telencephalon is most prominent. Thus Xuan *et al* (1995) proposed that BF-1 initially played no role or had any effect of the proliferation of the neuronal progenitor cells. However, as development progressed, BF-1 was required to maintain neuronal progenitor cell proliferation of the ventral telencephalon from E9.5 onwards, and of the dorsal telencephalon from E12.5 onwards. These results also suggest that there may be

regulators of neuronal progenitor cell proliferation other than BF-1 that exist within the developing forebrain (Xuan *et al.*, 1995).

It is suggested that BF-1 regulates the development of the forebrain in both a DNA-binding dependent (Dou *et al.*, 2000) and a DNA-binding independent manner (Hanashima *et al.*, 2002). To test that BF-1 functioned in the DNA-binding independent manner, Hanashima *et al* (2002) constructed BF-1 wherein the amino acids asparagines and histidine of the winged-helix domain, critical to the binding activity of the winged-helix domain, were mutated to alanine, BF-1^{NHAA}. Observation of BF-1^{NHAA} mice, in the BF-$1^{(-/-)}$ mutant background, showed that BF-1^{NHAA} was able to restore progenitor cell proliferation of the dorsal telencephalon to approximately wild type levels through a mechanism independent of the binding of BF-1 to DNA (Hanashima *et al.*, 2002).

Abnormalities in the proliferation of the dorsal telencephalic neuroepithelium continued to increase, in the BF-$1^{(-/-)}$ mice as development proceeded. Along with the smaller size of the cerebral hemispheres, the BF-$1^{(-/-)}$ mutant mice also had multiple eye abnormalities and a flattened frontal skull (Xuan *et al.*, 1995; Huh *et al.*, 1999). Hanashima *et al* (2002) observed that the BF-1^{NHAA} rescue transgenic mice had flattened skulls, displayed multiple abnormalities of the eyes and also died within minutes of birth. This suggested that the binding of BF-1 to DNA was required for the normal development of the dorsal telencephalon (Hanashima *et al.*, 2002).

By E12.5, only the wild type showed normal growth of the dorsal telencephalon, while the null mutant transgenic mice displayed an almost two-fold decrease in the number of proliferating cells of the anterior dorsal telencephalon to that of the posterior telencephalon (Xuan *et al.*, 1995). However, the dorsal telencephalon is able to survive until E12.5 without

BF-1 inducing the proliferation of the neuronal progenitor cells. Thus BF-1 can be seen here to play a role in the regionalisation of the telencephalon, rather than in the specification of the formation of the telencephalic vesicles (Xuan *et al.*, 1995).

Neuronal differentiation of the cerebral cortex in the mouse takes place between E11 and E18 of the developing mouse embryo (Xuan *et al.*, 1995). While neuronal proliferation is marked by the rapid and extensive increase in the number of neuronal progenitor cells, neuronal differentiation is marked by the exit of some of these neuronal progenitor cells from the cell cycle to enter into neurogenesis (Xuan *et al.*, 1995). At the E10 stage embryo, the neuroepithelium of the E10 stage embryo consists entirely of actively proliferating cells. A thickened cerebral cortex results from the migration of the differentiated cells away from the ventricular zone to the cerebral cortex as development proceeds (Xuan *et al.*, 1995).

Due to the significant decrease in the rate of proliferation of the ventral telencephalon, with proliferation ceasing completely by E10.5, the ventral telencephalon was absent in the E10.5 mutant (Xuan *et al.*, 1995). This loss of the ventral telencephalon suggested that the neuronal progenitor cells were exiting the cell cycle prematurely to enter neuronal differentiation, and migrating beyond the sub-ventricular zone to the cortex (Xuan *et al.*, 1995). The Microtubule-Associated Protein-2 (MAP2) was used as a marker of neuronal differentiation. Cells of the BF-1 null mutants showed high levels of MAP2 expression, whereas MAP2 expression of the E12.5 wild type counterparts was limited to the pre-plate neurons (Xuan *et al.*, 1995). Failure of the cells to incorporate BrdU confirmed that the cells were post-mitotic and already committed to a neuronal differentiation fate (Xuan *et al.*, 1995). Thus Xuan *et al* (1995) concluded that BF-1 was essential for the continual proliferation of the neuronal progenitor cells within the ventral telencephalon, from as early as E9.5.

The expression of BF-1 in both proliferating neuronal progenitor cells as well as in post-mitotic differentiating neuronal progenitor cells showed that BF-1 played a role in the neurogenesis of the mammalian embryonic forebrain. Furthermore, BF-1 was involved in the timing of differentiation of the glia, the neuronal supporting cells, and as well as in the normal growth and differentiation of the telencephalic neuroepithelium (Xuan *et al.*, 1995).

1.6.2 The molecular mechanisms by which BF-1 regulates neuronal progenitor cell proliferation and differentiation

Regionalisation of the neural tube is concomitant with the process of neurogenesis (Mariani *et al.*, 1998). Regionalisation of the neural tube and the differentiation of the neuronal progenitor cells (neurogenesis) are under the control of the neurogenic and proneural proteins (Guillemot *et al.*, 1993). These proteins act as positive or negative regulators of neuronal differentiation, thereby bringing about the development and spatio-temporal patterning of the neuroepithelium (Kageyama *et al.*, 1997). The expression of the proneural and neurogenic genes are in restricted domains within the developing neural plate and are surrounded by the region wherein prospective neuronal differentiation will occur (Chitnis *et al.*, 1995; Lee *et al.*, 1995). The expression of the proneural and neurogenic genes within restricted domains suggests that these genes are regulated spatially and temporally (Chitnis *et al.*, 1995; Hardcastle *et al.*, 2000), and thus play critical roles during development. In *Xenopus*, the delay of neuronal differentiation in the anterior neural plate until after neural tube closure, while posteriorly neuronal differentiation occurs at the neural plate stage, is suggestive of the temporal regulation of neurogenesis (Bourguignon *et al.*, 1998). Spatial regulation of neurogenesis in *Xenopus* is bordered by the region of *N-tubulin* expression (Bourguignon *et al.*, 1998). This region is represented by the three bilateral stripes found on either side of the dorsal midline in the posterior neural plate in the neurula stage (Bourguignon *et al.*, 1998). Anteriorly, neurogenesis is delayed until the tadpole stage and takes place within the

telencephalon, the olfactory placodes, the ventral diencephalons and the epiphysis early on in development, but spreads to the rest of the brain as development proceeds (Papalopulu *et al.*, 1996; Bourguignon *et al.*, 1998). The mechanisms by which the molecular control of the spatial and temporal regulation of neurogenesis occurs remain largely unknown (Bourguignon *et al.*, 1998). The expression of BF-1 in a restricted pattern within the developing telencephalon suggests that BF-1 may be required for the control of the temporal and spatial regulation of neuronal differentiation along the anterior-posterior axis of the developing CNS (Yao *et al.*, 2001), by co-ordinating or regulating cell division and neural cell fate specification (Hardcastle *et al.*, 2000).

1.6.3 The positive regulators of neuronal progenitor cell differentiation

Members of the transforming growth factor beta (TGF-β) signalling pathway have been shown to play a role in promoting neurogenesis thereby acting as positive regulators of neuronal differentiation (Guillemot *et al.*, 1993; Tanabe *et al.*, 1996; Furuta *et al.*, 1997; Kageyama *et al.*, 1997). TGF-β signalling acts by blocking the entry of cells released from contact inhibition back into the cell cycle. The bone morphogenetic protein (BMP4), a member of the TGF-β signalling pathway acts by inducing ectoderm to form epidermis (Tanabe *et al.*, 1996; Furuta *et al.*, 1997), and promotes neuronal differentiation by inhibiting neuronal progenitor cell proliferation (Dou *et al.*, 2000). Signals from the organiser have been suggested to counteract the action of BMP4 to bring about the neuronal induction of the ectoderm (Tanabe *et al.*, 1996). The *Xenopus* homologue of the mouse BF-1 (*X*BF-1) prevents the early differentiation of the neuronal progenitor cells in the anterior neural plate (Papalopulu *et al.*, 1996) whereby BF-1 antagonises the anti-proliferative action of TGF-β (Dou *et al.*, 2000). Knockout of BF-1 in mice resulted in the premature onset of neuronal progenitor cell differentiation in the mammalian forebrain (Xuan *et al.*, 1995). Also, the down-regulation of

*X*BF-1 by retinoic acid, a key regulator of the early development of the CNS (Blumberg *et al.*, 1997), resulted in the early onset of neuronal differentiation (Papalopulu *et al.*, 1996). Thus BF-1 is implicated in playing a role in the regulation of the differentiation of the neuronal progenitor cells during development.

1.6.4. The regulation of the TGF-β signalling pathway during neurogenesis

Dou *et al* (2000) have shown that the BF-1 $^{(-/-)}$ transgenic mice were more sensitive to the anti-proliferative action of TGF-β than the heterozygous or wild type mice, confirming that BF-1 was indeed required for the regulation of the timing of neuronal differentiation of the developing neocortex (Dou *et al.*, 1999; Dou *et al.*, 2000). As BF-1 is a nuclear protein, Dou *et al* (2000) initially hypothesised that BF-1 acted by interacting with members of the TGF-β signalling pathway, the Smad proteins. However, they found that BF-1 interacted with a C-terminal portion of FAST2, another winged helix transcription factor that binds to its gene targets along with and by interacting with Smad2. Interaction of BF-1 with FAST2 enabled BF-1 to interact with Smad4, and FAST2 to interact with Smad2 to bring about the inhibition of TGF-β –dependent gene expression by BF-1 (Dou *et al.*, 2000).

Rodriguez *et al* (2001) found that BF-1 does, however, interact with Smad proteins directly. Rodriguez *et al* (2001) used the Mink Lung cell line (Mv1Lu), a cell line characterised for its hyposensitive response to TGF-β signalling. As BF-1 had been implicated to antagonise TGF-β signalling (Dou *et al.*, 2000), Rodriguez *et al* (2001) then set out to investigate the mechanisms by which BF-1 regulated TGF-β –dependent signalling. They showed that the nuclear protein BF-1 interacted with the unphosphorylated Smad3, a cytoplasmic protein, and in the absence of TGF-β signalling, BF-1 was localised in the cytoplasm. Expression of BF-1 and Smad3 in the presence of the TGF-β signalling pathway,

resulted in the translocation of both of these proteins into the nucleus wherein BF-1 was able to inhibit the induction of the neuronal progenitor cells to differentiate by the TGF-β pathway (Rodriguez *et al.*, 2001). The translocation of Smad3 into the nucleus resulted in the interaction of Smad2 with Smad4, to bring about the transcription of genes involved in TGF-β signalling. However the interaction of BF-1 with Smad3 resulted in the negative regulation of TGF-β signalling (Rodriquez *et al.*, 2001).

Dou *et al* (2000) were able to show that BF-1 was required to interact with FAST2 in a DNA-independent manner in order to antagonise the anti-proliferative action of TGF-β in the nucleus. Rodriguez *et al* (2001) showed that BF-1 did, in fact, interact with another member of the Smad protein complex, the unphosphorylated Smad3 outside the nucleus to repress TGF-β signalling. However, the interaction of the phosphorylated Smad3 with BF-1 in the nucleus resulted in the abortion of the transcription of the TGF-β signalling gene targets (Rodriguez *et al.*, 2001). Hanashima *et al* (2002) later found that substitution of endogenous BF-1 with BF-1^{NHAA} was unable to repress the expression of *Bmp* genes, synonymous with that observed in BF-$1^{(-/-)}$ mutants. This demonstrated that the direct BF-1 DNA-binding activity was required for BF-1 to repress *Bmp* gene expression and thereby inhibit neuronal differentiation.

1.6.5 The negative regulators of neuronal progenitor cell differentiation

The neurogenic proteins work by limiting the number of neuronal progenitor cells that exit the cell cycle to undergo neuronal differentiation (Tanabe *et al.*, 1996). A regulatory interaction exists between the proneural and neurogenic proteins, that results in the activation of the neurogenic proteins by proneural genes, as well as the restriction of the activity of the proneural proteins by the members of the neurogenic family of bHLH proteins (Tanabe *et al.*, 1996). Proneural proteins belong to the basic helix-loop-helix (bHLH) family of transcription

factors that promote the neuronal differentiation of the neuronal progenitor cells (Guillemot *et al.*, 1993; Kageyama *et al.*, 1997). These neurogenic genes, the negative regulators of neuronal progenitor cell differentiation, comprise proteins that are components of the Notch signalling pathway (Yao *et al.*, 2001). The bHLH proteins, Hairy/Enhancer of split (Hes), a DNA-binding protein, and Groucho/transducin-like Enhancer of split (TLE), a transcriptional co-repressor, are intracellular factors that mediate responses to Notch signalling (Artavanis-Tsakonas *et al.*, 1999; Yao *et al.*, 2001).

The C-terminal domain of the chick homologue of BF-1, *Qin*, has been shown to play a role in transcriptional repression (Chang *et al.*, 1995; Li *et al.*, 1995). Thus Yao *et al* (2001) suggested that BF-1 might mediate its transcriptional repression activity by interacting with the bHLH proteins Hes and Groucho/TLE to bring about the regulation of the cell cycle and the differentiation of the neuronal progenitor cells in the development of the mammalian anterior neural plate. Yao *et al* (2001) showed that BF-1 and TLE were expressed together and interacted with each other *in vivo* in the telencephalic neuroepithelium to bring about the transcriptional repression activity of BF-1. As transcriptional co-repression activity of the Groucho/TLE is brought about when the Groucho/TLE proteins function as adaptors between the transcription factors and histone deacetylases, Yao *et al* (2001) wanted to investigate the role of the histone deacetylases during transcriptional repression by BF-1. They found that BF-1 interacted with TLE to recruit histone deacetylase-containing complexes in order to bring about the transcriptional repression activity of BF-1. Thus the complex formed by BF-1, TLE and Hes1 regulates cell cycle progression, transcriptional repression and neuronal cell differentiation during mammalian forebrain development (Yao *et al.*, 2001).

Hardcastle *et al* (2000) showed that injection of a high dose of *X*BF-1 into the *Xenopus* embryos resulted in the suppression of the $p27^{Xic1}$, a cyclin-dependent-kinase cell cycle

inhibitor that results in the inhibition of the cell division by inhibiting cyclin/cdk activity of the cell cycle and is only present in post mitotic non-dividing neuronal progenitor cells. This inhibition of $p27^{Xic1}$, the amphibian homologue of the mammalian $p27^{Kip1}$, by *X*BF-1 RNA is due to the fact that high dose of BF-1 is able to induce the ectopic proliferation of the neuronal progenitor cells (Hardcastle *et al.*, 2000). However, a low dose of *X*BF-1 RNA injected in the embryos resulted in the increased expression of $p27^{Xic1}$, and the concomitant ectopic expression of the neuronal differentiation marker *N-tubulin* (Hardcastle *et al.*, 2000). Hardcastle *et al* (2000) also showed that $p27^{Xic1}$ may be a direct target of high doses of *X*BF-1, with BF-1 promoting the progression of the cell cycle and thus neuronal proliferation. Hardcastle *et al* (2000) also suggest that high doses of BF-1 regulate proteins involved in the activation of neuronal progenitor cell proliferation, by suppressing proteins involved in the inhibition of cell cycle progression.

1.7 The regulation of BF-1 during forebrain development

Although BF-1 has been shown to play an important role in the development of the forebrain through the regulation of proliferation and differentiation of the neuronal progenitor cells, the question remains as to what regulates BF-1 expression. The expression of the fibroblast growth factor (*Fgf8*) has been shown to regulate tissue identity and anterior posterior patterning of the telencephalic neuroepithelium during development (Rubenstein *et al.*, 1998). *Fgf8* is expressed within the anterior neural ridge (ANR) before the expression of BF-1 is detected (Shimamura *et al.*, 1997). *Fgf8* has been shown to induce and regulate the expression of BF-1 (Shimamura *et al.*, 1997, Rubenstein *et al.*, 1998). Deletion of the ANR results in the elimination of BF-1 expression (Rubenstein *et al.*, 1998). However, the expression of BF-1 can be replaced by the ectopic addition of *FGF8* (Rubenstein *et al.*, 1998).

The expression of the *Bmp* genes have been shown to play critical role in the patterning and neuronal differentiation of the neuroectoderm (Furuta *et al.*, 1997). For example, BMP4 is expressed within the boundary between the telencephalic neuroepithelium and the underlying epidermis during gastrulation. The expression patterns of the *Bmp* genes play critical roles in the regulation of cell growth, proliferation and cell death, by inhibiting or repressing the expression of factors controlling telencephalic growth, such as BF-1 (Furuta *et al.*, 1997; Rubenstein *et al.*, 1998). The complementary expression patterns of BF-1 and BMP4 during neuronal progenitor cell differentiation in the telencephalon, suggested that the expression of BF-1 was regulated by BMP4 (Furuta *et al.*, 1997). Expression of other members of the *Bmp* family of genes, such as *Bmp2*, 4 and 7, are not directly involved in the inhibition of BF-1 in the telencephalon (Shimamura *et al.*, 1997). Instead, BMP2, and BMP4 and BMP7, induce the expression of *Msx I*, a marker of the dorsal CNS, in the ANR (Furuta *et al.*, 1997; Shimamura *et al.*, 1997) that inhibits BF-1 (Furuta *et al.*, 1997). Thus the development of the vertebrate neuroepithelium is regulated not only by signals derived from the mesoderm that antagonise epidermalising signals such as BMPs (Tanabe *et al.*, 1996), but also through the regulation of the induction or inhibition of BF-1 expression (Furuta *et al.*, 1997; Shimamura *et al.*, 1997).

1.8 Conclusion

Taken together, the importance of BF-1 in the regulation of forebrain development is clearly delineated. BF-1 displays a restricted pattern of expression that implicates its role in the spatial and temporal regionalisation and patterning of the developing embryo.

BF-1 regulates neuronal cell proliferation for the growth and development of the mammalian forebrain, whilst BF-1 also regulates the timing and the number of cells that enter into neuronal differentiation. Positive and negative regulators of neurogenesis activate and interact with each other to bring about the differentiation of the neuroectoderm. BF-1 has been shown to regulate and interact with proteins from the TGF-β and components of the Notch signalling pathways, to bring about the growth and differentiation of neuronal progenitor cells.

Fgf8 and the presence of the anterior neural ridge have been shown to control the induction of BF-1 during forebrain development. However, little is known of the interactions or the regulation of BF-1 that take place during neuronal development and result in the regulation of neuronal development.

1.9 Aims of the study

The molecular mechanisms by which BF-1 regulates neuronal progenitor cell proliferation and differentiation are currently being uncovered. However, the molecular mechanisms by which BF-1 function is regulated remain unclear. Hence, the aim of this study was to attempt to investigate how BF-1 function is regulated during neuronal development. To do this, this study was carried out using the olfactory placode neuroepithelial cell-lines generated by Boolay (1999) in the laboratory, as an *in vitro* system for use in the study of neuronal progenitor cell proliferation and neurogenesis (Illing *et al.*, 2002). BF-1 has been shown to be expressed in some of the OP cells (Boolay, 1999; Illing *et al.*, 2002), and thus these cell lines provide a system in which to study the regulation of BF-1 function and the interaction of BF-1 (*in vivo*), in an attempt to further characterise the role of BF-1 in the olfactory neuroepithelium during neuronal development.

Three main sections of this project were set up in order to address the likely mechanisms by which BF-1 and BF-1 function is regulated. The aim of the first part of the study was to further distinguish the interaction of the putative BF-1 interacting protein, BF1-IP$_1$ (Schwegmann, 2000), with BF-1, as a means of elucidating the regulation of BF-1 during neuronal development. The next part of the was to map the domains of BF-1 in order to investigate with of the three BF-1 domains were important for the protein-protein interactions identified by Schwegmann (2000) between BF-1 and BF1-IP$_1$. The last part of the study aimed to investigate the spatial localisation of BF-1 as a form of regulation of BF-1 function during neuronal development.

2 Introduction

In a study carried out by Boolay (1999), sixty permanent cells lines were established from the olfactory neuroepithelium of the embryonic day 10 (E10) olfactory placode (OP). Of these, forty-eight survived, without crisis or contamination, clonal isolation and expansion when grown at the permissive temperature of 33°C (Boolay, 1999; Illing *et al.*, 2002). All these cell lines were then tested, by PCR, to detect if they expressed any transcripts of the known olfactory or telencephalic neuroepithelial markers (Boolay, 1999, Illing *et al.*, 2002). The cell lines OP6, OP27, OP47 and OP55 were found to express different combinations of the markers tested, namely: transcription factors expressed early on in the olfactory receptor neuron (ORN) development, mainly in OP27 and OP47, as well as markers of the later stages of the development of the ORN lineage, mainly in OP6 and OP55 (Boolay, 1999). These four cells lines were thus selected for use in further study (Boolay, 1999).

In a previous study using the OP6 cell-line, four putative BF-1 interacting proteins, BF1-IP_1 to BF1-IP_4, were identified using the yeast two-hybrid screen (Schwegmann, 2000). Three of the four proteins, BF1-IP_2, BF1-IP_3 and BF1-IP_4, were shown to be homologous to extracellular matrix (ECM) proteins or contained EGF-like domains inherent of ECM proteins (Schwegmann, 2000).

The fourth putative BF-1 interaction protein, BF1-IP_1, was found to be novel as no homologous sequences were identified on the database (Schwegmann, 2000). Schwegmann (2000) had shown that nucleotides 2 to 18 of the sense strand of BF1-IP_1 were 100% homologous to 17 bp of the antisense strands of the genes encoding the human p38 interacting protein (accession number gb|AF093250.1|AF093250) and the human transcription factor (accession number emb|AJ130894.1|HS130894). However, homology of such a short

fragment of the gene to the antisense strands would require further verification before BF1-IP$_1$ is said to encode either of those proteins. Recently a BLAST search of the PUBMED sequence database (September 2002) identified nucleotides 78 to 303 of the 318 bp fragment of BF1-IP$_1$ to be 100% homologous to the antisense strand (nucleotides 1497 to 1272) of an expressed sequence tag (EST) that encodes a protein similar to a transcription factor that acts as a p38 interacting protein. The accession number of the EST is: XM_130880 (submitted 15 May 2002, and subsequently removed due to genomic annotation processing). Here again BF1-IP$_1$ still displays homology to the antisense strand of the EST and may not necessarily encode for this protein.

Of the four interacting proteins, BF1-IP$_1$ was isolated repeatedly in eight independent yeast two-hybrid screens, with BF1-IP$_1$ giving the strongest signal (Schwegmann *et al.*, 2000). BF1-IP$_1$ is a short twenty five amino acid C-terminal fragment with a cysteine rich domain, approximately twelve cysteines, located just prior to termination of the protein primary structure. Hence it was necessary to verify the interactions between BF1-IP$_1$ and BF-1 by determining that the expression of both BF1-IP$_1$ and BF-1 occurred within the same OP cell line at the same stage of development, as a first step to establishing whether the BF1-IP$_1$ and BF-1 interaction *in vitro* is reflective of an interaction occurring *in vivo*. Northern blot analysis, using the four OP cell lines, OP6, OP27, OP47 and OP55, was carried out for this purpose.

In the second part of this study, the expression patterns of BF-1 during neuronal progenitor cell development were investigated, by western blot analysis of the OP27 cell line, when the cells were grown at the permissive temperature of 33°C, and upon induction of the cells to differentiate, by the addition of RA and shifting the cells to the non-permissive temperature of 39°C. Ultimately, it is hoped that this experiment may provide suggestions with

regards to how BF-1 might be regulated during neuronal progenitor cell development within the olfactory neuroepithelium.

The OP27 cell line was chosen as the cells survived longer, after shifting them to the non-permissive temperature of 39°C, when compared to the other cell lines (Boolay, 1999). Also, the OP27 cell line is at the stage of development at which both early transcription factors and neuronal markers are expressed, when the cells are grown at the permissive temperature of 33°C (Boolay, 1999).

When *all-trans* retinoic acid is added, and the cells shifted to the non-permissive temperature of 39°C, the OP cell lines can be induced to differentiate into terminal, bipolar olfactory receptor neurons, forming long neurite outgrowths and expressing neuronal markers (Boolay, 1999; Illing *et al.*, 2002). These terminal, bipolar olfactory receptor neurons resembled those present *in vivo* in embryonic mice olfactory neuroepithelia (Boolay, 1999; Illing *et al.*, 2002).

RA is a morphogen that has been shown to play a role in the growth, maturation and differentiation of the neuronal progenitor cells within the developing olfactory neuroepithelium. In the early stages of the developing olfactory neuroepithelium, it is suggested that RA may govern the identity and function of the neuronal progenitor cells (Calof *et al.*, 2002). In the later stages of the developing olfactory neuroepithelium, however, RA may play a role in the growth and adhesion of the olfactory receptor neurons (ORN), as the neurons extend into and make contact with the olfactory bulb (Whiteside *et al.*, 1998). Hence, in the attempt to study BF-1 expression during neuronal progenitor cell differentiation, the cells would be induced to differentiate by the addition of RA and shifting them to the non-permissive temperature of 39°C, in this study as well.

2.1 Materials and Methods

2.1.1 Cell culture of olfactory placode cells

Olfactory placode (OP) cell line cells were cultured in Dulbecco's Modified Eagle Medium (DMEM; Gibco), supplemented with 3.7 g/l sodium bicarbonate and 10% heat-inactivated foetal calf serum (FCS; Sigma), hereafter referred to as DMEM-10. Each 1 ml of 1×10^4 cells/ml of OP cell line stocks, frozen in 10% (dimethylsulfoxide) DMSO in DMEM-10 in liquid nitrogen at –180°C, was briefly thawed at 37°C. The cells were carefully transferred to fresh culture medium and centrifuged at 1000 ×g for five minutes. The medium was aspirated off and the cell pellet resuspended in fresh DMEM-10. Each 1 ml of thawed cells was used to seed a single 25 cm^2 tissue culture flask and the flasks incubated at 33°C 10% CO_2. Cell growth was observed daily using an inverted phase-contrast light microscope (Nikon) at 10× and 20× magnification. Cells were passaged when they were 70 - 80% confluent. The old culture medium was aspirated off and the cells rinsed once in 1×PBS (140 mM NaCl, 2.7 mM KCl, 8 mM $Na_2HPO_4.7H_20$, pH 7.3), to remove all traces of serum. Cells were then trypsinised with 0.25% trypsin-0.04% EDTA solution in 1× PBS, at a tenth volume of the culture medium for one minute or until the cells had detached. After the addition of DMEM-10 to terminate trypsinisation, the cell suspension was centrifuged at 1000 ×g for five minutes to pellet the cells. The cells were resuspended in fresh medium and seeded into two 75 cm^2 tissue culture flasks, per 25 cm^2 flask sub-cultured. Once cells had reached 70% confluency again, they were sub-cultured into one 150 cm^2 petri-dish per 75 cm^2 flask used. After further incubation to reach 70% confluency in the petri-dishes, cells were harvested by trypsinisation, pelleted at 1000 ×g for five minutes and the supernatant aspirated off. The cell pellet was immediately stored at –70°C until further processing.

2.1.2 Single step method for isolation of total RNA from OP cell lines

Keeping all samples and solutions on ice, the OP cell pellets were lysed and homogenised in 500 µl of DEPC-treated guanidinium-thiocynate solution, solution D (Chomzyinski *et al.*, 1990), by repeatedly drawing up the sample through a 1G × 40 mm needle attached to a 1 ml syringe. Solution D was comprised of 4 M guanidinium thiocynate, 25 mM sodium citrate pH 7, 0.5 % sarkosyl and 0.1 M β-mercaptoethanol in DEPC-treated water, and prepared using RNAse-free reagents. The RNA was extracted from the homogenate using an equal volume of phenol pH 4, and the thoroughly vortexed mixture was centrifuged at 13 000 ×g for five minutes at 4°C. The aqueous RNA-containing phase was re-extracted with an equal volume of chloroform, at 13000 ×g at 4°C for five minutes. The RNA was then recovered from the aqueous phase by ethanol precipitation and the RNA pellet resuspended in DEPC-treated water.

2.1.3 Northern blot analysis

Using total RNA extracted from the olfactory placode cell lines OP6, OP27, OP47 and OP55, 20 µg of each RNA sample was electrophoresed on a 1% agarose-1× MOPS- 6% formaldehyde gel for sixteen to eighteen hours at 30 V at room temperature.

2.1.4 Transferring the RNA onto the Hybond membrane

The gel was rinsed in distilled water for one hour at room temperature, with gentle agitation. The gel was prepared and mounted onto Hybond N (Amersham) membrane for northern blot analysis, and transferred in 20 × SSC (3M NaCl, 0.3M Na_3citrate) buffer following the manufacturers instructions. The RNA was transferred onto the membrane by capillary action for twelve to sixteen hours, at room temperature.

The transfer apparatus was dismantled and the membrane was marked for orientation. The membrane was rinsed briefly in 2 × SSC (0.3 M NaCl and 30 mM $Na_3C_6H_5O_7.2H_2O$, pH 7) buffer and blotted onto Whatman paper. The membrane was dried for ten minutes at 60°C, and the RNA was permanently fixed onto the membrane using an UV-crosslinker (Amersham) for approximately twenty seconds. The membrane was stained in a 0.3% methylene blue in 0.03% DEPC-treated sodium acetate solution for two hours, and then rinsed in water for ten minutes. The membrane was blotted dry briefly to remove excess liquid, wrapped in cling film and photocopied to capture the stained RNA bands visible on the membrane. The membrane was then dried completely and stored in cling film at 4°C until further processing.

2.1.5 Preparation of the probe

Plasmid F3.2 comprised the 300bp fragment of BF1-IP_1 cDNA cloned into the pGAD424 yeast two-hybrid vector (CLONTECH) (Schwegmann, 2000). Plasmid pBF-1 comprised the full-length mouse BF-1 cDNA cloned into pBluescript SK (Li *et al.*, 1996). A single colony of *E. coli* transformed with each of these plasmids, from a freshly streaked plate, was used to inoculate 100 ml Luria-Broth medium containing 100 µg/ml ampicillin each, and incubated at 37°C for twelve to sixteen hours with vigorous shaking. Plasmid DNA was isolated from the overnight cultures using the Wizard Midi-Prep kit (Promega), following the manufacturer's instructions. Briefly, the 100 ml cultures were pelleted at 15,000 ×g (Beckman J2-21 centrifuge) at 4°C for fifteen minutes. The supernatant was aspirated off and the pellet resuspended in the cell resuspension solution (50 mM Tris-HCl, pH 7.5, 10 mM EDTA, 100 µg/ml RNAse A). The bacteria were lysed with the cell lysis solution (0.2 M NaOH, 1% SDS) and neutralised in the neutralisation solution (1.32 M KCH_3COO, pH 4.8). The samples were then centrifuged at 15,000 ×g for fifteen minutes at 4°C, to pellet the cell debris. The plasmid

DNA-containing supernatant was allowed to enter a silica-resin column, by drawing the liquid using a vacuum source, and the column washed twice in the column wash solution (80 mM KCH_3COO, 8.3 mM Tris-HCl, pH 7.5, 40 µg EDTA, 55% ethanol). The DNA was eluted from the column with 300 µl of sterile water.

Each 10 µg of the plasmid preparations was digested with *EcoR I* for the F3.2 and *EcoR I* and *Kpn I* for the pBF-1, in a 50 µl reaction with three units of enzyme at 37°C overnight. The digest was heat inactivated at 65°C for twenty minutes, and the digests were electrophoresed on a 1% low-melting point agarose gel (SeaPlague® GTG ® agarose; FMC) in 1× TAE buffer, in 1× DNA loading dye, at 100 V for one hour. The gel was visualised briefly using the short wavelength UV transilluminator. The 300 bp BF1-IP_1 fragment and the 1264 bp BF-1 fragment were excised from the gel for labelling.

The DNA was recovered from the gel slices using the GENECLEAN kit (BIO101), following the manufacturer's instructions, into 20 µl of sterile water. The DNA concentration was estimated on an ethidium bromide plate, using serial dilutions of lambda DNA.

2.1.6 Labelling the DNA

After gel purification of the DNA, 25 ng of each of DNA fragments were used as the template for the labelling of the probe. The DNA fragments were labelled with ^{32}[P]-dCTP (Amersham) using the Megaprime DNA labelling kit (Amersham), according to the manufacturers instructions. The labelled DNA was denatured at 95°C for five minutes, and chilled immediately on ice. To calculate the percentage incorporation, 2 µl of the denatured sample was placed in a scintillation vial for Cerenkov counting.

2.1.7 Removal of unincorporated nucleotides

A short-stemmed Pasteur pipette was plugged with silanised glass wool. The pipette was then filled with 1× STE (10 mM Tris-HCl, pH 7.5, 10 mM NaCl and 1 mM EDTA)-equilibrated Sephadex G-50 slurry, by gravity flow, until the column bed had been packed to the indentation at the top of the pipette. Using 1 ml of 1× STE buffer, the buffer was passed three times through the column, to equilibrate it. The labelled DNA sample, to which a Dextran blue-Orange G tracking dye had been added, was applied to the column and allowed to enter the top of the column bed. The column was carefully topped with 0.5 ml of 1× STE buffer to a total of 1.5 ml, and four-drop fractions were collected immediately into 1.5 ml centrifuge tubes. Using the Geiger counter, the three or four fractions with the highest counts per second were pooled together. From the pooled sample, 2 µl was placed into a scintillation vial, and the two 2 µl samples were counted using the Cerenkov method on the scintillation counter.

2.1.8 Hybridisation

The membrane was placed RNA side up in a glass hybridisation tube. The membrane was pre-hybridised in 20 ml/75 cm^2 warmed hybridisation buffer (0.1% SDS, 50% formamide, 5× Denhardt's solution, 50 mM sodium phosphate pH 6.8, 0.1% sodium pyrophosphate and 50 mg/ml salmon sperm DNA) for at least six hours at 42°C. The pre-hybridisation buffer was replaced with 10 ml fresh hybridisation solution, and the denatured labelled probe was carefully mixed into the solution. Hybridisation was carried out using 1×10^6 counts/ml of hybridisation solution, calculated from the total counts of the pooled sample. The membrane was hybridised with the probe for thirteen to sixteen hours at 42°C, with gentle agitation.

2.1.9 Washing and exposing the membrane to X-ray film

The membrane was washed in excess 2× SSC, 0.1% SDS solution for fifteen minutes at room temperature with gentle agitation, following a protocol by McCaughern-Carucci, 1997, posted online. The stringency of the subsequent washes were increased until only two to five counts per second were detected, using a Geiger counter, on the membrane. The membrane was briefly blotted onto blotting paper, to remove excess liquid, and wrapped in cling wrap. The membrane was exposed to sensitive X-ray film and incubated in an X-ray cassette at –70°C for up to eight days. The X-ray film was developed in fresh X-ray developing solution until bands appeared, rinsed briefly in 3% acetic acid solution and fixed in X-ray fixing solution for six minutes. The X-ray was then washed for thirty minutes under de-ionised running water and air-dried completely.

2.1.10 Stripping the blot for re-probing

As the membrane was hybridised with first the BF1-IP_1 and then the BF-1 DNA probe, the membrane was stripped, between each hybridisation, by placing in a heated 0.5% SDS solution at room temperature for thirty minutes. The membrane was then briefly blotted dry, wrapped in cling film and stored moist at 4° C until further processing.

2.1.11 Bacterial culture and isolation of fusion protein

The histidine, proline and glutamine rich region and DNA-binding domain of the rat BF-1 (Tao *et al.*, 1992; Xuan *et al.*, 1995) cDNA, amino acids 38 to 271 or nucleotides 554 to 1255, had been cloned into the *EcoR I* site of pGEX-3X (Pharmacia Biotech) glutathione S-transferase (GST) fusion vector (Rumback, and Schwegmann, personal communication). This construct is referred to as pGST-BF-1 for the plasmid DNA and GST-BF-1 for the expressed protein. The pGEX-3X was used as the control, and has been referred to as pGEX-3X for the plasmid DNA and GST for the expressed protein. The experimental pGST-BF-1 construct and

the control pGEX-3X construct were transformed into the BL 21 DE3 pLysS and BL 21 DE3 *Escherichia coli* strains, respectively. The expressed GST protein ran at approximately 27.5 kDa and the expressed GST-BF-1 fusion protein ran at approximately 53 kDa on the SDS-PAGE.

A single colony from each of pGEX-3X and pGST-BF-1 was used inoculate 5 ml each of 2× YT (Ausubel *et al*, 1987) medium containing 100 μg/ml ampicillin in each, as well as 30 μg/ml chloramphenicol for the pGST-BF-1, and incubated overnight at 37°C with vigorous shaking. The overnight cultures were used to inoculate 5 ml of fresh 2× YT medium, with the appropriate antibiotics, at a 1 in 50 dilution, and these were incubated at 37°C with vigorous shaking until they reached an OD_{600} of 0.9 to 1.2. Removing 1 ml of the culture as a time zero or non-induced sample, 0.4 mM IPTG was added to the cultures, to induce protein at 30°C overnight with vigorous shaking. Three ml of the bacterial cells were harvested into 1.5 ml tubes at 13 000 ×g for two minutes at 4°C. The supernatant was discarded and the pellets were stored overnight at –20°C to aid in the lysis of the bacterial cultures. The thawed pellets were resuspended in 150 μl TNT (40 mM Tris-HCl pH 7.5, 1 mM EDTA, 150 mM NaCl and 0.1% (v/v) Triton X-100) buffer to which the protease inhibitor cocktail (2μg/ml Leupeptin, 2 μg/ml Pepstatin, 10 mM DTT and 1mg/ml PMSF) was added, and the samples incubated on ice for five minutes. The protease inhibitor cocktail was added to the TNT buffer, the glutathione slurry and reduced glutathione solution in the subsequent steps. 20 μl of Lysozyme (20 mg/ml) was added and the samples incubated on ice for thirty minutes. This was followed by the addition of 1.6 μl of 10% (v/v) Triton X-100, 1.6 μl of 1 M $MgCl_2/MgSO_4$ and 10 μl of DNAse I (10 mg/ml), and the samples mixed thoroughly by tapping the tube after each addition. The samples were then incubated at 37°C for thirty minutes and the cell debris pelleted at 13 000 ×g for thirty minutes at 4°C. The supernatant was transferred to a clean tube

and 20 µl of 50% (w/v) glutathione Sepharose slurry (Pharmacia Biotech) was added and the samples incubated at room temperature for five minutes. The glutathione Sepharose beads were harvested by centrifugation at 5000 ×g for five minutes at 4°C. The bead pellet was washed 3× in 10× bed volume of TNT buffer, and centrifuged at 5000 ×g for five minutes at 4°C after each wash. The bead pellet was resuspended in an equal volume of TNT to which 10 mM ATP and 10 mM $MgCl_2$ added. The sample was incubated at room temperature for ten minutes and then centrifuged at 5000 ×g for five minutes at 4°C. The pellet was washed in an equal volume of TNT buffer and spun down at 5000 ×g for five minutes at 4°C. The bound fusion protein was eluted from the beads using an equal volume of 10 mM reduced glutathione (in ice cold 50 mM Tris-HCl pH 8) by incubating the eluate on ice for ten minutes and then centrifuging the sample at 5000 ×g for five minutes at 4°C. The elution of the fusion protein from the beads was repeated twice more and the supernatants were pooled together. To the flow-through sample was added 20 µl of the 50% (w/v) glutathione sepharose slurry, and the protein was re-extracted twice more as indicated above. The three protein elutions were pooled together, and the protein concentration was approximated using the Bradford Protein assay (BIORAD).

2.1.12 Cell culture, retionic acid induction and protein extraction from the OP27 cell line

OP27 cells were normally cultured in DMEM-10 at 33°C 10% CO_2, as indicated in section 2.1.7 above. Cells were sub-cultured when they reached 70% confluency. 20 µl of the resuspended cells was counted in 5 µl of 4mg/ml Trypan Blue in 1× PBS. The cells were then seeded at 0.5×10^5 to 1×10^5 cells/ml into 10 cm tissue culture petri dishes in 6 ml DMEM-10 per dish. The cells were incubated at 33°C 10% CO_2 until they were 70% confluent.

Cells were harvested by washing the cells twice in 1× PBS. Using a cell-scraper the cells were scraped off the dish in 1× PBS. The cells were centrifuged at 100 ×g for five minutes and the supernatant was discarded. Cells were lysed in 50 µl of homogenisation buffer (50 mM Tris-HCl, pH 7.5, 150 mM NaCl, 1% NP-40 and 5 mM EDTA) with the protease inhibitor cocktail (used above) added, by pipetting up and down. The lysed cells were stored at –20°C for at least one hour or until further processing. The lysed cells were centrifuged at 10 000 ×g for twenty minutes at 4°C and the supernatant was carefully transferred to a clean tube.

OP27 cells were synchronised in 100 ng/ml colcemid solution (Gibco), added directly to the culture medium, for 27.5 hours. Synchronisation was carried out to ensure that all the cell sin culture were at the same stage of the cell cycle. The culture medium was replaced with retinoic acid (RA) differentiation medium, that was comprised of DMEM/F12 (Gibco) supplemented with 3.7 g/l of sodium bicarbonate (Sigma) and 1% N2 Supplement (Gibco). The RA differentiation medium was further supplemented with 2% heat-inactivated FBS (Sigma) and 100 µM ascorbic acid (Sigma), and the cells induced to differentiate with the addition of 10 µM retinoic acid (Sigma) and the immediate incubation of the samples at 39°C 10% CO_2. Cell pellets were collected from cells harvested at zero hour, one day, two days and four days in retinoic acid. Retinoic acid was replenished forty-eight hours after the cells were shifted to 39°C 10% CO_2.

The Bradford Assay (BIO-RAD) was used to determined protein concentration. Sample protein concentrations were determined from the standard curve generated by the BSA standards. The protein concentrations estimated for each of the samples were: approximately 1.6 µg/µl for the non-synchronised non-RA treated sample, the synchronised non-RA treated,

and for the one day and two days synchronised and RA treated samples; 100 ng/µl of the purified GST sample and 18 ng/µl of the purified GST-BF-1 sample.

2.1.13 SDS-PAGE resolution and transfer of the protein onto membrane

15 µl of the samples were electrophoresed, in duplicate, on a semi-discontinuous 10% SDS-polyacrylamide gel (Maniatis *et al.*, 1983) at 100 V in 1× running buffer (25 mM Tris, 192 mM glycine and 0.1% SDS) for 1 hour at room temperature, using the BIO-RAD Mini-Protean II gel system. The first gel was stained in Coomassie blue staining solution (50% (v/v) methanol, 0.05% (w/v) Coomassie brilliant blue R-250 and 10% (v/v) acetic acid) for thirty minutes and then de-stained overnight in destaining solution (5% (v/v) methanol and 7% (v/v) acetic acid), with gentle agitation. SDS-PAGE solutions, stain and destaining solution were prepared according to Ausubel *et al* (1987), unless otherwise stated.

For the second gel, the stacking gel was carefully removed and the gel orientation marked by cutting off one corner. The gel was soaked in chilled transfer buffer (25 mM Tris, 192 mM glycine and 20% Methanol) for 10 minutes. Hybond-P membrane (Amersham) was hydrated immediately before use, or when allowed to dry by wetting briefly in methanol, rinsed in distilled water for five minutes and soaked in transfer buffer to ten minutes. Hybond-P (Amersham) membrane was cut to the gel dimensions and wetted as indicated. The gel and membrane were assembled into the transfer cassette, and the proteins transferred onto the membrane in chilled transfer buffer for one hour at 100 V, using the BIO-RAD Mini Trans-Blot Electrophoretic Transfer unit.

2.1.14 Western blot analysis and chemiluminescence detection of BF-1

The membrane was carefully removed, marked for orientation and incubated in 5% fat-free milk powder in 1× TBS (10 mM Tris-HCl, pH 7.5 and 150 mM NaCl) for one hour at 4°C, with gentle agitation. The membrane was incubated overnight at 4°C in 1:1000 dilution of rabbit anti-BF-1 primary antibody (Schwegmann, personal communication) in 2% fat-free milk in a heat sealed bag, with gentle agitation. The membrane was washed 3× in 0.1% Tween-20 in 1× TBS at room temperature, for five minutes each wash with gentle agitation. The membrane was incubated for one hour at room temperature in 1:1000 dilution of goat anti-rabbit biotinylated secondary antibody (DAKO) in 2% fat-free milk in 1× TBS, in a heat-sealed bag with gentle agitation. The membrane was washed 3× in 0.1% Tween-20 in 1× TBS at room temperature, for five minutes each wash with gentle agitation. The membrane was incubated for one hour at room temperature in 1:1000 dilution of horseradish peroxidase (HRP)-conjugated streptavidin (DAKO) in 2% fat-free milk in 1× TBS. The membrane was washed 3× in 0.1% (v/v) Tween-20 in 1× TBS at room temperature, with gentle agitation for five minutes each wash.

The chemiluminescence reagents were made up prior to use as follows: Solution 1: 100mM Tris-HCl pH 8.5, 60 µg/ml p-Coumaric Acid (Sigma), in DMSO, and 0.0166% (m/v) hydrogen peroxide, made up to volume in sterile water; Solution 2: 100 mM Tris-HCl pH 8.0 and 0.44 mg/ml 5-Amino-2,3-dihydro-1,4-phthalazinedione (Luminol; Sigma), in DMSO, made up to volume in sterile water. Solution 1 was added to an equal volume of solution 2 immediately prior to use. The membrane was blotted onto paper towel briefly, to remove excess liquid, and placed onto cling film. The membrane was then incubated protein-side up in 0.1 ml/cm^2 of the chemiluminescence reagent mixture (mixture of solution 1 and 2) for two to five minutes. The membrane was briefly blotted onto paper towel to remove excess liquid and

then wrapped in cling film and placed into the X-ray cassette. In the dark, a sheet of X-ray film (Konica) was exposed to the membrane and incubated in the cassette for one minute. The X-ray film was developed, until the signals was detected and fixed for six minutes in X-ray developer and fixer. Fresh X-ray film was exposed to the membrane for twenty minutes and even overnight, for the detection of the signal, and the X-ray developed as normal. The fixed X-ray was washed for thirty minutes under running water and air-dried at room temperature.

2.2 Results

2.2.1 Northern blot analysis of BF1-IP$_1$ and BF-1 in the OP cell line

The first study was undertaken to verify that BF1-IP$_1$ was indeed present and expressed in the same olfactory placode cell lines and at the same time as BF-1 was expressed. From this study, the molecular weight of the full-length BF1-IP$_1$ transcript could also be estimated. To do this, northern blot analysis was performed. All four cells lines, OP6, OP27, OP47 and OP55, were utilised and would enable the comparison of the expression of BF1-IP$_1$, and BF-1, within the different cell lines.

The membrane onto which the gel-resolved 20 μg total RNA had been transferred, was stained with methylene blue to assess for equal loading, Figure 2.1 A. The different lanes show equivalent amounts of RNA.

Northern blot analysis identified two mRNA transcripts that hybridised to the BF1-IP$_1$ probe in the total RNA extracted from the OP6, OP27 and OP55 cell lines (Figure 2.1 B). No mRNA transcripts hybridised to the BF1-IP$_1$ probe in the total RNA extracted from the OP47 cell line. Using a standard curve generated in Microsoft Excel, the BF1-IP$_1$-positive RNA transcripts were estimated to be 1.6 kb and 3.2 kb in size (Figure 2.1 B), compared to the 1.9 kb and 4.1 kb of the 18S and 28S RNA species, respectively (Figure 2.1 A). Mouse 18S and 28S RNA species are given to be approximately 1.9 kb and 5.1 kb (Darnell *et al.*, 1990), respectively, although the 28S RNA species in our samples were only resolved to approximately 4.1 kb (Figure 2.1 A). The absence of the BF1-IP$_1$ hybridisation signals in the OP47 total RNA sample strengthens the case that the BF1-IP$_1$ transcripts observed in the three OP cell lines were positive signals and not the result of non-specific hybridisation.

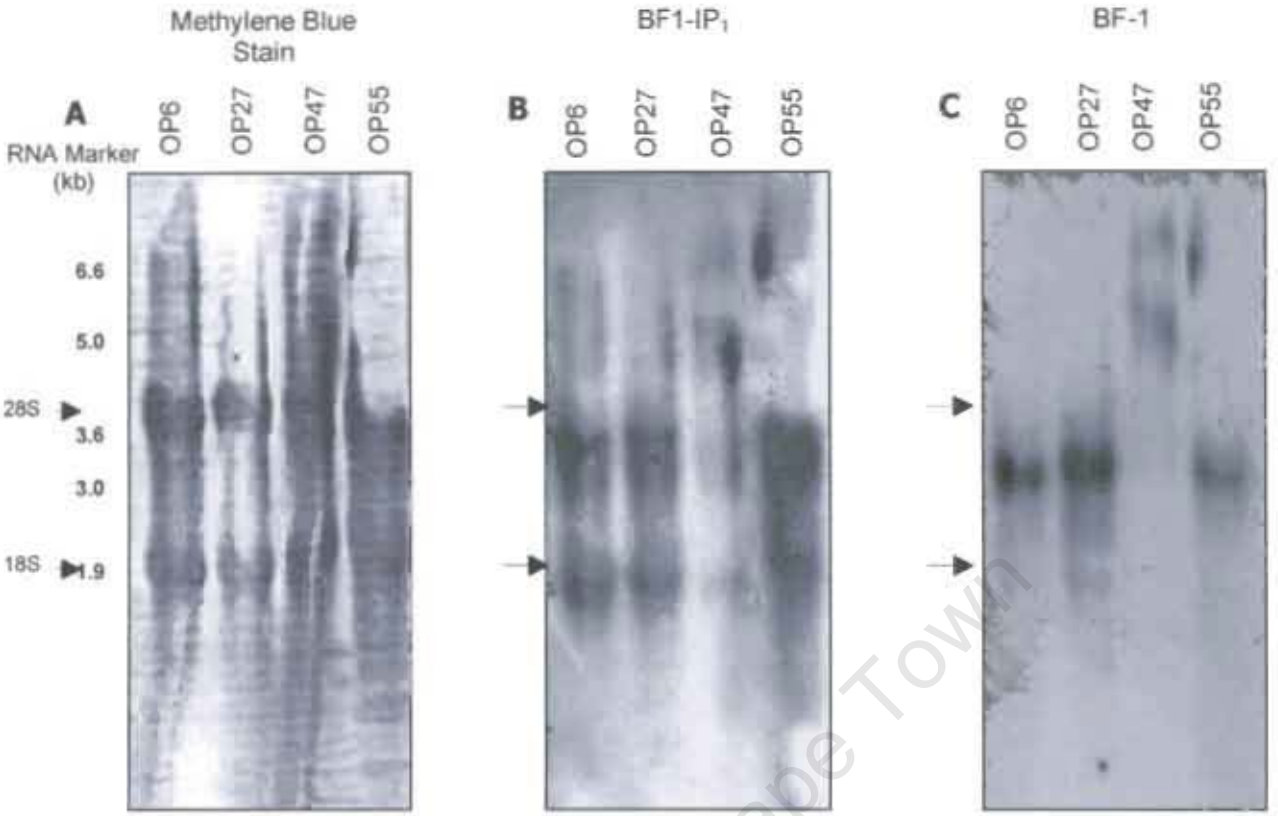

Figure 2.1: Northern blot analysis of OP cell-lines, OP6, OP27, OP47 and OP55, using BF1-IP$_1$ (B) and BF-1 (C) as probes. The positions of the 28S and 18S RNA species, stained in (A) are indicated on blots (B) and (C) by the black arrows. The BF1-IP$_1$ probe hybridised to the two transcripts of 3.2 kb (top) and 1.9 kb (bottom) (B), and the BF-1 probe hybridised to the 2.8 kb transcript (C), respectively. (A) is a photographic image of the membrane after methylene blue staining to show equal loading of the total RNA sample. An RNA molecular weight marker was used (Promega), with the transcript sizes indicated in kilobases (kb).

To confirm that if BF1-IP$_1$ was a putative interacting protein of BF-1, both BF-1 and BF1-IP$_1$ would be expressed within the same cell line at the same stage of development, the [^{32}P]-dCTP labelled *EcoR I-Kpn I* BF-1 fragment was hybridised to the stripped membrane. A single 2.8 kb BF-1 transcript was identified in the OP6, OP27 and OP55 total RNA samples (Figure 2.1 C). This 2.8 kb transcript was absent in the OP47 RNA sample, as had the BF1-IP$_1$ transcripts been absent in the OP47 total RNA sample too. The results show that BF1-IP$_1$ and BF-1 are co-expressed in the same cell lines at the same stage of development.

2.2.2 Western blot analysis of BF-1 in OP cell line

Once the BF1-IP$_1$ and BF-1 mRNA transcripts been had detected in the in the OP6, OP27 and OP55 cell lines, the expression of the BF-1 protein, using the OP27 cell line, was

investigated. Antibodies had been generated in rabbit against the purified GST-BF-1 recombinant fusion protein, and the resultant polyclonal IgG fractions collected (Schwegmann, personal communication). The anti-BF-1 immune IgG were affinity purified from the polyclonal fraction using a glutathione sepharose CN-4B (Amersham) bead column, with the elution of the non-binding anti-BF-1 antibodies free of the affinity- or column-bound anti-GST antibodies (Shacker, personal communication). A dot blot assay that had been used to check the specificity of the different fractions showed that the anti-BF-1 was able to recognise only the recombinant BF-1, that is the GST-BF-1, and not the GST control protein too (Shacker, personal communication).

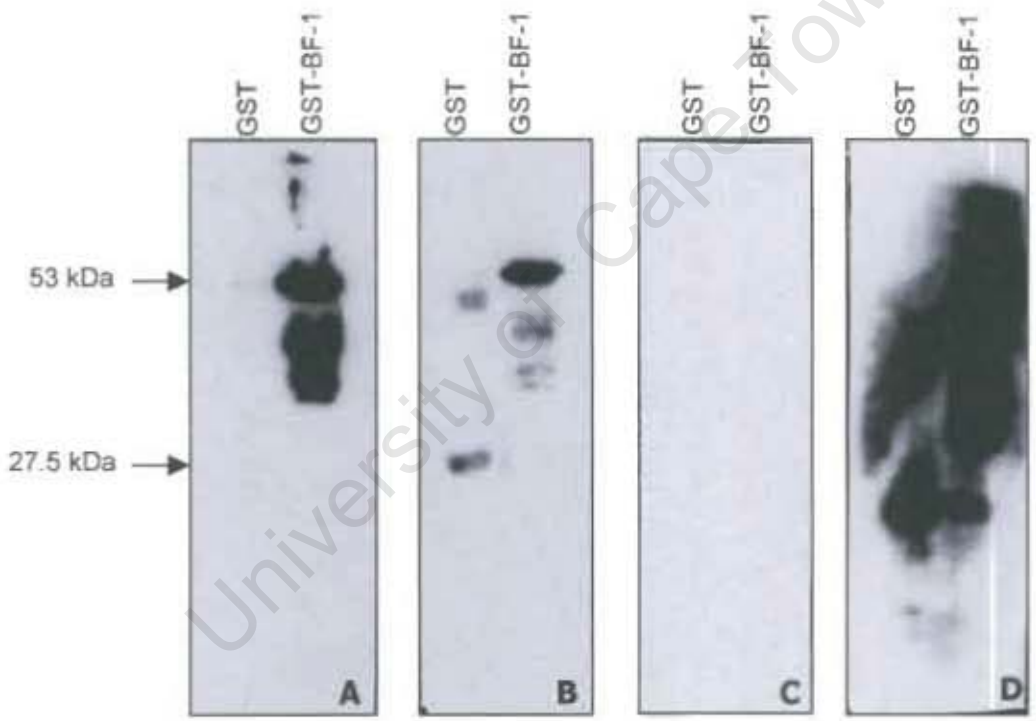

Figure 2.2: Testing the specificity of the gluthatione-sepharose purified antibodies on the GST-recombinant fusion, GST-BF-1, that had been resolved by SDS-PAGE and transferred onto Hybond-P membrane. Membrane A was incubated with affinity purified anti-BF-1; membrane B was incubated with affinity-bound anti-GST, membrane C was incubated with the non-immunised IgG fraction, and membrane D was incubated with the non-purified polyclonal fraction.

To assess the specificity of the purified anti-BF-1 antibody fraction, recombinant GST and GST-BF-1 protein, expressed in *E. coli*, that had been resolved on an SDS-PAGE gel and transferred onto PVDF (Hybond-P) membrane, were immunoblotted with the different polyclonal purification fractions. These polyclonal purification fractions were the affinity-

purified anti-BF-1 (Figure 2.2 A); the affinity bound anti-GST (subsequently eluted by addition of reduced glutathione to the sepharose column; Figure 2.2 B), the non-purified IgG fraction (Figure 2.2 D) and a non-immunised IgG fraction (Figure 2.2 C). Antibodies from the non-purified IgG fraction recognised both the 53 kDa GST-BF-1 proteins as well as the 27.5 kDa GST protein (Figure 2.2 D). The affinity purified anti-BF-1 antibody recognised the 53 kDa GST-BF-1 protein and degradation proteins (Figure 2.2 A). The eluted affinity bound anti-GST antibody fraction recognised the 27.5 kDa GST protein as well as the 53 kDa GST-BF-1 protein (Figure 2.2 B). This fraction would still recognise the GST epitope of the 53 kDa recombinant GST-BF-1 protein. No antibodies were present in the non-immunised fraction that recognised the GST-BF-1 or the GST proteins (Figure 2.2 C). This experiment showed that the purified anti-BF-1 was specific for the BF-1 of the GST-BF-1 fusion protein only, and not the GST protein as well. Thus the affinity-purified anti-BF-1 could be used to identify BF-1 proteins specifically.

Western blot analysis was used to monitor the levels of BF-1 protein in the OP27 cell line in when cells were grown at the permissive temperature of 33°C, and when the cells were induced to differentiated, in the presence of retinoic acid (RA), and grown at the non-permissive temperature of 39°C. Recombinant GST (lane 6) and recombinant GST-BF-1 (lane 7) protein were used as controls. The affinity-purified anti-BF-1 antibodies recognised the recombinant GST-BF-1 protein (Figure 2.3, lane 7), but not the GST protein (Figure 2.3, lane 6), as shown previously. Lanes 1 to 4 (Figure 2.3) were loaded with equivalent amounts of protein, approximately 24 μg (15 μl of 1.6 μg/μl). Only 6 μg (15 μl of 0.4 mg/ml) of protein was loaded into lane 5, since the cells had died and detached from the surface of the petri-dish after the second addition of RA to the cultured cells, resulting in very little sample remaining for extraction on day four.

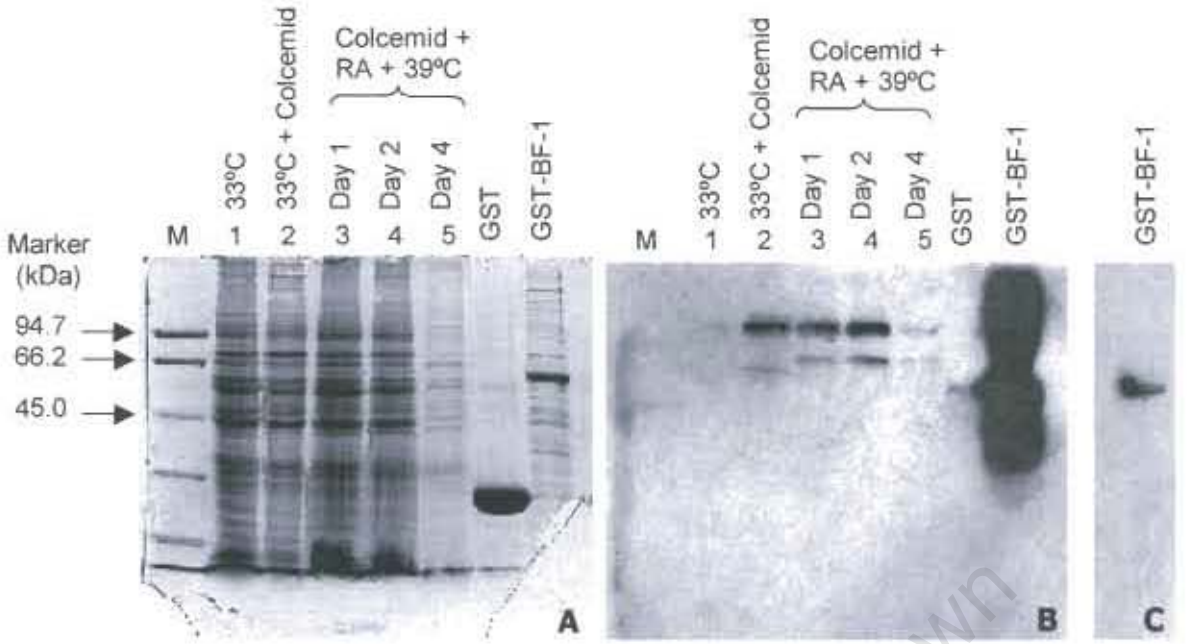

Figure 2.3: Coomassie blue stained SDS-PAGE (A) and membrane of the transferred proteins (B) of OP27 total protein extracted after synchronisation (lanes 2 to 5) and addition of retinoic acid (RA); lanes 3 to 5). (A) shows equivalent loading of the protein samples in lanes 1 to 4. Sample 5 had a lower protein concentration due to high loss of cultured cells with the progression of cell culture in the presence of RA. Lanes are: 1: non-synchronised at 33°C; 2: synchronised, non-RA treated, at 33°C; 3, 4 and 5: synchronised and 1, 2 and 4 days, respectively, in RA (10 μ M). (C) depicts the immunoreactive GST-BF-1, with anti-BF-1 under low exposure, to show the size of the GST-BF-1 protein. The BIORAD Low Range Marker (M) was used with the molecular weights indicated in kilo Daltons (kDa).

Lanes 1 is a whole cell lysate from actively proliferating OP27 cells culture at 33°C. Lane 2 contains whole cell lysate of cells whose cell cycle had been halted at the metaphase stage by addition of the synchronising agent colcemid, whilst lanes 3 to 5 consists of whole cell lysates from cells that had been induced to differentiate by culturing the OP27 cells at 39°C in the presence of RA, after they had been synchronised with colcemid. Synchronisation was carried out to ensure that all the cells in culture were at the same stage of the cell cycle prior to the addition of RA to induce the cells to differentiate when they were placed at the non-permissive temperature of 39°C.

Two anti-BF-1 immunoreactive products were detected in whole cell lysate of the synchronised cells (lane 2), a 62 kDa and a 95 kDa product. When the synchronised cells were induced to differentiate by the addition of RA and placed at 39°C (lanes 3 to 5), the 66 kDa

product and 95 kDa protein products were recognised by the anti-BF-1 antibodies. The 95 kDa protein product remained the predominant protein product recognised by the anti-BF-1 antibodies (lanes 2, 3, 4 and 5). A weak 95 kDa protein was detected in lane 1 (Figure 2.3). The 66 kDa product corresponds to the 67 kDa product identified by Tao *et al* (1992) who showed that the 480 amino acid protein of the rat BF-1 ran at a higher molecular weight of approximately 67 kDa on an SDS-PAGE gel, than that of the predicted molecular weight of 53 kDa.

Synchronisation of the OP27 cells with colcemid resulted in an increase of BF-1 expression, lanes 2, 3, and 4 (Figure 2.3 B); however, very little protein product was recognised by the anti-BF-1 antibodies in the non-colcemid treated cells, lane 1 (Figure 2.3). Synchronised cells treated with RA at the non-permissive temperature showed a 66 kDa protein product, lanes 3 to 5 (Figure 2.3), a shift from the 62 kDa protein product identified in the synchronised non-RA treated cells grown at 33°C (lane 2). No conclusions could be drawn with regards to the protein levels of the protein products observed in lane 5, as the amount of protein used was not equivalent to that used in lanes 1 to 4 (Figure 2.3), and no comparisons or similarities could be observed.

2.3 Discussion

2.3.1 BF1-IP$_1$ and BF-1 expression in the olfactory placode (OP) cell lines

In this study two RNA transcripts were identified for the full-length BF1-IP$_1$, the 1.6 kb and 3.2 kb transcripts (Figure 2.1 B). Identification of the two transcripts suggest that BF1-IP$_1$ is either transcribed from two different genes, undergoes post-transcriptional modification such as splicing events, or that transcription of BF1-IP$_1$ could be initiated from two different promoters. It is unknown, yet, whether both of the expressed transcripts will yield functional protein. In a study to characterise how BF-1 expression is regulated during forebrain development, Li *et al* (1996) investigated the structure and function of the BF-1 gene and the BF-1 primary transcripts. Li *et al* (1996) found that BF-1 was transcribed from two promoters, generating two classes of BF-1 transcripts. This it is not surprising that the two BF1-IP$_1$ transcripts were identified, possibly to interact with or regulate the protein expressed from the two classes of transcripts. At present, however, the full-length cDNA of BF1-IP$_1$ is unknown, and because of this, neither is the protein known. Hence the function of BF1-IP$_1$ or how it interacts with BF-1 is unknown. Therefore the isolation of the full-length cDNA of BF1-IP$_1$ would enable the identification and the characterisation of the function of BF1-IP$_1$, and thus suggest a possible role for BF1-IP$_1$ when it interacts with BF-1.

Only one RNA transcript was identified for BF-1 by northern blot analysis in this study. These results confirm those obtained by Boolay (1999) and Illing *et al* (2002) wherein the RT-PCR analysis of the OP cells lines identified only one BF-1 transcript. The size of the BF-1 transcript, obtained in this study, was estimated at 2.8 kb fragment (Figure 2.1 C), similar to the predominant 2.8 kb BF-1 cDNA clone isolated from the rat whole-brain λgt11 cDNA library (Tao *et al.*, 1992). The BF-1 transcript identified in this study was shown to only be expressed in the OP6, OP27 and OP55 cell lines, but not in the OP47 cell line. A similar

expression pattern was observed BF1-IP_1 in this study. Thus the interaction of BF1-IP_1 with BF-1 can be confirmed as the transcripts for both BF1-IP_1 and BF-1 are expressed within the same cell lines at the same stage of development.

Western blot analysis of the OP27 whole cell lysate identified the three BF-1 immunoreactive products of 62 kDa, 66 kDa and 95 kDa. The 62 kDa protein identified in the whole cell lysates obtained from OP27 cells that were synchronised at 33°C (lane 2, Figure 2.3 B), corresponds to the approximate 62 kDa protein product observed by Yao *et al* (2001). This 62 kDa protein was observed by Yao *et al* (2001) when they used anti-TLE antibodies to co-immunoprecipitate BF-1 from E15 mouse embryo telencephalonic preparation. The approximately 66 kDa protein product identified in lanes 3, 4 and weakly in lane 5 (Figure 2.3 B), correspond to the molecular weight of 480 amino acid rat BF-1 protein that had been observed by Tao *et al* (1992) to resolve at 67 kDa, a higher molecular weight than the 53 kDa protein that had been calculated.

BF-1 protein levels were low when non-synchronised OP27 cells were grown at the permissive temperature of 33°C, where the SV40 large T antigen drives their proliferation. Upon synchronisation, the levels of BF-1 were increased dramatically (lanes 2 to 5, Figure 2.3). As the cells were now all at the same stage of the cell cycle, at the same stage of development, expression of any of the transcripts or proteins during this time would be more distinct than when the cell were operating asynchronously, that is, when some are expressing protein while others are dividing and still others are in senescence, and so forth. This was further supported by the weak 95 kDa protein product observed in lane 1 (Figure 2.3), before the cells were synchronised.

Addition of RA to the synchronised cells, however, resulted in the shift of the 62 kDa protein product to the 66 kDa protein product observed in days one, two and four (lanes 3 to 5, Figure 2.3 B). This suggests that some form of interaction exists between BF-1 and RA. However, further study would be required in order to elucidate how RA regulates the expression or function of BF-1 during neuronal development. High levels of BF-1 expression have been required to regulate the progression of neuronal progenitor cell proliferation by regulating the cell cycle (Hardcastle *et al.*, 2000). The 62 kDa immunoreactive product observed in the synchronised cells at 33°C (lane 2, Figure 2.3 B) suggests that BF-1 may have been cleaved or that the larger molecular weight of 66 kDa is the result of another form of post-translational modification of the protein during growth of the cells in the presence of RA at 33°C.

The post-translational modification of proteins has been shown to be important in the regulation of protein function and protein degradation (Alberts *et al.*, 1994; Lodish *et al.*, 2000). Many transcription factors require activation before they are able to recognise and bind to their specific response elements (Albert *et al.*, 1994). Activation of these transcription factors may result from the phosphorylation, dephosphorylation, disassociation from inhibitory subunit or the dimerisation of the transcription factors (Alberts *et al.*, 1994; Lodish *et al.*, 2000). For example, the nuclear localisation of transcription factors can be controlled by the phosphorylation or dephosphorylation of these regulatory proteins. Here phosphorylation inactivates the nuclear localisation signal (Alberts *et al.*, 1994), preventing translocation of these transcription factors into the nucleus. Hence the transcription of the target sequence does not occur.

The detection of the 95 kDa protein that is recognised by the anti-BF-1 antibodies migrates substantially slower than the 66 kDa protein product (lanes 2 to 5; Figure 2.3 B), or

the 67 kDa protein observed by Tao *et al.*, 1992, suggesting that BF-1 may be extensively modified by post-translational mechanisms. Rodriguez *et al* (2001) showed that BF-1 bound to the phosphorylated Smad3 protein resulting in the translocation of this complex into the nucleus, whilst binding to the non-phosphorylated Smad3 resulted in the repression of the transcription of the TGF-β gene targets. Thus it is possible that BF-1 may undergo a similar modification in order to bind to its response element to bring about the regulation of neuronal growth and development.

Similarly, the 62 kDa protein product was identified (lane 2, Figure 2.3 B) suggesting that BF-1 may be cleaved to enable it to interact with membrane proteins, or to be activated to be functional protein within the cell. Interaction of transcription factors or gene regulatory proteins with the cell membrane results in the prevention of the protein from entering the nucleus to carry out its function there (Alberts *et al.*, 1994), and thus it is hypothesised that BF-1 could be localised outside of the cell during this time. However, further experiments would need to be carried out to assess the presence and the level of post-translational control of BF-1 as a means of regulating BF-1 function and nuclear translocation.

Lanes 3, 4 and 5 (Figure 2.3) contained whole cell lysates of the OP27 cells at one, two and four days after induction to differentiation. A slight increase of the 66 kDa product is observed two days after addition of RA. It would be interesting to find out whether these observations are reproducible, since this experiment was only performed once. This might well indicate or propose an interaction of RA with BF-1, not only for RA to generate a post-mitotic, non-BF-1 producing neuronal progenitor cell population, but also the up regulation of BF-1 to stabilise the proliferative neuronal progenitor cell population as a subset of these cell are being lost to differentiation and maturation in the presence of RA. It is also unknown, however, at this stage how the levels of expression compare as differentiation proceeds, as the

amount of protein loaded into lane 5 is almost four times lower in this lane as compared to lanes 1, 2, 3 and 4 (Figure 2.3 A). Thus no comparative conclusions could be deduced here.

This study provides further evidence of the usefulness of an *in vitro* model system of conditionally immortalised cell lines for *in vivo* study of neuronal development. This study has also alluded to the control of BF-1 at the protein level during these processes. However, further study is needed to conclude the preliminary results obtained thus far. Also the identification of the full-length BF1-IP_1 protein and the further investigation of the possible modifications that BF-1 undergoes remain to be carried out. These investigations could provide further evidence of how BF-1 is regulated during neuronal progenitor cell proliferation and upon induction of the cells to differentiate in the olfactory neuroepithelium.

3 Introduction

Several methods have been used to identify protein-protein interactions and protein function that occurs in cells. These include yeast two-hybrid screens and co-immunoprecipitation of cell extracts. The yeast two-hybrid assay allowed for the identification of proteins involved in these protein-protein interactions by expressing the bait protein and the library of candidate interaction proteins as fusions to the DNA-binding domain and the activation domain of yeast expression vectors, respectively. The validation of the interaction of the bait protein with a putative interacting protein was measured by of the amount of β-galactoside units observed here relative to the amount of β-galactoside units observed for the control assay.

The yeast two-hybrid system was employed in a previous study to identify proteins that interact with BF-1 (Schwegmann, 2000). A library of cDNA's from the OP6 cell-line cloned upstream of the GAL4 activation domain was co-transformed with rat BF-1 (amino acids 26 to 480) fused in frame to the GAL4 DNA binding domain. Four putative interacting proteins were identified, and upon characterisation, three of these were found to be homologous to extra-cellular matrix proteins (Schwegmann, 2000). An attempt to further characterise the function and interactions of the fourth BF-1 interacting protein, BF1-IP$_1$ was undertaken in this study.

In the study carried out by Schwegmann (2000), BF1-IP$_1$ was found to be a short 318 bp C-terminal cDNA fragment for which no function or homologous protein or DNA could be identified. Hence this study aimed to investigate and verify the protein-protein interactions between BF-1 and BF1-IP$_1$.This would be carried out to by identifying the domains of BF-1 that were important for the protein-protein interactions between BF-1 and BF1-IP$_1$. The results

3.1 Materials and Methods

3.1.1 Construction of the domain-deleted plasmids

The AS1.5 construct contained the open reading frame, nucleotides 515 to 2238 or amino acid residues 26 to 480, of rat BF-1 cDNA (Tao *et al.*, 1992) cloned in frame to the Gal4 DNA binding domain of the yeast two-hybrid vector, pGBT9 (Schwegmann, 2000). To delete all three BF-1 domains, 10 μg of AS1.5 was double digested with five units of each of the restriction enzymes *BstE II* and *BamH I*, incubated overnight at 37°C. An ethanol precipitation (Maniatis *et al.*, 1983) was performed between the *BstE II* and the *BamH I* digest, as the buffer requirements for the two enzymes were different. The digested plasmid was resolved on a 1% low-melting point agarose gel (SeaPlague, FMC) with 0.1 mg/ml ethidium bromide in 1× tris acetate (40 mM Tris acetate and 2 mM $Na_2EDTA.H_20$) electrophoresis (TAE) buffer. The fragment of interest was purified from the gel slice using the GENECLEAN kit (BIO101). Briefly, the gel slice was dissolved in 2.5× the volume of the weight of the gel slice of 3 M sodium iodide (NaI) solution at 45°C for five minutes. Once dissolved, 10 μl of resuspended glassmilk was added and the sample was vortexed for five seconds to mix. The sample was incubated on ice for five minutes and then centrifuged in a benchtop microfuge at top speed (approximately 13000 rpm) for ten counts. The supernatant was carefully removed and pellet was resuspended in 700 μl of NEW WASH (NaCl, EDTA, Tris-HCl pH 7, and ethanol) solution by pipetting up and down. The sample was pelleted in the microfuge for ten counts at full speed and the supernatant was discarded. The wash was repeated twice more, and the pellet was vacuum-dried at approximately 13000 rpm for five minutes at room temperature. The dried pellet was resuspended in 10 μl of sterile water and incubated at 45°C for three minutes. The DNA was eluted by centrifuging the sample in the benchtop microfuge at top speed for ten counts, transferring the supernatant to a clean tube. Another 10 μl of sterile water

was added to the pellet and the sample incubated and centrifuged as above. The resultant supernatant was pooled with the previous one.

The DNA fragment was filled-in, to generate blunt ends, using 18 µl of the gel purified DNA elute, 500 µM dNTP mix and 2.5 units of Klenow DNA polymerase (Amersham) in a 50 µl reaction. The sample was incubated at 30°C for thirty minutes and then at 75°C for ten minutes to inactivate the polymerase. The sample was resolved on a 1% low-melting point agarose gel (NuSieve, FMG) in 1× TAE buffer, and the DNA purified from the gel slice using the GENECLEAN kit (BIO101) as instructed. The blunted ends were ligated together using two units of T4 DNA ligase (Amersham) in a 20 µl reaction, at 16°C for sixteen hours. The entire 20 µl ligation reaction was transformed into 200 µl XL-1 Blue competent cells using the heat-shock method (Maniatis *et al.*, 1983) at 42°C for thirty seconds. The transformed cells were incubated at 37°C in 800 µl of SOC (Ausubel *et al.*, 1982) transformation buffer. For each of the dilutions, 10^0, 10^{-1} and 10^{-2}, 100 µl of each of the transformed cells were plated out onto Luria-Broth plates containing 100 µg/ml ampicillin (LB-Amp plates), and the plates were incubated overnight at 37°C. Transformants were screened using *Hind III* under standard conditions.

3.1.2 Sequencing of the deletion constructs

Putative positive transformants were sequenced manually using the dideoxy chain termination method of Sanger *et al* (1977), to confirm that there was no sequence rearrangement. Plasmid DNA was obtained from the putative positive transformants using the manual mini-preparation protocol (Maniatis *et al.*, 1983), and prepared for sequencing as described in the T7 Sequenase™ version 2 DNA Sequencing Kit (Amersham) manual. Briefly, 0.5 pmol plasmid DNA with 5 pmol of the AS1.5 3' sequencing primer (Table 1) was

denatured in 1 µl of 2 M NaOH/2 mM EDTA solution in a 20 µl total volume, for fifteen minutes at 37°C. The DNA was precipitated with the addition of 3 µl of 3 M sodium acetate and 75 µl of ice-cold absolute ethanol and then place at –20°C for thirty minutes. The sample was centrifuged at 13000 rpm for thirty minutes at 4°C, the supernatant aspirated off and the pellet washed in 70% ice-cold ethanol, at 13000 rpm for ten minutes. The DNA and primer pellet was dried under vacuum for five to ten minutes, and then resuspended in 8 µl of sterile water. To the mixture, 2 µl of Sequenase buffer was added and the reaction was incubated at room temperature for ten minutes. The DNA was labelled with ^{35}S-dATP in the Sequenase 1× dGTP labelling reaction mix for exactly five minutes at room temperature. The labelling reaction was terminated with the dideoxy nucleotide termination cocktail for exactly five minutes, after which the dideoxy reaction was terminated with the addition of the formamide stop mix and incubated at 95°C for five minutes. The sequencing reactions were run on a pre-run 6% urea-polyacrylamide DNA gel for one and a half hours. The gel was incubated in a 5% methanol, 5% acetic acid fixing solution for twenty minutes and dried at 80°C for one hour. The dried gel was exposed to Konica X-ray film for one to three days in an X-ray cassette at room temperature. The autoradiograph was developed and fixed in X-ray developer and fixer, as per manufacturer's instructions. The sequences were read and analysed by alignment with their corresponding theoretical sequences. Plasmid DNA from which confirmed correct sequences were obtained, were used in further analyses.

3.1.3 PCR-mediated site-directed mutagenesis

PCR-mediated site-directed mutagenesis was carried out on the deletion construct as illustrated in the flow diagram below:

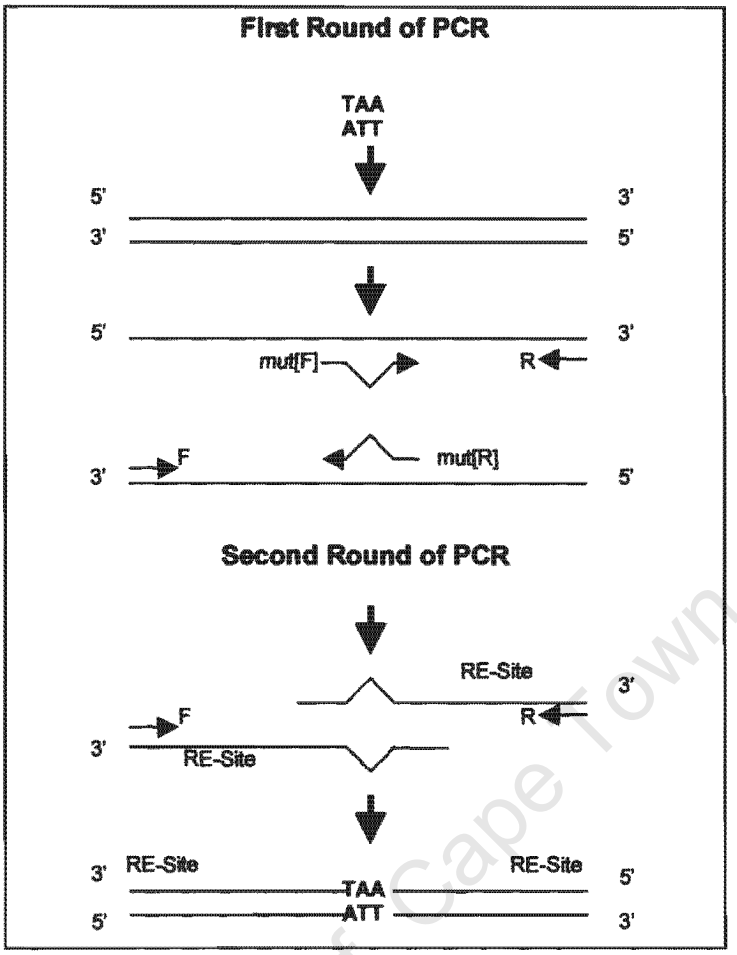

Figure 3.1: A flow diagram to summarise the design and application of the PCR-mediated site-directed mutagenesis of the AS1.5 $\Delta_{HPQ, DBD, TRD}$ and the AS1.5 $\Delta_{DBD, TRD}$ deletion constructs to introduce the stop codon into the double stranded deletion constructs. The stop codon would be inserted immediately after the 3' end of the BF-1 insert, at the site of ligation of the deletion construct. Two rounds of PCR would be required to do this, the first an asymmetric PCR to introduce the stop codon into each strand of the construct, and the second PCR to generate a full-length mutagenesis construct. Restriction enzyme digests, to subclone the mutagenesis fragment back into the AS1.5$\Delta_{BsrG\ I\text{-}NgoM\ IV}$ vector, using these 2 enzyme sites for directional cloning, would then follow the PCR reactions.

PCR-mediated site-directed mutagenesis is a method used to introduce sequence-specific changes into a DNA sequence. Using Figure 3.1 as a guide, primers are designed to introduce a site-specific change in the DNA sequence. PCR-mediated site-directed mutagenesis is carried out in two rounds of amplification. The first round of amplification is used to introduce the mutagenised sequence into the DNA sequence by asymmetric amplification. The second round of amplification is used to join the asymmetric fragments generated in the first round of amplification to give rise to the full-length mutagenised DNA sequence. The first round of PCR is generally carried out at lowered annealing temperature in duplicate, where one

duplicate contains the normal and mutagenesis primer pair for the first half of the DNA sequence, and the other duplicate reaction consists of the normal and mutagenesis primer pair for the second half of the DNA sequence. Each of these PCR reactions generated asymmetric PCR products of the template sequence. In the second round, the two sets of asymmetric products are mixed together into one reaction and the PCR is carried out to join the two products together, using the normal primers only, to generate a full length DNA sequence consisting of the mutagenesis sequence. The mutagenesis primers herein refer to the primers designed to incorporate the mutagenesis sequence, for example Bst-mut[F], while normal primers refer to the primers designed to recognise the DNA sequence wherein no changes to the DNA sequence have been made, for example Bst-F.

Mutagenesis primers were designed to incorporate the stop codon TAA into the sense strand (and ATT into the complement strand) of the deletion construct, at the site of ligation. In the one reaction, the forward primer (F) was used with the mutagenesis reverse primer (mut[R]), and in the other reaction, the reverse primer (R) was used with the mutagenesis forward primer (mut [F]). The PCR reaction mix was performed using 10 pg of template DNA (the AS1.5 $\Delta_{HPQ, DBD, TRD}$ or the AS1.5 $\Delta_{DBD, TRD}$ deletion construct), 0.4 µM of each primer, 0.2 mM dNTP mix, 2 mM $MgCl_2$, 1× *Taq* DNA polymerase buffer, and 2.5 units of *Taq* DNA polymerase (Promega) per 50 µl reaction. The PCR cycling parameters were comprised of an initial denaturation of 94°C for 5 minutes, 94°C for 30 seconds, 61°C for 1 minute and 72°C for 1 minute, for 30 cycles, with a final extension at 72°C for 7 minutes.

The asymmetric PCR products from the first round were resolved on a 1% low melting point agarose gel in 1× TAE buffer. The DNA fragments were purified from the gel slice using the GENECLEAN kit (BIO101), as described previously. The purified fragments were added

together to the PCR mix, as the template, along with the F and R primers, to carry out the second round of amplification. The PCR reaction and cycling parameters used were as described above, except that 1 µl of each of the eluted DNA fragments was used in the reaction. The resultant PCR products were purified from a 1% low melting point agarose gel in 1× TAE buffer using the GENECLEAN kit (BIO101), as described above.

3.1.4 Screening and sequencing of the mutagenised fragment

Ligation of the full-length AS1.5 $\Delta_{DBD, TRD, TRD}$ mutagenesis construct to pGEM-T Easy vector (Promega) was performed using 3 µl of the gel-purified DNA, 1 µl of pGEM-T Easy vector, 1 µl of 1 unit/µl T4 DNA ligase and 1× ligation buffer, in a 10 µl reaction. The samples were incubated at 16°C for sixteen hours. The entire ligation reaction was transformed into 200 µl of XL-1 Blue competent cells using the heat-shock method (Maniatis *et al.*, 1983), and incubated at 37°C in 800 µl SOC transformation buffer for one hour. 100 µl of the transformations were plated onto LB-Amp plates and incubated overnight at 37°C.

Transformants were screened in a double digest to isolate the approximately 450 bp mutagenesis fragment from the pGEM-T Easy vector (Promega) using the restriction enzymes *BsrG I* and *NgoM IV* under standard conditions. Putative positive transformants were sequenced in the MegaBACE automated sequencer by the dideoxy chain termination method (Sanger *et al.*, 1977). The DNA sequences were then analysed using DNAMAN software to verify the incorporation of the stop codon and to confirm that no sequence rearrangements had been introduced during the amplification and cloning procedures.

3.1.5 Subcloning of the Full-Length AS1.5 $\Delta_{HPQ, DBD, TRD}$ Mutagenesis Fragment

Using 10 µg of the full-length AS1.5 $\Delta_{HPQ, DBD, TRD}$ mutagenesis fragment in pGEM-T, a 100 µl digest reaction was carried out with 2 µl of *EcoR I* at 37°C overnight. The digest was resolved on a 1% low-melting point agarose gel (SeaPlague; FMC) in 1× TAE buffer. The 0.85 kb insert fragment was excised from the gel, and the DNA purified from the gel slice using the GENECLEAN kit (BIO101) method, following the manufacturer's instructions. The gel-purified fragment was then digested with *BsrG I* and *NgoM IV*, with an ethanol precipitation step carried out between the two digests, as the buffer requirements of the two enzymes were different. The digest was electrophoresed on a 1% low-melting point agarose gel in 1× TAE buffer. The approximate 450 bp fragment was excised from the gel, and the gel slice used for in-gel ligation.

To subclone the AS1.5$\Delta_{HPQ, DBD, TRD}$ full-length mutagenesis fragment back into the yeast two-hybrid vector, AS1.5, 10 µg of the AS1.5 plasmid DNA was also digested with *BsrG I* and *NgoM IV* restriction enzymes in 100 µl reactions at 37°C overnight. An ethanol precipitation (Maniatis *et al.*, 1983) was carried out as the two restriction enzymes had different buffer requirements. The digested plasmid was electrophoresed on a 1% low-melting point agarose gel in 1× TAE buffer, and the 5.1 kb fragment was excised from the gel. The DNA was purified from the gel slice using the GENECLEAN kit (BIO101) method as described previously.

In-gel ligation reactions were carried out using the pGEM-T Easy ligation method (Promega), DNA ligase and reaction buffer. The gel slice containing the full-length AS1.5 $\Delta_{HPQ, DBD, TRD}$ mutagenesis fragment was heated at 70°C for ten minutes and then incubated at 37°C briefly to set up the ligation reaction mix. Using the molten gel-DNA mixture, 3 µl of

this was added to 1 µl of the purified *BsrG I-NgoM IV*-digested AS1.5 fragment, along with 1 µl of the 1 unit/µl T4 DNA ligase and 1× reaction buffer in a 10 µl reaction. The samples were incubated at 15°C for two days. Only 5 µl of the ligation reaction was transformed into 100 µl of XL-1 Blue competent cells, using the heat-shock method (Maniatis *et al.*, 1983) at 42°C for thirsty seconds. The transformations were incubated in 1 ml Luria Broth (LB) medium at 37°C for one hour, and 100 µl and 900 µl of the transformations were plated out on LB-Amp plates and incubated overnight at 37°C.

Double digests using *Xho I* and *Pst I* restriction enzymes under normal conditions were used to screen the forty of the eighty-six transformants. As the expected 0.3 kb fragment was not visible on the 1% agarose gel when the digested samples were resolved by electrophoresis, the transformants were further screened by PCR amplification using the Bst-F and Bst-R primers. For a 50 µl reaction, 2 µl of the sample DNA was used, as detailed in section 3.2.1 above, under the same cycling parameters. The 10 µl of the PCR reactions were resolved on a 1% agarose gel in 1× TAE buffer to visualise the PCR products. As no PCR product was visualised on the gel, the remaining forty-six transformants were screened by a *Hind III* digest. The digests were resolved on a 1% agarose gel in 1× TAE buffer.

3.2 Results

3.2.1 Deletion of BF-1 domains

The open reading frame of rat BF-1 (Tao *et al.*, 1992), nucleotides 515 to 2238, has previously been inserted into the yeast two-hybrid vector pGBT9 at the *EcoR I* site, in frame at its N-terminal end with the open reading frame of the GAL4 DNA binding domain (Schwegmann, 2000). For ease of identification, this construct will hereafter be referred to as AS1.5 (Figure 3.2 A) in this study. In this study we wanted to generate deletion constructs of AS1.5, wherein the three BF-1 domains, namely the transcriptional repressor domain (TRD), the DNA-binding domain (DBD) and the histidine, proline and glutamine (H, P, Q)-rich region, would be sequentially deleted. As the N-terminal end of BF-1 had already been cloned in frame with the open reading frame of the pGBT9 (CLONTECH) GAL4 DNA-binding domain (Schwegmann, 2000), the deletion constructs were generated from the C-terminal end of BF-1, to preserve the correct frame of the construct. The stop codon was introduced by PCR mutagenesis.

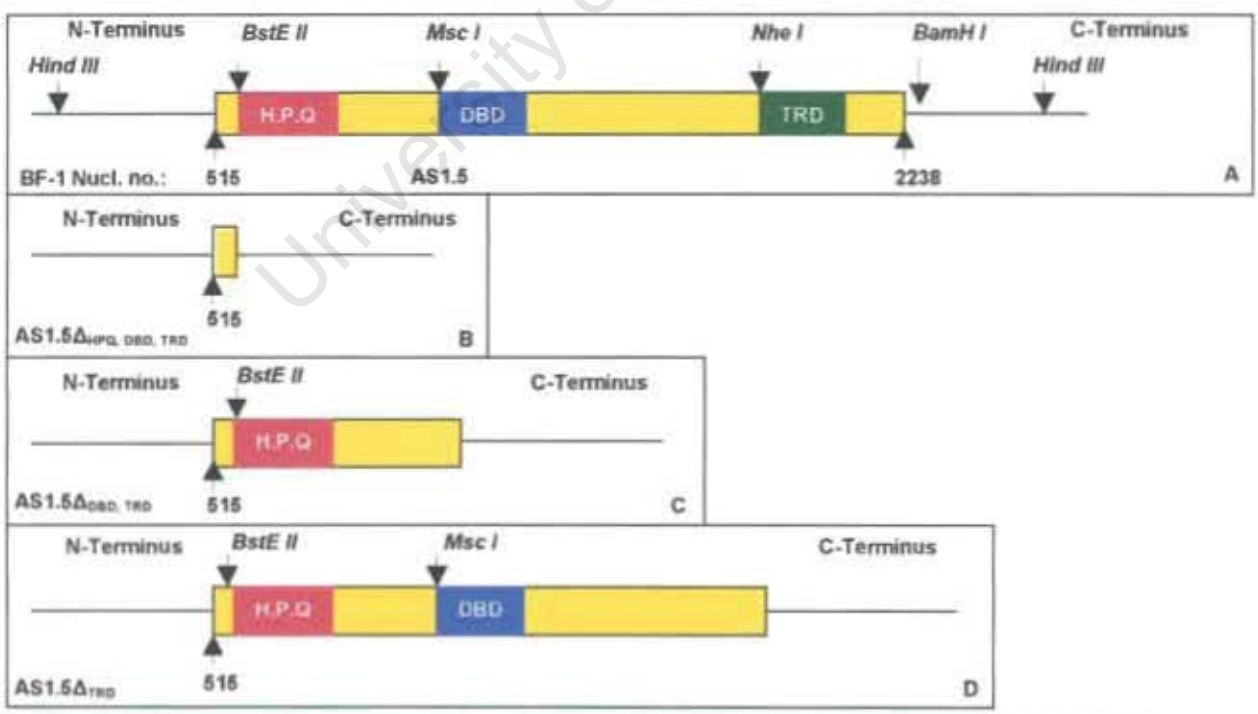

Figure 3.2: Diagrammatic representation of the rat BF-1 open reading frame cloned into pGBT9 (A). The location of the restriction enzyme sites: *BstE II, Msc I* and *Nhe I* with *BamH I*, used to delete the all three domains, generating: AS1.5$\Delta_{H,P,Q, DBD, TRD}$ (B), the DBD and the TRD domains, generating AS1.5$\Delta_{DBD, TRD}$ (C), and TRD domain, generating AS1.5Δ_{TRD} (D), respectively, are indicated. H, P, Q: Histidine, Proline, Glutamine rich region; DBD: DNA-binding domain; TRD: transcriptional repressor domain; —— denotes pGBT9 vector sequence

Figure 3.2 is a diagrammatic representation of the rat BF-1 open reading frame and the planned deletion constructs. The restriction enzymes *BstE II*, *Msc I* and *Nhe I*, were identified for use in the double digests, with *BamH I*. The *BamH I* restriction site of AS1.5 was located close to the C-terminal end of the rat BF-1 cloned into the pGBT9 (CLONTECH) multiple cloning site. Double digests performed using of each of the three BF-1 restriction enzymes, namely *BstE II*, *Msc I* and *Nhe I* with *BamH I*, would each result in the successive removal of the following domains:

- *BstE II-BamH I* to delete all three domains: histidine, proline and glutamine-rich region (H, P, Q), the DNA binding domain (DBD) and the transcriptional repressor domain (TRD), to generate AS1.5 $\Delta_{HPQ, DBD, TRD}$
- *Msc I-BamH I* to remove the DNA binding domain (DBD) and the transcriptional repressor domain (TRD), to generate AS1.5 $\Delta_{DBD, TRD}$
- *Nhe I-BamH I* to remove the transcriptional repressor domain only, to generate AS1.5Δ_{TRD}

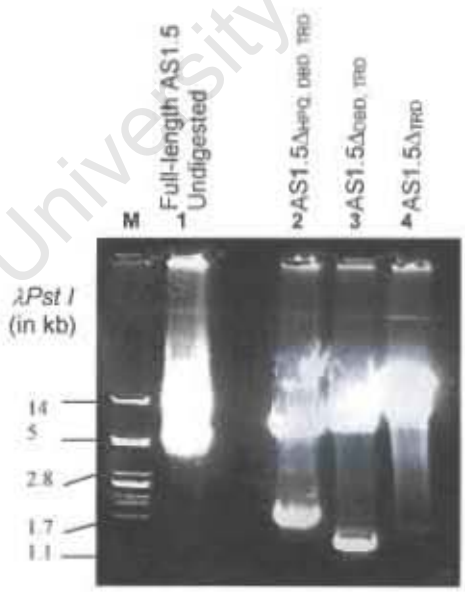

Figure 3.3: Restriction enzyme digests for the preparation of the deletion constructs of BF-1: AS1.5$\Delta_{HPQ, DBD, TRD}$ (lane 2), AS1.5$\Delta_{DBD, TRD}$ (lane 3), and AS1.5Δ_{TRD} (lane 4), and undigested AS1.5 (lane 1). The digests were electrophoresed on a 1% LMP agarose gel. Molecular weight marker (M) was λ*Pst I* (lambda *Pst I*), with the sizes shown in kilo base pairs (kb) as indicated. LMP = low melting point; H, P, Q = histidine, proline, glutamine; DBD = DNA binding domain; TRD = transcriptional repressor domain.

Figure 3.3 shows the complete digestion of AS1.5 with *BstE II-BamH I*, to generate two fragments of 1.68 kb ($\Delta_{HPQ, DBD \text{ and } TRD}$) and 5.56 kb, and *Msc I-BamH I*, to generate two fragments of 1.24 kb ($\Delta_{HPQ \text{ and } DBD}$) and 6.0 kb. The *Nhe I-BamH I* double digest was incomplete, with only a linearised fragment at 7.2 kb. The 5.6 kb AS1.5 $\Delta_{HPQ, DBD, TRD}$ fragment, the 6 kb AS1.5 $\Delta_{DBD, TRD}$ fragment from the digest, and the 7.2 kb AS1.5 control, were purified from the deleted domains by gel electrophoresis. The resolved fragments were excised from the gel, purified, filled in, re-circularised and transformed.

Transformants were screened using a *Hind III* digest (Figure 3.2 (A) for the location of *Hind III*). Figure 3.4 shows confirmation of the AS1.5 deletion constructs made. All three AS1.5$\Delta_{HPQ, DBD, TRD}$ construct transformants (lanes 7, 9 and 11), and five of the seven AS1.5$\Delta_{DBD, TRD}$ construct transformants screened (lanes 13, 15, 21, 23, and 25), resulted in the expected digest products. The expected digest products were 0.8 kb and 4.3 kb for the AS1.5$\Delta_{HPQ, DBD, TRD}$ construct, lanes 7, 9 and 11 (Figure 3.4), and 1.6 kb and 4.3 kb for the AS1.5$\Delta_{DBD, TRD}$ construct, in lanes 13, 15, 21, 23 and 25 (Figure 3.4).

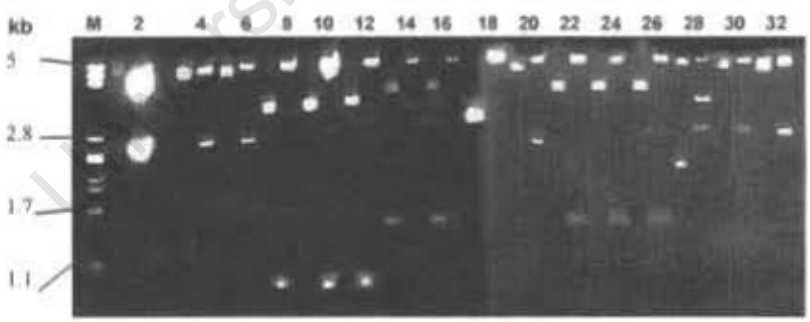

Figure 3.4: *Hind III* restriction enzyme digests to screen putative positive transformants. Undigested and digested plasmid of each transformant screened, were analysed on a 1% agarose gel, along with the undigested and digested AS1.5 as the control in lanes 1 and 2. Lanes 3 to 6 represent the re-transformed undigested AS1.5 sample from Figure 3.2 (lane 1), which was digested with *Hind III*. The lane between 2 and 3 is empty and has not been assigned a number. The samples in lanes 7 to 27 were loaded in the order digested-undigested for each transformant screened. Only the even-numbered lanes have been marked for clarity in labelling. λ*Pst I* was used as the molecular weight marker (M), and the molecular weights are indicated in kilo base pairs (kb) as shown.

As the digest to generate the AS1.5Δ_{TRD} construct had not been successful, no further manipulation of this construct were carried out.

One putative positive transformant from each of the AS1.5$\Delta_{HPQ, DBD, TRD}$ and AS1.5 $\Delta_{DBD, TRD}$ deletion constructs was chosen for manual sequencing, in the reverse direction by the T7 Sequenase version two DNA sequencing kit method, using the AS1.5 3' sequencing primer (Table 1). The plasmids were sequenced in the reverse direction only, as only the sequence across the ligation site was required to confirm that no rearrangements had occurred during the cloning procedure.

Generation of the AS1.5$\Delta_{HPQ, DBD, TRD}$ and AS1.5$\Delta_{HPQ, DBD}$ deletion constructs would result in the deletion of the BF-1 stop codon. Thus, to ensure that only the truncated BF-1 would be expressed when the constructs were re-introduced into the yeast two-hybrid assay, and not a nonsense protein, a stop codon would be introduced at or near the ligation site of the deletion constructs generated. PCR-mediated site-directed mutagenesis was used for this purpose, Figure 3.1 (Materials and Methods). Thus the sequence directly flanking the site of ligation was verified, as this site was required for the design of the mutagenesis primers.

The sequences were aligned in DNAMAN (Lynnon BioSoftware, version 4.13) and compared to their respective theoretical sequences, generated in DNAMAN, to check sequence rearrangements. As the ligation sites of the sequenced deletion constructs were free of rearrangements, the sequenced AS1.5$\Delta_{HPQ, DBD, TRD}$ and AS1.5$\Delta_{HPQ, DBD}$ deletion constructs were selected for further manipulation.

3.2.2 PCR-mediated site-directed mutagenesis

For use of the PCR-mediated site-directed mutagenesis technique, the mutagenesis primers, mut[F] and mut[R], Figure 3.1, were designed to have between 9 and 15 nucleotides on either side of the mutagenic sequence or base. This was to stabilise the primer and to ensure

specificity of annealing of the primers to the template during amplification. The stop codon was designed to be in the middle of the mutagenesis primers to minimise mis-priming at the 3' end and non-specific sequence recognition at the 5' end. It was essential too that the mutagenesis primers are the exact reverse and complement of each other (Figure 3.7). Mutagenesis primers designed at slightly different loci would not result in the amplification of the correct full-length mutagenesis fragment, as there would not be enough sequence recognition between the two asymmetric PCR products to prime extension across its asymmetric partner.

The forward and the reverse primers were chosen to give rise to at least a 250 bp fragment upstream or downstream of the introduced stop codon, when amplification was conducted using the respective mutagenesis primers (Figure 3.7). This would enable the precise recovery of the mutagenesis PCR products from the agarose gel, devoid of and unobstructed by primer-dimer products that range at 50 to 100 bp in length.

Figure 3.5 shows the amplification of the AS1.5$\Delta_{HPQ, DBD, TRD}$ deletion construct using the mutagenesis primers in the asymmetric PCR reaction. In lane 1 (Figure 3.5) the Bst-forward (Bst-F) with the Bst-mutagenesis reverse (Bst-mut[R]) primers were used. In lane 2 (Figure 3.5), the Bst-reverse (Bst-R) with the Bst-mutagenesis forward (Bst-mut[F]) primers were used. These gave rise to the 300 bp fragment upstream of the introduced stop codon and the 250 bp fragment downstream of the stop codon respectively. The samples in lanes 1 and 2 (Figure 3.5) were excised from the gel and used as template for the second round of PCR.

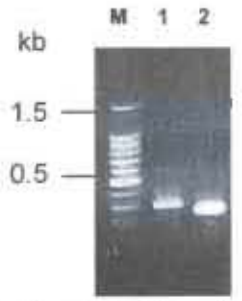

Figure 3.5: PCR-mediated site-directed mutagenesis was performed to introduce a stop codon into the AS1.5$\Delta_{HPQ, DBD, TRD}$ deletion construct. The first round of PCR was performed using the Bst-F with the Bst-mut[R] primers (lane 1), and Bst-mut[F] with the Bst-R primers (lane 2), to generate the 300 and 250 bp products respectively. Samples were electrophoresed on a 1.2% LMP agarose gel, and the gel purified samples in lanes 1and 2 were placed into 1 tube and used as the template for the second round of PCR. The 100 bp ladder (Promega) was used as the molecular weight marker (M) with the fragment sizes indicated in kilo base pairs (kb).

The gel-purified products were used in the second round of PCR, as templates for the amplification of the full-length AS1.5$\Delta_{HPQ, DBD, TRD}$ mutagenesis sequence to generate the 550 bp fragment.

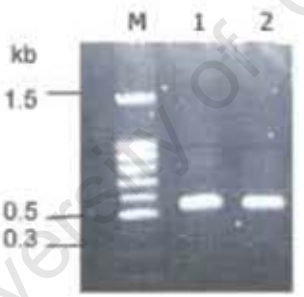

Figure 3.6: The full-length 550 bp product was generated from the amplification of the 250 bp and 300 bp mutagenesis fragments as templates, using Bst-F and Bst-R primers only. Combining the two mutagenesis fragments as the template of the reaction generated the samples in lanes 1 and 2. A 100 bp ladder (Promega) was used as the molecular weight marker (M), with the fragment sizes indicated in kilo base pairs (kb) as illustrated.

The full-length mutagenesis sequence was cloned into the pGEM-T Easy (Promega) vector. Putative positive transformants of the full-length AS1.5$\Delta_{HPQ, DBD, TRD}$ mutagenesis fragment, in pGEM-T Easy were sequenced on an automated sequencer (ABI MegaBACE Sequencer; Amersham Biosciences) using the T7 and the T3 primers. Figure 3.7 shows the alignment of the forward and reverse sequences of the pGEM-T Easy AS1.5$\Delta_{HPQ, DBD, TRD}$ full-

length mutagenesis sequence with a theoretical sequence generated in DNAMAN. This alignment was used to confirm the introduction of the stop codon into the AS1.5$\Delta_{HPQ, DBD, TRD}$ deletion construct.

The introduced stop codon, resulting from the base substitutions of cytosine (C) to thymidine (T) and thymidine (T) to adenine (A) have been highlighted in white on the alignment (Figure 3.7). There were a few minor nucleotide changes introduced, but as they occurred downstream of the introduced stop codon, this full-length AS1.5$\Delta_{HPQ, DBD, TRD}$ mutagenesis fragment was used in further manipulations.

During the design of the mutagenesis primers the *NgoM IV* restriction site was incorporated towards the 3' end of the Bst-R primer, whilst the *BsrG I* restriction site was located at least fifty base pairs downstream of the Bst-F primer (the two restriction sites are highlighted in yellow in Figure 3.7). These sites would be used for the directional sub-cloning of the full-length AS1.5$\Delta_{HPQ, DBD, TRD}$ mutagenesis fragment back into the AS1.5 vector backbone.

Figure 3.7: The T7- and SP6-sequenced full-length AS1.5$\Delta_{HPQ, DBD, TRD}$ mutagenesis products cloned into the pGEM-T Easy (Promega) vector were aligned with the theoretical sequence generated in DNAMAN. The T7 and SP6 primers have been shown in green. The mutagenesis forward (mut[F]) and reverse primers (mut-[R]) have been indicated in purple. The introduced stop codon has been highlighted in white. The Bst-mut[F] and Bst-mut[R] primers (purple) were constructed for the exact same segment of sequence in the forward and reverse directions respectively. The Bst-F and Bst-R primers are shown in red. The *BsrG I* and *NgoM IV* restriction enzyme sites are highlighted in yellow, to show their location with respect to the Bst-F and Bst-R primers. As a second *NgoM IV* site is located in the pGEM-T vector sequence, the full-length mutagenesis fragment would have to be excised with *EcoR I* first, before digesting with *BsrG I* and *NgoM IV*, to eliminate double digestion when the *NgoM IV* enzyme is used. pGEMT+BF-1 refers the theoretical full-length sequence with the AS1.5$\Delta_{HPQ, DBD, TRD}$ mutagenesis fragment inserted into pGEM-T Easy, which was generated in DNAMAN. Mut_ AS1.5$\Delta_{HPQ, DBD, TRD}$ _T7 and mut_ AS1.5$\Delta_{HPQ, DBD, TRD}$ _SP6 sequences were obtained from the MegaBACE automated sequencer. No significant substitutions or sequence rearrangements were found in the region that would be subcloned back into AS1.5 using *BsrG I* and *NgoM IV*. The full-length AS1.5$\Delta_{HPQ, DBD, TRD}$ mutagenesis sequence has been highlighted in blue.

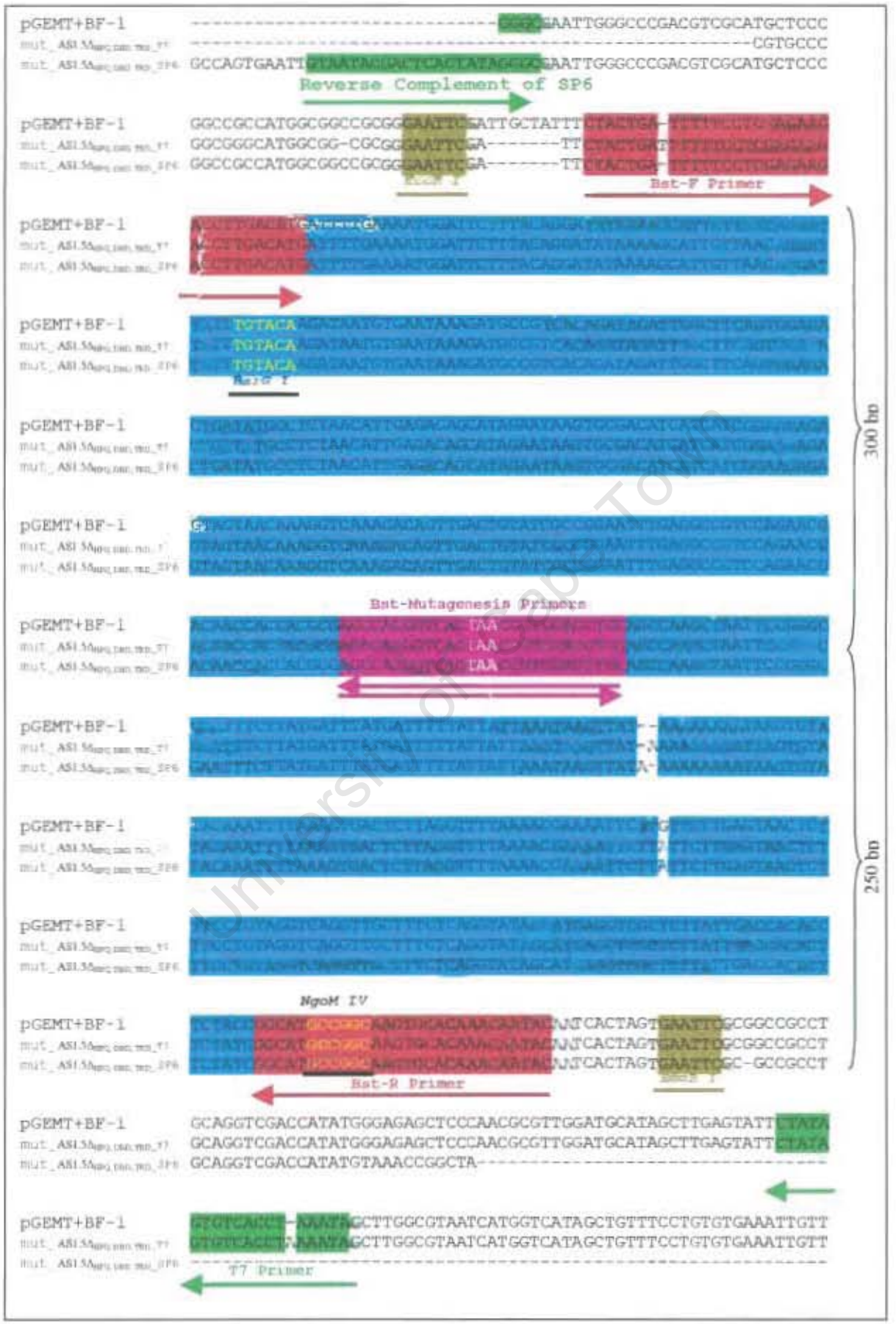

Asymmetric amplification of the AS1.5$\Delta_{HPQ, DBD}$ deletion construct was performed using the Msc-forward (Msc-F) with the Msc-mutagenesis reverse (Msc-mut[R]) primers and the Msc-reverse (Msc-R) with the Msc-mutagenesis forward (Msc-mut[F]) primers. No PCR products were visualised when the samples were electrophoresed on the 1% agarose gel in 1× TAE buffer (data not shown). Further PCR amplifications of the AS1.5$\Delta_{HPQ, DBD}$ deletion construct were attempted using different combinations of primers. However, as no PCR products were obtained, this construct was not used in further manipulations.

3.2.3 Subcloning of the AS1.5$\Delta_{HPQ, DBD, TRD}$ full-length mutagenesis sequence into AS1.5

The full-length AS1.5$\Delta_{HPQ, DBD, TRD}$ mutagenesis sequence was digested from pGEM-T Easy (Promega) vector using *EcoR I*, restriction site shown in dark yellow in Figure 3.7 (Figure 3.8). This was required to ensure that the subcloning of the full-length AS1.5$\Delta_{HPQ, DBD, TRD}$ mutagenesis fragment using *BsrG I* and *NgoM IV* would be without interference of the *NgoM IV* restriction site that was also present on the pGEM-T Easy vector. The gel purified *EcoR I* fragment was then digested with *BsrG I* and *NgoM IV*, with an ethanol precipitation step carried out between the two digests, as the buffer requirements were different for the two enzymes: *BsrG I* and *NgoM IV*.

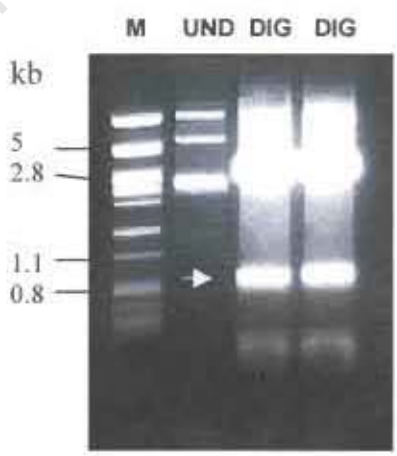

Figure 3.8: The full-length AS1.5$\Delta_{HPQ, DBD, TRD}$ mutagenesis fragment was digested from pGEM-T Easy (Promega) using *EcoR I*. The 100 µl digest was electrophoresed on a 1% LMP agarose gel in two 50 µl aliquots per lane (DIG), with 1 µl of the undigested sample used as the undigested control (UND). The 0.9 kb fragment (white arrow) was excised from the gel for purification using the GENECLEAN kit (BIO101). λPst I was used as the molecular weight marker, with the fragment sizes indicated in kilo base pairs (kb). LMP= low melting point

AS1.5 was also digested with *BsrG I* and the *NgoM IV* restriction enzymes, with an ethanol precipitation step, to generate the backbone vector into which the full-length mutagenesis construct would be ligated. This would result in a directional and in-frame cloning of the AS1.5 deletion construct. This would ensure that only the correct GAL4-BF-1 protein would be expressed in the subsequent yeast two-hybrid assay.

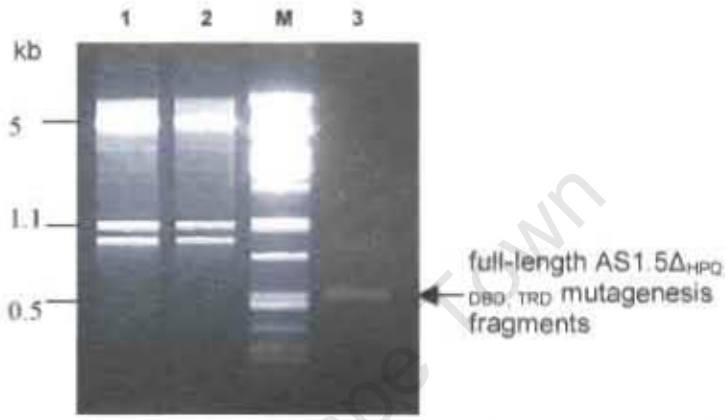

Figure 3.9: AS1.5 and the full-length AS1.5$\Delta_{HPQ, DBD, TRD}$ mutagenesis fragment, after digestion with *NgoM IV* and *BsrG I*, were electrophoresed on a 1% LMP agarose gel. The 100 µl AS1.5 digest was run in two 50 µl aliquots (lanes 1 and 2), and the 20 µl ethanol-precipitated full-length AS1.5$\Delta_{HPQ, DBD, TRD}$ mutagenesis fragment was loaded into lane 3. λPst I was used as the molecular weight marker (M), with the molecular weights indicated in kilo base pairs (kb). LMP = low melting point

The digested AS1.5 (AS1.5$\Delta_{BsrG\ I\text{-}NgoM\ IV}$ vector) was electrophoresed on a 1.2% low melting point agarose gel, Figure 3.11, and purified from the gel slice using the GENECLEAN kit (BIO101). As the efficiency of purification of DNA fragments of less than 500 bp is greatly reduced when using the GENECLEAN method (BIO101), the gel purified mutagenesis fragment, after *BsrG I-NgoM IV* digestion, was excised from the gel, and the gel slice used for in-gel ligation (as indicated by the arrow (◄—) in Figure 3.9).

3.2.4 Screening of the AS1.5$\Delta_{HPQ, DBD, TRD}$ full-length mutagenesis construct

Eighty-six colonies, in total on the plates, were picked and used to inoculate 5 ml Luria-Broth medium containing 100 µg/ml ampicillin. Using of forty of the eighty-six transformants, *Xho I-Pst I* restriction enzyme double digest was used to screen these transformants for the

insertion of the AS1.5$\Delta_{HPQ, DBD, TRD}$ full-length mutagenesis fragment subcloned into the AS1.5$\Delta_{BsrG\ I\text{-}NgoM\ IV}$ vector. These digests only resulted in a linearised DNA fragment of approximately 5.5 kb, rather than the 0.3 and 5.2 kb fragments, when the samples were electrophoresed on a 1% agarose gel (Figure 3.10).

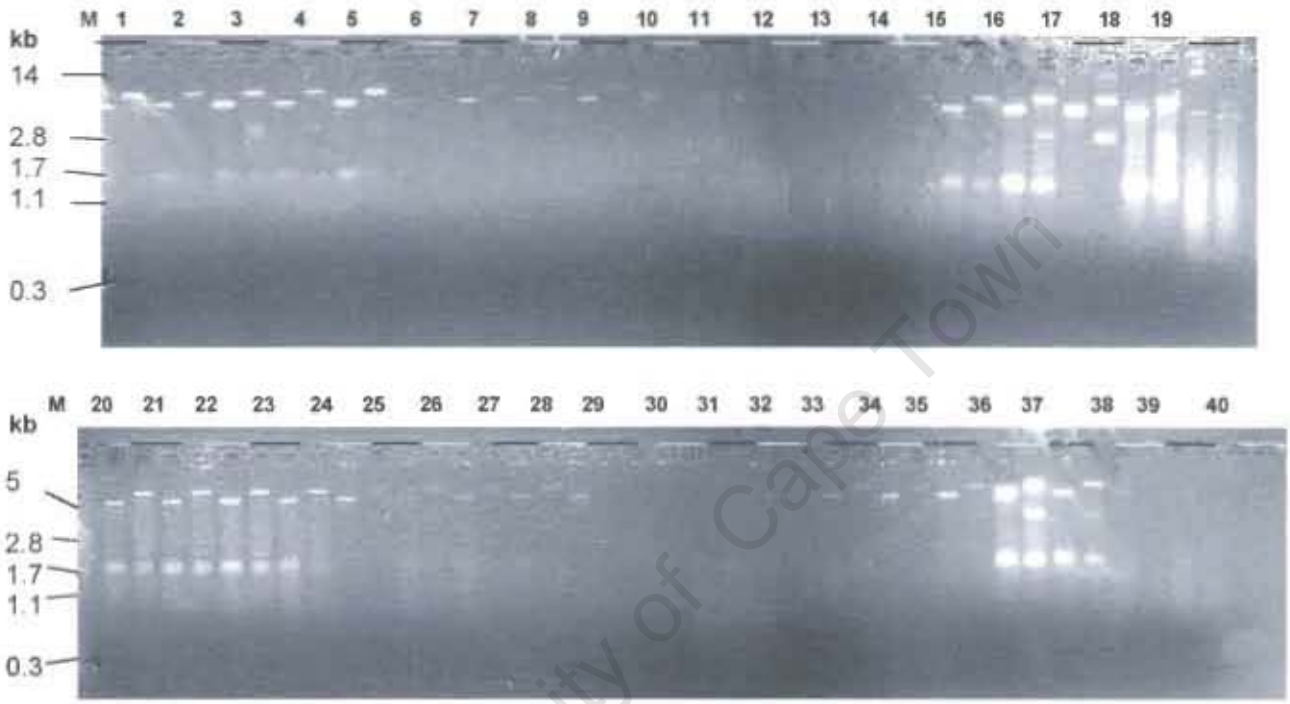

Figure 3.10: 40 of the 8 AS1.5$\Delta_{HPQ, DBD, TRD}$ mutagenesis transformants were digested with *Xho I* and *Pst I*. The expected 0.3 kb fragment was not visualised when the samples were run on a 1% agarose gel. A 1.7 kb fragment was found in both the digested and undigested samples. A white or black bar at the top of the gel represents the paired digested and undigested sample. All the samples were loaded in the digested-undigested orientation.

A 1.7 kb fragment was visualised in both the digested and undigested samples resolved on the agarose gel (Figure 3.10). As this band was common to both the digested and undigested samples, this indicated that the digested had not been successful. The absence of the expected 0.3 kb fragment on the gel suggested that either the insert may not have been ligated into the AS1.5 vector backbone, or the concentration of the DNA digested was too low for the visualisation of the fragment on the gel.

PCR amplification of the mutagenesis fragment was performed, using the Bst-F and Bst-R primers. PCR amplification of the 550 bp product, of the full-length mutagenesis fragment, would be easier to visualise than the 0.3 kb product. No product was visualised when the samples were electrophoresed on a 1% agarose gel (data not shown). As the amplification of AS1.5 with the BF R1474 and BF Fs10 primers, used as a PCR positive control, also yielded no product, the PCR parameters were likely to have been less than optimal for amplification. Hence, the PCR amplification of the AS1.5$\Delta_{HPQ, DBD, TRD}$ deletion clone (Figure 3.11) with Bst-F and Bst-R (lane 2), with Bst-F and Bst-mut[R] (lane 4), and with Bst-R and Bst-mut[F] (lane 3) primer combinations, along with AS1.5 with BF R1474 and BF Fs10 (lane 1), as the control, was performed.

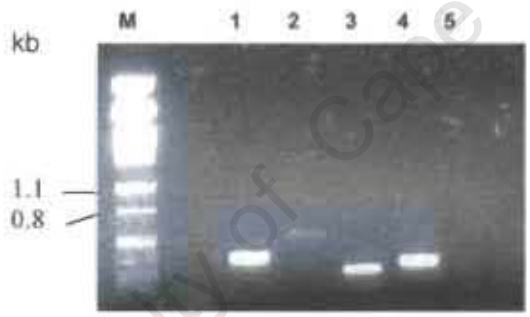

Figure 3.11: PCR amplification of the AS1.5$\Delta_{HPQ, DBD, TRD}$ deletion clone was amplified with Bst-F and Bst-R (lane 2), Bst-mut[F] and Bst-R (lane 3), and Bst-F and Bst-mut[R] (lane 4). AS1.5 was amplified with BF R1474 and BF Fs10 in lane 1. λ*Pst I* was used as the molecular weight marker (M), with the molecular weights indicated in kilo base pairs (kb).

All yielded product when the samples were visualised on the 1% agarose gel, under the same conditions and when a fresh dilution of the primer stock was used (Figure 3.11). Amplification of the AS1.5$\Delta_{HPQ, DBD, TRD}$ deletion construct with Bst-F and Bst-R (lane 2; Figure 3.11) was successful, although the amount of product produced only resulted in a faint band. PCR amplification was repeated once again, using the transformant samples with the Bst-F and Bst-R primers, and the SuperTherm (Molecular Research) DNA polymerase in place of the *Taq* DNA polymerase used previously. Only smears were visible in the transformants' sample lanes (lanes 1 to 40; Figure 3.12). The PCR controls, AS1.5 and the AS1.5$\Delta_{HPQ, DBD,}$

$_{TRD}$ deletion clone, resulted in the correct product size when the samples were electrophoresed on a 1% agarose gel, Figure 3.12.

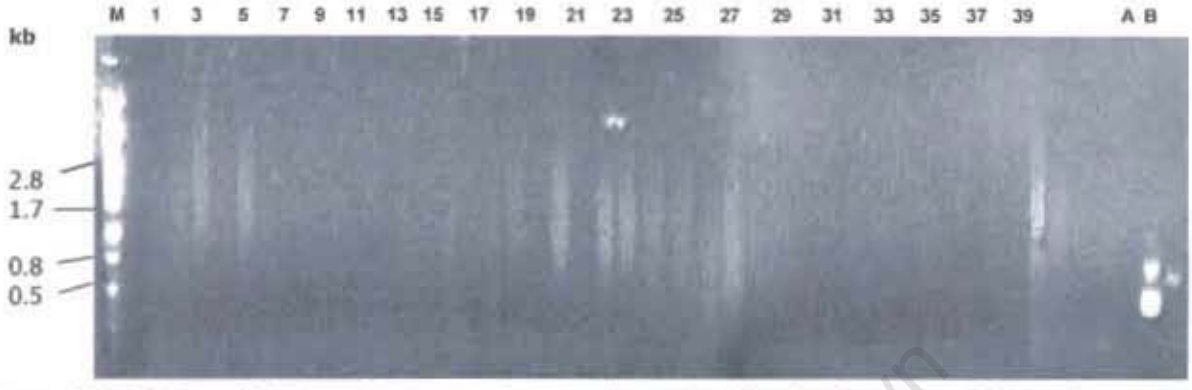

Figure 3.12: PCR amplification of the 40 transformants (lanes 1 to 40) using SuperTherm DNA polymerase and Bst-F and Bst-R primers, resulted in smeared products in many of the sample lanes. All the smears are larger than the 0.5 kb product expected from the primer and template used. The AS1.5 PCR positive control (A) was amplified with BF R1474 and BF Fs10, and the AS1.5$\Delta_{HPQ, DBD, TRD}$ deletion construct (B) was amplified with the Bst-F and Bst-R, both giving the 350 base pair (bp) and 550 bp products expected, respectively. λ*Pst I* was used as the molecular weight marker (M), with the molecular weights indicated in kilo base pairs (kb).

Using the remaining 46 transformants, the samples were digested with *Hind III*, to verify the ligation of the AS1.5$\Delta_{HPQ, DBD, TRD}$ full-length mutagenesis fragment into the AS1.5$\Delta_{BsrG\ I\text{-}NgoM\ IV}$ vector. Samples were electrophoresed on a 1% agarose gel and visualised under UV (data not shown). The 0.9 kb and 3.7 kb fragments expected from this digest were not visualised on the gel, indicating that the full-length mutagenesis fragment had not been ligated to the AS1.5$\Delta_{BsrG\ I\text{-}NgoM\ IV}$ vector. Thus the subcloning of the AS1.5$\Delta_{HPQ, DBD, TRD}$ full-length mutagenesis fragment into the AS1.5$\Delta_{BsrG\ I\text{-}NgoM\ IV}$ vector was not successful.

3.3 Discussion

BF-1 is made up of three domains, the N-terminal histidine, proline and glutamine (H, P Q)-rich region, the winged helix DNA-binding domain, and the C-terminal transcriptional repressor domain (Figure 3.2; Tao *et al.*, 1992). This study was set up in an attempt to investigate which of the BF-1 domains were required for interaction with the BF-1 interacting protein, specifically BF1-IP$_1$. Restriction enzyme digests were designed to delete each of the three domains of BF-1. Deletions were generated sequentially from the C-terminal end of the BF-1 cloned into the yeast two-hybrid vector pGBT9 (CLONTECH), to preserve the reading frame of the deletion construct.

3.3.1 Deletion of the transcriptional repressor domain

The *Nhe I-BamH I* double digest had been unsuccessful and the deletion construct that was devoid of the transcriptional repressor domain, AS1.5 Δ_{TRD}, could not be generated. As *BamH I* was used in the construction of the two additional deletion constructs, this site was functional. Further digestion of the AS1.5 Δ_{TRD} construct with *Hind III*, *Msc I* and *BstE II* (data not shown) had been performed successfully. Thus the *Nhe I* site was either non-functional due to rearrangement or modification of the recognition site on the AS1.5 sequence or a fresh batch of the restriction enzyme itself was required. Perhaps an alternate site could be used with which to delete the transcriptional repressor domain.

The transcriptional repressor domain was identified by homologous study with the chick oncogene *Qin*, the avian homologue to BF-1 (Li *et al.*, 1995). Mapping of the domains of *Qin* located the transcriptional repressor domain to the carboxy-terminal end of *Qin*, and that although *Qin* had strong transcriptional activator activity, it also functioned in direct repression by sequence specific transcriptional regulation (Li *et al.*, 1995). Thus deletion of the

transcriptional repressor domain of BF-1 could have identified whether or not BF-1 was involved in transcriptional repression in the OP6 E10.5-neuroepithelial cell-line.

3.3.2 Deletion of the DNA-binding and the transcriptional repressor domains

The AS1.5 $\Delta_{DBD, TRD}$ deletion construct was cloned successfully, generating the desired BF-1 open reading frame devoid of the DNA-binding domain and the transcriptional repressor domain. However, subsequent experiments to introduce a stop codon by PCR-mediated site-directed mutagenesis into this construct were unsuccessful.

3.3.3 Deletion of the H, P, Q-rich, DNA-binding and transcriptional repressor domains

The construction of the AS1.5 $\Delta_{HPQ, DBD, TRD}$ domain deleted plasmid was successful in our study. Of the 1.7 kb BF-1 open reading frame cloned into the yeast two-hybrid vector, only 39 bp of the N-terminal region of BF-1 remained with the construction of this plasmid. This construct would be useful as it would allow the verification of whether the putative BF1-IP_1 interaction with BF-1 was specific. This truncated GAL4-BF-1 deletion construct, AS1.5 $\Delta_{HPQ, DBD, TRD}$, is devoid of the H,P,Q, the DBD, and the TRD domains and is thus unlikely to interact with BF1-IP_1 in a yeast two hybrid assay. If the BF1-IP_1-GAL4 activation domain construct (Schwegmann, 2000) is able to still able to activate expression of *lacZ* when co-transformed with AS1.5 $\Delta_{HPQ, DBD, TRD}$, it would mean that either BF1-IP_1 is acting non-specifically, or that it interacts with the first thirteen amino acids of BF-1.

3.3.4 Amplification of the AS1.5 $\Delta_{DBD, TRD}$ construct

The difficulties encountered in the amplification of the AS1.5 $\Delta_{DBD, TRD}$ deletion construct could, in part, have resulted from the inability to overcome the strong DNA-DNA self-hybridisation inherent in the highly repetitive DNA sequence that codes for the histidine, proline and glutamine rich region of BF-1. This highly repetitive region was absent in the

4 Introduction

Little is known of how BF-1 regulates neuronal progenitor cell proliferation or differentiation at the molecular level during embryonic development, or how BF-1 is itself regulated during neuronal development. To this end Schwegmann (2000) employed the yeast two-hybrid system to identify proteins that interacted with BF-1 in an attempt to characterise the molecular mechanisms by which BF-1 regulates or is regulated during neuronal development. The BF-1 coding region was fused in frame to the GAL4 DNA binding domain yeast vector, whilst a library of cDNA generated from the OP6 cell line were fused to the GAL4 activation domain yeast vector. Four interacting proteins were identified in this assay, BF-1 interacting protein (BF1-IP) 1, 2, 3 and 4 (Schwegmann, 2000). Of these interacting proteins, BF1-IP_2, BF1-IP_3 and BF1-IP_4, showed 100% homology to MBP1 (mutant p53 binding protein 1), acrogranin and fibulin 2, respectively. As all these proteins were extracellular matrix proteins (ECM), or contained the EGF-like domain characteristic of all ECM proteins, it was concluded that BF-1 would need to be localised outside the cell, that is, in the extracellular matrix in order to interact with these proteins (Schwegmann, 2000). Hence the cellular and extracellular localisation of BF-1 would need to be investigated. Consequently this study was set up to investigate and elucidate the spatial localisation of BF-1 in the OP cell line.

Mouse olfactory placode (OP) cell-lines were generated from the embryonic day 10 (E10) mouse olfactory neuroepithelium (Boolay, 1999), to enable the study of the growth and regulation of the neuronal progenitor cells during the development of the embryonic forebrain (Illing *et al.*, 2002). To address the question of BF-1 localisation, fluorescent protein fusions with the open reading frame of mouse BF-1 (mBF-1) were constructed. The mBF-1-

fluroescent protein fusions were then injected into *Xenopus* embryos to study the functionality of the BF-1 in these constructs.

Experiments carried out by Bourguignon *et al* (1998) and Hardcastle *et al* (2000) showed that the injection of *X*BF-1 mRNA into *Xenopus* embryos resulted in the perturbation of the *XSox3* and *N-tubulin* domains. Thus the experiments carried out in this study were compared to those performed previously by Bourguignon *et al* (1998) and Hardcastle *et al.*, (2000), to assess the functionality of the expressed mBF-1 as a fluorescent fusion protein, and when mBF-1 was expressed on its own.

Ectopic expression of a high dosage of *X*BF-1 mRNA, the *Xenopus* homologue of the mouse BF-1, in the *Xenopus* embryos, resulted in the suppression of the medial and lateral domains of the endogenous *N-tubulin* (Bourguignon *et al.*, 1998). *N-tubulin* is a tissue-specific marker used to specify differentiated primary neurons. *N-tubulin* was not found distributed within the region of high *X*BF-1-expressing cells, and the *N-tubulin* domains were shifted more ventrally. These results indicated that *X*BF-1 down-regulated neuronal differentiation in the cells in which it was highly expressed (Bourguignon *et al.*, 1998). However, a border of neuronal cells, expressing the neuronal differentiation marker *N-tubulin*, was formed adjacent to and surrounding those cells in which ectopic XBF-1 was expressed, (Bourguignon *et al.*, 1998; Hardcastle *et al.*, 2000). Expression of *N-tubulin* within this region has suggested that *X*BF-1 may function to control the spatial patterning of the anterior neural plate, by controlling the positioning of the population of highly proliferating neuronal cells within a boundary of cells undergoing neurogenesis (Hardcastle *et al.*, 2000). Ectopic expression of a high dosage of *X*BF-1 has also been correlated with the expansion of the *Xenopus* embryo neuroepithelium (Bourguignon *et al.*, 1998).

Contrary to this, the ectopic expression of a low dosage of *X*BF-1 mRNA resulted in the expansion of the endogenous lateral domains of *N-tubulin* (Bourguignon *et al.*, 1998). There was no ectopic expression of *N-tubulin* observed nor was there the formation of boundary of *N-tubulin* expressing cells surrounding the *X*BF-1 expressing cells in these embryos. Low dosage of *X*BF-1 resulted in the failure of ectopically expressed XBF-1 to suppress neuronal differentiation, with the expansion of the lateral *N-tubulin* domains into the *X*BF-1-expressing ectoderm (Bourguignon *et al.*, 1998).

Expression of the *XSox3*, an early neural marker (Bellefroid *et al.*, 1998), however, was expanded in regions of high *X*BF-1 expressing cells, whilst the region of *XSox3* expression was not affected in the ectopic expression of a low dosage *X*BF-1 mRNA (Bourguignon *et al.*, 1998). Concomitant with *XSox3* expression, was the absence of *N-tubulin* expressing cells within the regions of *XSox3* expression, whether or not *X*BF-1 was expressed at the high or low dosage (Bourguignon *et al.*, 1998).

The experiments carried out in this study, where the mBF-1 constructs were injected into *Xenopus* embryos, would be correlated to the experiments carried out by Bourguignon *et al* (1998) and Hardcastle *et al* (2000), with regards to how the injected constructs would affect the distribution of the *XSox3* and *N-tubulin* domains. Also the distribution and functionality of mBF-1 would be investigated in *Xenopus* embryos first, before the mBF-1 fusion constructs would be introduced into the OP cells.

Once the functionality of mBF-1 is verified, the mBF-1 fluorescent fusion constructs would them be transfected into the OP cell line to address the question of the localisation of BF-1 during neuronal development. The localisation of BF-1 was observed by visualising the cells under fluorescent microscopy.

4.1 Materials and Methods

4.1.1 Construction of plasmid DNA

PCR primers were designed to amplify the full-length mouse BF-1 coding region, to incorporate the ACC Kozak sequence (Kozak, 1991) on the N-terminal of the ATG start codon, and to eliminate the stop codon as well as the last four amino acid codons preceding the stop codon. The final concentration of the 50 µl PCR reaction mix was as follows: 8 ng/µl mouse BF-1 cDNA template (Li *et al.*, 1996), 4 ng/µl of each of the forward (mBF-1 sense2) and reverse (mBF-1 antisense2) primers, 0.25 mM dNTP mix (Roche), 1× Deep Vent polymerase buffer (NEB), 5% and 10% DMSO (Sigma), and two units Deep Vent polymerase (NEB). The PCR cycling parameters, using the Whatman Biometra thermocycler (Anachem Ltd), were as follows: an initial denaturation cycle at 95°C for 30 seconds, followed by 30 cycles of denaturation at 94°C for 1 minute, annealing at 60°C for 45 seconds, extension at 72°C for 3 minutes, with a final extension cycle at 72°C for 10 minutes. The PCR products were resolved on a 1% agarose gel, with the PCR products from the 5% and 10% DMSO reactions pooled together after resolving on the gel. The PCR fragments were electro-eluted from the gel slice, by electrophoresis of the DNA in the gel slice into dialysis tubing in 1× TAE, followed by a 1× phenol (pH 8.0) and 1× chloroform extraction and ethanol precipitation (Maniatis *et al.*, 1983). The PCR fragments were then phosphorylated using polynucleotide kinase (Roche).

The pCSGFP3 vector, derived from βGFP-R3N (Zernika-Goetz *et al.*, 1996) by Pines J. (personal communication), was digested with *Sma I* for five to eight hours, to generate blunt ends. The digested vector was purified from a 1% agarose gel, as above, and dephosphorylated with calf alkaline phosphatase (CIP) (Roche). The pECFP-N1 and pEYFP-N1 (CLONTECH) vectors were digested with *BamH I* for five to eight hours, and the overhangs filled in with T4 DNA polymerase (Roche) to generate blunt ends. These two blunted vectors were then

dephosphorylated with CIP. The pCS2 (Rupp *et al.*, 1994; Turner *et al.*, 1994) vector, previously digested with *Stu I* to generate blunt ends, was also dephosphorylated with CIP.

The phosphorylated PCR fragments were ligated into all these vectors using Quick Stick (QS) ligase (BIOLINE) in 1× QS buffer, for fifteen minutes at room temperature. The ligated DNA constructs were transformed into *E. coli* DH5α cells using the heat shock method (Maniatis *et al.*, 1989). The bacteria were plated out onto LB plates containing 100 μg/ml ampicillin, for the pCSGFP3 and pCS2 derived constructs, and 20 μg/ml kanamycin, for the pECFP-N1 and pEYFP-N1 derived construct. The plates were incubated overnight at 37°C.

4.1.2 Verification of DNA constructs and insert orientation

The integrity of the mBF-1 plasmid constructs were checked by analysis of restriction enzyme digests under standard conditions.

4.1.3 Sequencing of positive clones

After screening the transformants by restriction enzyme digests, one putative positive clone from each of the different constructs generated above was selected. The constructs were sequenced in the forward and reverse directions using the T7 and SP6 promoter primers or sequence-specific primers as dictated by the plasmid concerned. The constructs were sequenced on the ABI Megabase automated dye terminator sequencer (Amersham), following the manufacturer's instructions. Details of all the primers used are given in Table 1. As the mBF-1 insert was 1434 bp long, a primer was designed to sequence from the middle of the mBF-1 gene in the sense direction to check for fidelity during amplification. The sequencing results were either aligned against the predicted theoretical sequence generated in DNAMAN, or entered into the basic local alignment sequence tool (BLAST) programme (Altschul *et al.*,

1990) on the PUBMED database (Appendix 2), to check that no sequence substitutions or frameshifts had been incorporated during the construction of the mBF-1 plasmids, as well as to confirm that the fusions were in frame.

4.1.4 Embryo culture and DNA injections

Embryos were obtained from albino and pigmented *Xenopus laevis* adult frogs by hormone-induced egg laying and *in vitro* fertilisation using standard methods (Nieuwkoop *et al.*, 1967), and chemically de-jellied in 3% (w/v) cysteine in 0.1× Marc's Modified Ringer's solution (MMR), pH 7.9 (Newport *et al.*, 1982). Embryos were staged according to Nieuwkoop *et al* (1967). One or both blastomeres of two-cell stage embryos were injected with 100 pg of experimental plasmid DNA in a volume of 10 nl. Experimental plasmid DNA was also co-injected with a CMV-driven *lacZ* tracer mRNA (kindly provided by Dr R. M. Grainger; Coffman *et al.*, 1990) that served as a lineage label for cells that had inherited the injected DNA mixture (Bourguignon *et al.*, 1998). As negative controls, embryos were similarly injected (100 pg/10 nl) with a CMV-driven *lacZ* mRNA alone or not injected at all. At the neural plate stage, the injected embryos were fixed in MEMFA solution (0.1 M MOPS buffer at pH 7.4, 2 mM EGTA, 1 mM $MgSO_4$ and 3.7% (v/v) formaldehyde solution, in DEPC-treated water) and then stained with X-gal histochemical stain (Sive *et al.*, 2000) to reveal the distribution of the *lacZ* tracer. The stained embryos were then analysed by whole-mount *in situ* hybridisation. The *lacZ* tracer used in this study carries a nuclear localisation signal and therefore the blue staining is localised in the nucleus. In contrast, the *in situ* hybridisation signals, *N-tubulin* and *XSox3*, are predominantly cytoplasmic.

4.1.5 *In situ* hybridisation

In situ hybridisation was basically performed according to the protocol described by Harland (1991). Briefly, embryos were rehydrated into PBS-Tween-20, incubated in

triethanolamine with acetic anhydride and rinsed in PBS-Tween-20. The rinsed embryos were pre-hybridised in hybridisation buffer and incubated overnight with the digoxygenin-labelled probe, *N-tubulin*, in fresh hybridisation buffer. The embryos were rinsed in saline sodium citrate (SSC) buffer and incubated with blocking reagent in maleic acid buffer (MAB). The embryos were incubated overnight in MAB with the anti-digoxygenin antibody, followed by washes in MAB. The embryos were then incubated with the NBT/BCIP substrates in the chromogenic reaction buffer until the purple colour had developed, usually fifteen minutes to one hour, and the reaction was terminated with fresh MEMFA. Antisense RNA probes had been prepared from linearised DNA templates of *XSox3* (kindly provided by Dr R. M. Grainger) and *N-tubulin* (Chitnis *et al.*, 1995) by *in vitro* transcription in the presence of fluoroscein-12-UTP digoxygenin-11-UTP (Boehringer Mannheim) respectively, using the protocol described by Harland (1991).

Double *in situ* hybridisations were carried out as described by Knecht *et al* (1995), and as adapted in Bellefroid *et al* (1998). Briefly, primary hybridisation of the samples with the fluorescein-labelled and digoxygenin-labelled probes was carried out simultaneously. Secondary hybridisation was carried out starting with the alkaline conjugated anti-fluorescein antibody followed by the alkaline conjugated anti-digoxygenin antibody. Probes were then visualised sequentially using BCIP first for the anti-fluorescein-alkaline phosphate conjugated-probe (blue colour), and NBT/BCIP second for the anti-digoxygenin-alkaline phosphate-conjugated probe (purple or magenta colour).

4.1.6 X-gal histochemical stain

The embryos were grown to the desired stage, staged according to Nieuwkoop *et al* (1967), at 21°C. The vitelline membrane was carefully removed manually using watchmaker's forceps, and the embryos were fixed in MEMFA for one hour. Following a five-minute wash

in 0.1 M phosphate buffer (pH 6.3), embryos were transferred into the X-gal staining solution (Coffman *et al.*, 1993) until the staining was apparent, typically thirty minutes to two hours. Rinsing in the 0.1 M phosphate buffer, pH 6.3, terminated the reaction. The embryos were then dehydrated through an ethanol series and stored in absolute ethanol at –20°C until further processing. The X-gal staining solution was prepared as follows: 10 mM potassium ferricyanide and 10 mM potassium ferrocyanide in 0.1 M phosphate buffer pH 6.3, to which 15 mg X-gal (5-bromo-4-chloro-3-indolyl-β-D-galactopyranoside) dissolved in 100 µl DMSO, per 10 ml solution, was added.

4.1.7 Cell culture of olfactory placode cells

OP cells were maintained in high glucose Dulbecco's Modified Eagle Medium (DMEM; Gibco) supplemented with 3.7 g/l sodium bicarbonate and 10% (v/v) heat-inactivated foetal bovine serum (FBS; Sigma). This complete medium is hereafter referred to as DMEM-10. The cells were incubated in a humidified incubator at 33°C and 10% CO_2. The cultured cells were first rinsed in 1× PBS and then passaged by trypsinising the adherent cells with a tenth volume of 0.25% (w/v) trypsin – 0.04% (w/v) EDTA solution (Gibco) in 1× PBS, for one minute or until the cells had detached. The reaction was terminated by the addition of DMEM-10. The cells were recovered by centrifuging at 100 ×g for five minutes at room temperature. The cells were resuspended in a small volume of fresh DMEM-10, and 10 µl of the resuspended cells were counted using a haemocytometer. The cells were then seeded at 5×10^4 cells/cm^2 or 1×10^5 cells/ml and incubated for twenty-four hours at 33°C, 10% CO_2. The PBS was prepared using tissue culture grade reagents as follows: 0.8% (w/v) sodium chloride, 0.02% (w/v) potassium chloride, 0.115% (w/v) di-sodium phosphate and 0.02% (w/v) potassium di-hydrogen phosphate, with a pH of between 7.2 and 7.4. All culture solutions

were warmed to 37°C before use, with plasmid DNA and the FuGene6 Transfection Reagent (Roche) used at room temperature.

4.1.8 Transient transfection of the OP6 cell line

OP6 cells were transfected with the FuGene6 Transfection Reagent (Roche) guided by the manufacturers instructions. Transfections were carried out when the cells were approximately 60% confluent. This was achieved by seeding six-well plates or 35 mm tissue culture dishes with 1×10^5 cells/ml per well of rapidly growing cells (approximately 75% confluent), in 2 ml DMEM-10, twenty four hours before transfection. Using the Qiagen EndoFree Plasmid kit, 5 µg of endotoxin-free plasmid DNA was prepared, following the manufacturer's instructions, and added to 6 µl of FuGene6 Transfection Reagent and 94 µl of serum-free DMEM, in a 5 ml polystyrene tube. The mixture was incubated at room temperature for fifteen to thirty minutes. Old culture medium was removed from the wells and replaced with 2 ml serum-free DMEM. The DNA/FuGene6/DMEM mix was added drop-wise uniformly across the well and the plates swirled once to mix. The plates were incubated at 33°C, 10% CO_2 for four to six hours. The DNA/FuGene6/DMEM culture medium was aspirated off the cells and replaced with fresh DMEM-10, and the cells incubated for sixteen to twenty four hours at 33°C, 10% CO_2.

Transfections were carried out using endotoxin-free pCSGFP3 as the control plasmid, pCMVβ-Gal (MBS Transfection kit, Stratagene) to calculate transfection efficiency, and mBF-1-GFP as the experimental plasmid DNA.

4.1.9 Calculating transfection efficiency

Transfection efficiency was calculated by co-transfecting 5 μg of each of pCMVβ-Gal with pCSGFP3. Twenty-four hours after transfection, the transfected cells were stained with the X-gal histochemical stain according to Coffman *et al* (1993), in 1× PBS instead of the 0.1 M phosphate buffer. The culture medium was aspirated off and the cells washed in 1× PBS for five minutes at room temperature. The cells were fixed in 4% formaldehyde solution made up in 1× PBS, for fifteen minutes at room temperature. The fixed cells were washed in 1× PBS and permeablised in 1× detergent stock solution (10× detergent stock: 2%SDS and 10% Triton X-100 in water) in 1× PBS for thirty minutes at room temperature. The X-gal staining solution was added to the permeablised cells and the cells incubated at room temperature until the colour developed, usually five to thirty minutes. Visualising three different field views and taking the average of the cells counted in all three views, the number of blue-stained cells, expressed as a fraction of the unstained cells was used to calculate the transfection efficiency. The number of GFP fluorescent cells as a fraction of the number of non-fluorescent cells was also used to estimate the transfection efficiency.

4.1.10 Synchronisation of the OP6 cell line

Cells were grown until they were 90% confluent at 33°C, 10% CO_2, before they were trypsinised and seeded at 1×10^6 cells/ml or 5×10^5 cells/cm^2. Cells were incubated for twenty-four hours at 33°C, 10% CO_2. The colcemid (Sigma) was made up in 1× PBS, and was added directly to the culture medium. The cells were then incubated in the colcemid-containing culture medium for eighteen to twenty four hours at 33°C, 10% CO_2. The cells were then transfected as indicated above, and incubated at 33°C, 10% CO_2 for twenty-four hours. Cells were viewed under the fluorescent microscope twenty-four hours after transfection.

4.1.11 Staining OP6 cells with Hoechst

Old culture medium was aspirated off the cells and the cells washed once in 1× PBS. Cells were fixed in 4% formaldehyde in 1× PBS for fifteen minutes at room temperature. Cells were washed three times in 1× PBS, with gentle agitation for five minutes per wash, and then permeablised in the 1× detergent stock in 1× PBS for thirty minutes at room temperature. The cells were washed three times as above, and a 1:10000 dilution in 1× PBS, of 10 mg/ml Hoechst (33342; Sigma) stock solution, was used to stain the cells for five minutes at room temperature. The cells were rinsed once in 1× PBS and all liquid was aspirated off. One drop, dispensed using an eye-dropper, of Vectashield mounting medium (Vector Laboratories) was placed in the middle of the well, a coverslip was carefully lowered over the drop and the cells were visualised with a Hoechst filter on the Zeiss Axiophot-2 microscope.

4.1.12 Tracking cells

When the cells were 80% confluent, the cells were trypsinised and seeded into six-well plates into which a single CELLocate micro-grid coverslip (Eppendorf) with a 175 μm grid size, had been placed per well. Cells were incubated at 33°C 10% CO_2 for twenty-four hours. Cells were transfected with 5 μg of pCSGFP3 or mBF-1-GFP using the FuGene6 method, as indicated above, and incubated at 33°C 10% CO_2 for four to six hours. Transfection medium was replaced with fresh culture medium and cells incubated at 33°C for a further eighteen to twenty four hours. Visualising with fluorescence microscopy identified cells expressing GFP, and their location recorded under bright field onto corresponding paper grids, using the grid marks engraved into the coverslip for identification of location. Cells were returned to the incubator and followed over three days.

4.1.13 Visualisation of embryos and cell cultures

Embryos were visualised using a Leica MZ12.5 epi-fluorescent stereomicroscope fitted with GFP, ECFP and EYFP filters. Using a PVCAM (Roper Scientific Inc.) digital camera, the images were captured onto the OPENLAB (Improvisions) software, at 1.65 × to 2.25 × magnification.

For live non-fixed cells, images were visualised using a SONY (Sony) digital camera, attached to the Olympus IX70 microscope, and captured onto the Northern Eclipse version-2 (Empix Imaging) analysis software programme. Fixed and Hoechst-stained cells were visualised using the PVCAM digital camera on the Zeiss microscope, with images captured onto the OPENLAB (Improvisions) analysis software programme. For both the Olympus and Zeiss microscopes, images were captured at either the 10 × or the 20 × magnifications.

4.2 Results

4.2.1 Cloning of mBF-1 and verification of the mBF-1 fusion constructs

To generate mouse BF-1 (mBF-1) fusion constructs, the mBF-1 open reading frame was amplified using the mBF-1 sense2 and mBF-1 antisense2 primers. The mBF-1 sense2 primer was designed to incorporate the ACC Kozak sequence to the 5' end of the open reading frame, to increase the translational efficiency of the mRNA transcript and its expression in mammalian cells (Kozak, 1991). The mBF-1 antisense2 primer was designed to terminate at the last four amino acid codons preceding the stop codon. The last four amino acid codons were eliminated due to the formation of DNA-DNA hybrids that prevented the amplification of the mouse BF-1 open reading frame. The stop codon of the mBF-1 gene was also eliminated to enable the transcription of the entire fusion construct from the mouse BF-1 start codon to the fluorescent gene stop codon. The 1434 bp PCR amplified mBF-1 product is shown in Figure 4.1.

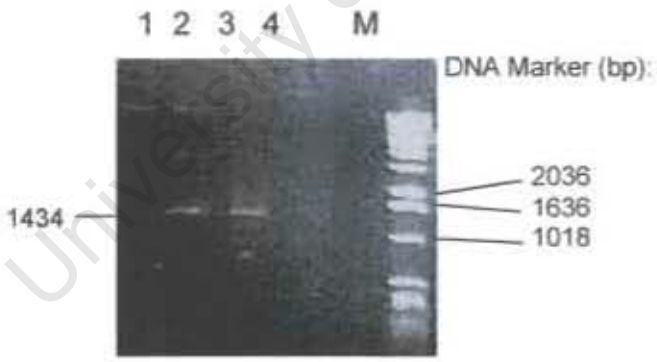

Figure 4.1: The amplified mBF-1 open reading frame resolved on a 1% agarose gel. Only product amplified in 5% and 10% (v/v) DMSO was visible, lane 2 and 3, respectively. No DMSO or even 12.5% (v/v) DMSO (lanes 1 and 4, respectively) in the PCR mix resulted in no product amplification. DNA marker X (Roche) was used, with the molecular weights indicated in base pairs (bp) as shown.

The mBF-1 PCR product was cloned into the following three fluorescent vectors: pCSGFP3, pECFP-N1 and pEYFP-N1, containing the genes encoding the green fluorescent protein (GFP), the enhanced cyan fluorescent variant and the enhanced yellow-green fluorescent variant of the *Aequorea victoria* GFP, respectively (Figure 4.2 A, B and C).

Construction of mBF-1-GFP from the pCSGFP3 vector enabled for the use of pCSGFP3 as the control construct for the monitoring of the localisation and function of mBF-1 distinct from the GFP under fluorescence. The mBF-1-ECFP and mBF-1-EYFP fusion constructs were designed for use of each of these constructs in double labelling experiments, in the simultaneous analysis of the localisation of and the protein-protein interactions of BF-1 and BF-1 interacting proteins in the cell lines. That is, the BF-1 interacting protein (BF1-IP) would also be cloned into either pECFP-N1 or pEYFP-N1 to generate BF1-IP fluorescent fusion proteins. Thus the resultant fluorescence from the respective protein fusions, BF-1 and BF-1 interacting protein, could then be resolved from each other using filters that distinguish the one fluorescent fusion protein from the other when viewed under a fluorescent microscope. Maps of the resultant fusion constructs are shown diagrammatically in Figure 4.2, in which mBF-1 has been cloned upstream of the fluorescent gene. mBF-1 was also cloned into the pCS2 vector to generate a control construct (Figure 4.2 D). The pCS2 vector is similar to the pCSGFP3 vector but lacks the fluorescent gene. The mBF-1-CS2 construct would enable the monitoring of the function of BF-1, to ensure that the effects observed for BF-1 when using mBF-1-GFP were not influenced by the GFP, that is BF-1 was functional.

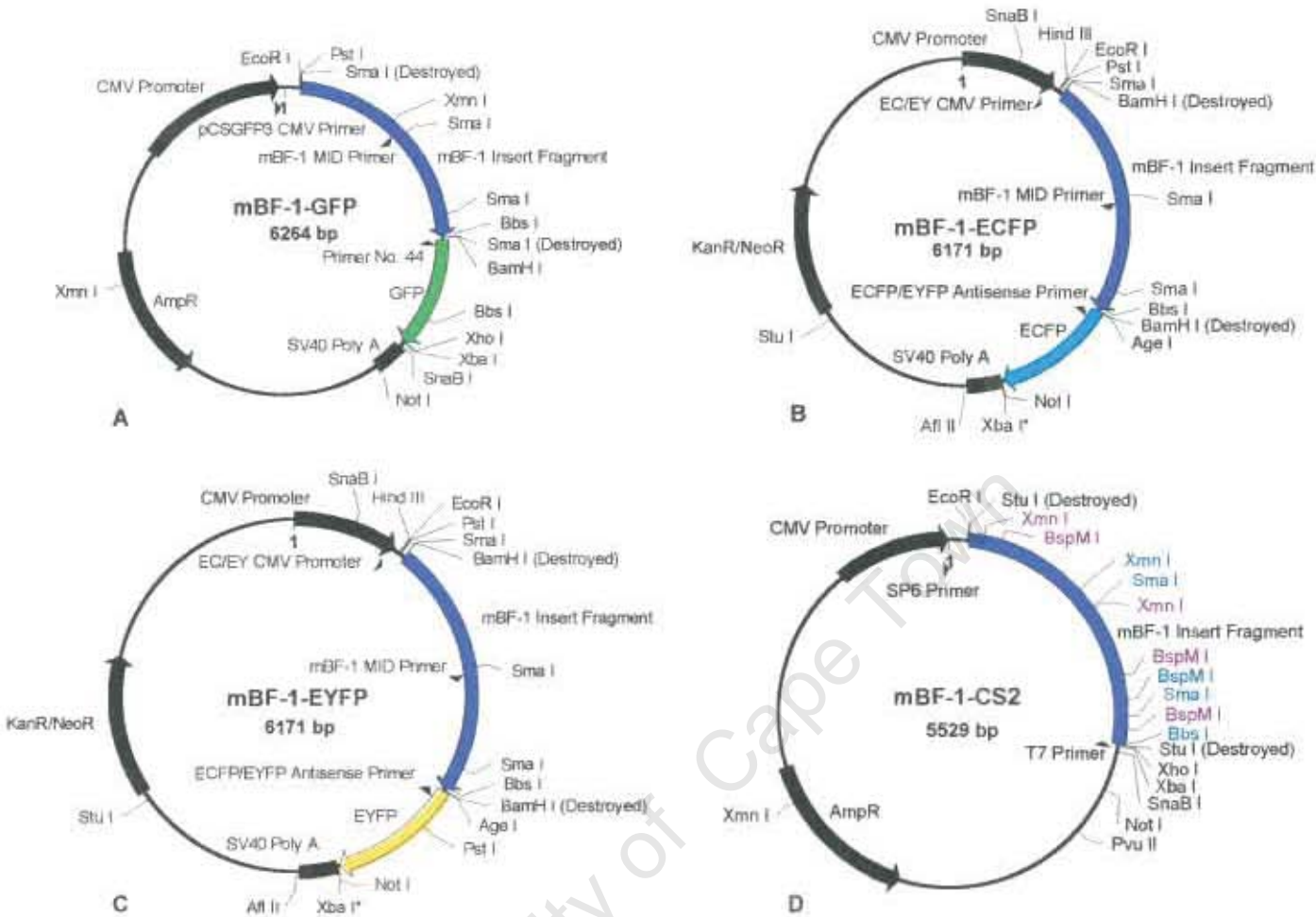

Figure 4.2: Diagrammatic representation of the fluorescent fusion construction, mBF-1-GFP (A), mBF-1-ECFP (B) and mBF-1-EYFP (C), generated to study the localisation of BF-1 in the OP cell line. The mBF-1-CS2 construct (D) was generated as a control, where mBF-1-CS2 is similar to mBF-1-GFP, but does not have a fluorescent gene. The restriction enzymes in mBF-1-CS2 (D) are in purple, when the mBF-1 insert fragment is in the incorrect orientation, and in green when the mBF-1 insert fragment is in the correct orientation. The diagrammatic vector representations were generated in DNAMAN version 4.13 (Lynnon BioSoftware).

The constructs were confirmed by restriction analysis (Figure 4.3 A). *EcoR I* and *BamH I* digest of the mBF-1-GFP transformants identified mBF-1 containing clones. Of the twenty-four transformants screened, five contained the 1.4 kb insert released from the 4.8 kb vector.

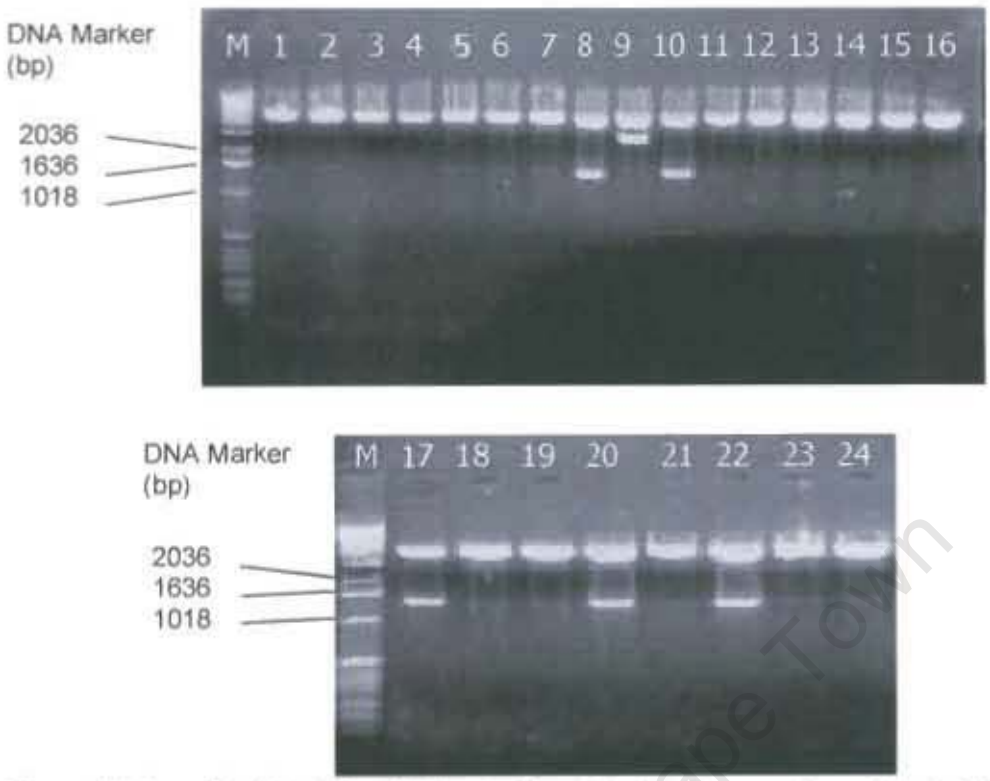

Figure 4.3 A: *EcoR I* and *BamH I* digest of the mini-plasmid preparations of the (mBF-1-GFP) positive transformants, to verify insert ligation. The following clones were selected for further analysis: plasmids no. 8, 10, 17, 20 and 22. DNA Marker X (Roche) was used, with the molecular weights indicated in base pairs (bp) as shown.

To select for the correct orientation of the inserts, clones 8, 10, 17, 20 and 22 (lanes 8, 10, 17, 20 and 22, respectively) were digested with *Bbs I*. Clones 10 and 17 gave rise to the expected fragment sizes of 0.5 kb and 5.7 kb (Figure 4.3 B).

Figure 4.3 B: *Bbs I* digest of the mBF-1-GFP constructs to verify insert orientation. Of the 5 putative positive clones identified in Fig. 4.3 A, only two of these have the insert in the correct orientation, plasmids number 10 and 17 and were chosen for further studies. DNA marker X (Roche) was used with the molecular weights indicated in base pairs (bp).

The mBF-1 containing clones of the mBF-1-ECFP and mBF-1-EYFP fusion construct transformants were verified by *EcoR I* and *Not I* digestion. Eleven out of the sixteen mBF-1-ECFP and two out of the four mBF-1-EYFP transformants screened showed the predicted 4.0 kb vector fragment and a 2.1 kb fragment consisting of the mBF-1 insert (1.4 kb) fused to the fluorescent gene (0.7 kb) (Figure 4.4 A).

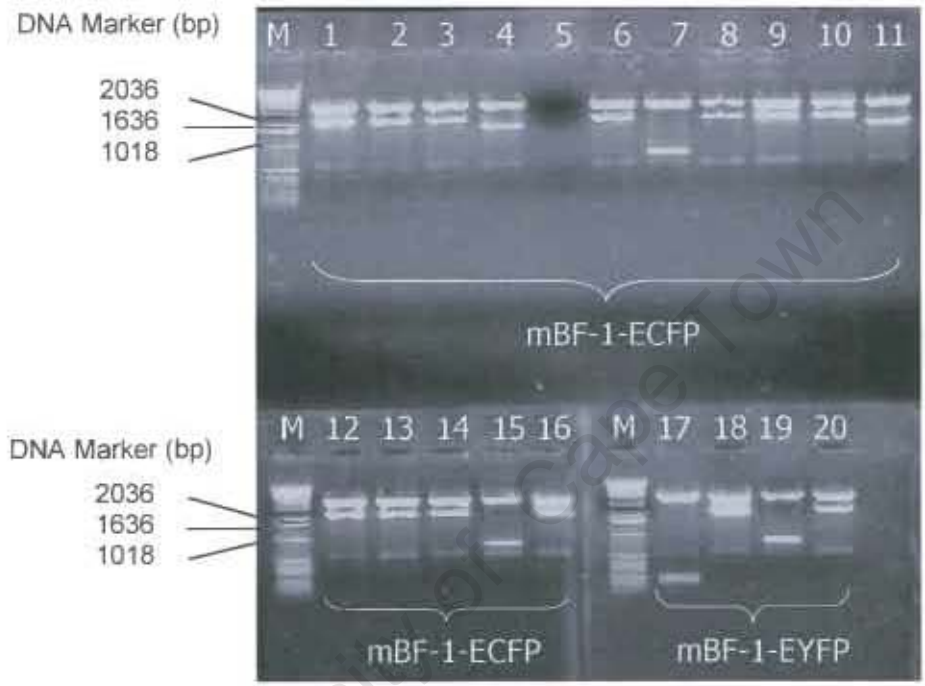

Figure 4.4 A: *EcoR I* and *Not I* digests of mini-plasmid preparations of the mBF-1-ECFP and mBF-1-EYFP positive transformants, to verify the ligation of the insert. The following clones were selected for further analysis: plasmid no. 1, 2, 3, 6, 8, 9, 10, 12, 13, 14, 16, 18 and 20. DNA marker X (Roche) was used with the molecular weights indicated in base pairs (bp).

To select for the correct orientation of the inserts, the eleven mBF-1-ECFP clones and the two mBF-1-EYFP samples, clones 1, 2, 3, 6, 8, 9, 10, 12, 13, 14, 16, 18 and 20 (in lanes 1, 2, 3, 6, 8, 9, 10, 12, 13, 14, 16, 18 and 20, respectively), Figure 4.4 A, were digested with *Bbs I* and *Hind III* (Figure 4.4 B).

Figure 4.4 B: *Bbs I* and *Hind III* digest of the putative positive clones of mBF-1-ECFP and mBF-1-ECFP to verify insert orientation. Of the positive clones, plasmids no. 3 and 10, of the mBF-1-ECFP transformants, and plasmid no. 18 of the mBF-1-EYFP transformants were chosen for further studies. DNA marker X (Roche) was used, with the molecular weights indicated in base pairs (bp) as shown.

Digestion of mBF-1-ECFP and mBF-1-EYFP with these two restriction enzymes, *Hind III* and *Bbs I*, would result in the release of the 1.4 kb and 4.7 kb fragments if the insert were inserted in the correct orientation. The location of these restriction enzymes is shown in Figure 4.2 B and C. Clones 2, 3, 10, 12 and 13 of the mBF-1-ECFP constructs, and clone 18 of the mBF-1-EYFP construct gave rise to the expected fragment sizes (Figure 4.4 B).

mBF-1 was also cloned into the *Stu I* site of the pCS2 vector by blunt end ligation. To verify the ligation of insert to generate the control construct, twenty-four transformants were screened with *Xho I* and *EcoR I* restriction enzymes. The 1.4 kb insert fragment and the 4 kb vector fragment were identified in clones 4, 8, 11, 12 and 16 (lanes 4, 8, 11, 12 and 16, respectively) of the mBF-1-CS2 transformants, Figure 4.5 A.

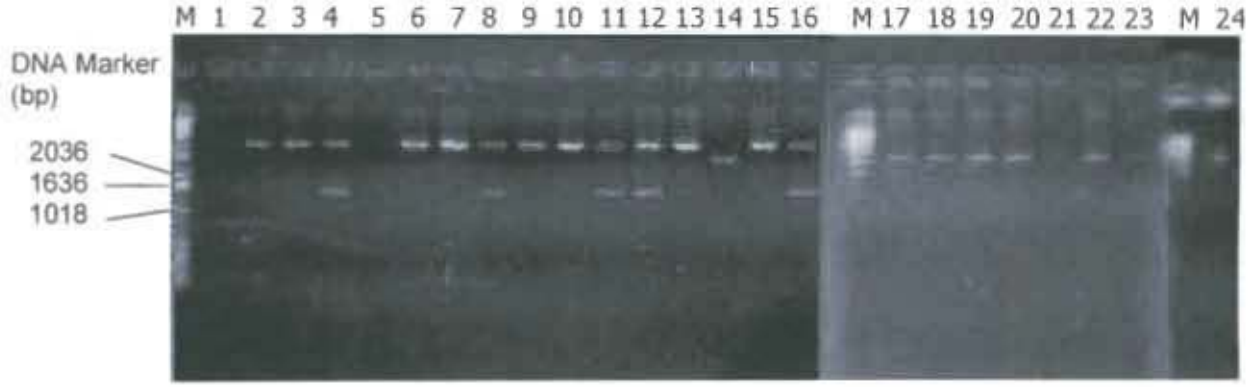

Figure 4.5 A: *EcoR I* and *Xho I* digest of mini-plasmid preparations of the mBF-1-CS2 transformants to verify insert ligation into vector. The following clones were chosen for further analysis: plasmids no. 4, 8, 11, 12, 16 and 17. DNA marker X (Roche) was used, with the molecular weight sizes indicated in base pairs (bp) as shown.

The insert orientation was determined by digestion of the five mBF-1-CS2 clones using *BspM I* with *Not I* and *Bbs I* with *Pvu II*. Using *BspM I* with *Not I* the 0.5 kb and 5 kb fragments were expected, with 0.4 kb and 5 kb fragments expected from the *Bbs I* with the *Pvu II* digest. Clones 11 and 16 gave rise to the correct fragments in both digests, while clone 8 was positive for the *Bbs I* and *Pvu II* digest only (Figure 4.5 B).

Figure 4.5 B: *BspM I* and *Not I*, and *Bbs I and Pvu II* digests of the putative positive clones of mBF-1-CS2 plasmids, to select for correct insert orientation. Plasmids no. 8, 11 and 16 were chosen for further assays. As shown, plasmid no. 8 is in the incorrect orientation, but was chosen as such for use in RNA interference studies and to generate an antisense RNA probe. DNA marker X (Roche) was used with the molecular weight sizes indicated in base pairs (bp) as shown.

Although clone 8 had the mBF-1 insert inserted in the incorrect orientation, as shown in the *Bbs I* and *Pvu II* digest (Figure 4.5 B), clone 8 was selected along with clones 11 and 16 for

sequencing as well. Clone 8 was chosen as it could be useful in future work in RNA interference studies and to generate an antisense RNA probe.

mBF-1-GFP clones 10 and 17, mBF-1-ECFP clone 3 and mBF-1-CS2 clones 8, 11 and 16 were selected for sequencing in the forward and reverse directions. Sequencing was performed to verify the full-length insert and the integrity of the ligation sites to ensure that no sequence frameshifts or rearrangements had been introduced during the cloning procedure. The sequence results showed that no rearrangements had been introduced into the insert or at the ligation site (Appendix 2) during cloning.

4.2.2 Visualisation of fluorescent fusion-protein expression in *Xenopus* embryos

The mBF-1-GFP, mBF-1-ECFP and mBF-1-EYFP DNA constructs were injected into approximately fifty *Xenopus* embryos, for each construct used, to verify that the fluorescent protein fusion constructs were being expressed. On average, twenty embryos for each of the injections, survived to the neurula stage embryo, stage 15/16 (Nieuwkoop *et al.*, 1967). Using different filter sets for each of the three different fluorescent proteins, the injected embryos, grown to the neurula stage (stage 15/16; Nieuwkoop *et al.*, 1967), were visualised under the fluorescent microscope.

Figure 4.6 shows that the mBF-1-GFP injected embryos (1) expressed the green coloured fluorescent protein fusions (2), the mBF-1-ECFP injected embryos (3) expressed the blue coloured fluorescent protein fusions (4), and the mBF-1-EYFP injected embryos (5) expressed the yellow-green coloured fluorescent protein fusions (6). Expression of the fluorescent protein confirmed that no frameshifts or mutations were introduced into the fusion constructs. Each of the embryo sets visualised, had been imaged using the exact same views for both the bright field (top row) and the fluorescent images (bottom row), Figure 4.6.

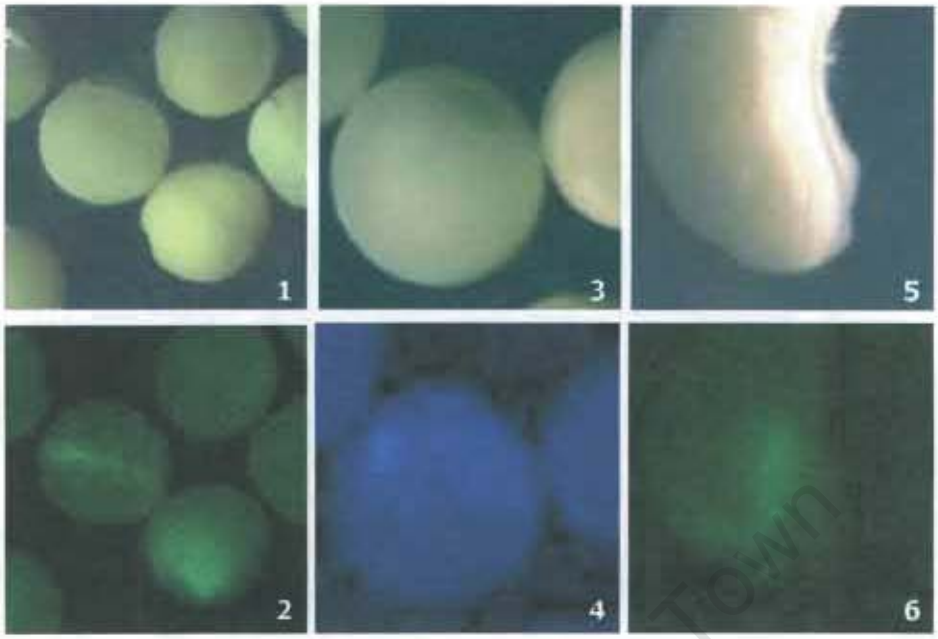

Figure 4.6: Injection of mBF-1-GFP (1 and 2), mBF-1-ECFP (3 and 4) and mBF-1-EYFP (5 and 6) DNA into *Xenopus* embryos to detect the colour of the expressed fluorescent gene, where images 1, 3 and 5 are the embryos under bright field, and images 2, 4 and 6 are the same respective embryos under fluorescent microscopy, using the GFP, ECFP and EYFP filters respectively.

To investigate the utility of the fusion constructs for double labelling experiments, the mBF-1-ECFP and the mBF-1-EYFP DNA constructs were injected into a different cell each of two-cell stage embryos and visualised at the neurula stage (stage 15/16; Nieuwkoop *et al.*, 1967). No inter or intra-cellular interference was observed in these embryos when the embryos were visualised under the different filter sets for each respective protein (Figure 4.7). Visualisation of the same embryo at exactly the same view using the ECFP filter (Figure 4.7) enabled the visualisation of the mBF-1-ECFP (blue) expressed protein only, while under the EYFP filter (Figure 4.7) only the mBF-1-EYFP (yellow-green) protein could be visualised. Whilst both proteins were expressed in the same region of the embryo, the different fluorescent proteins were not visualised within the same cell, that is, they were mutually exclusive of each other.

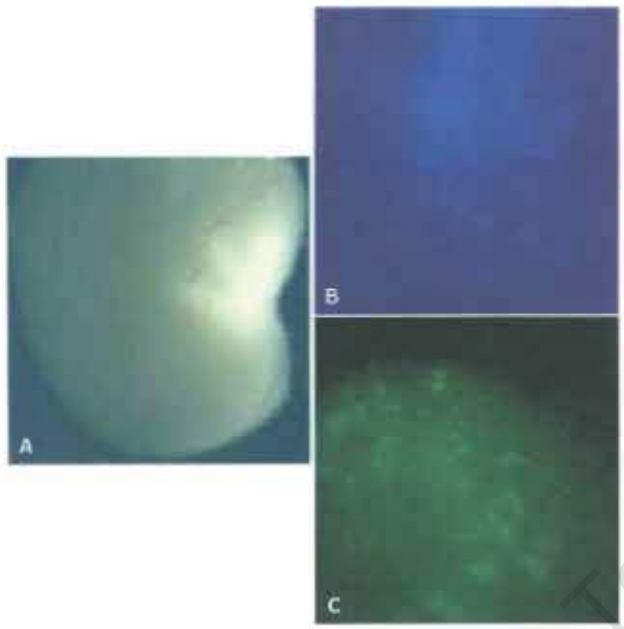

Figure 4.7: Visualisation of an embryo (A), in the exact same lateral view, that had been injected with both mBF-1-ECFP (B) and mBF-1-EYFP (C) into one blastomere each of the same four-cell stage embryo, under the different filters, bright field (A), ECFP (B) and EYFP (C), shows that there is no inter or intra-cellular interference between mBF-1-ECFP and mBF-1-EYFP when the two constructs are used together. The fluorescent proteins of mBF-1-ECFP and mBF-1-EYFP are far apart enough in wavelength for use of these fluorescent fusions together in double labelling experiments.

To investigate the localisation of the mBF-1-GFP in the *Xenopus* embryos, the control GFP DNA, pCSGFP3, and mBF-1-GFP were injected into two-cell stage *Xenopus* embryos and visualised under the fluorescent microscope (Figure 4.8). The pCSGFP3 injected embryos showed a diffuse distribution of the GFP protein in comparison to the punctate distribution of the mBF-1-GFP expression (Figure 4.8, 1A and 1B). The punctate distribution of the mBF-1-GFP expression indicated that mBF-1 was able to direct the GFP to the nucleus, while the expression of pCSGFP3 was not directed and thus had a diffuse cytoplasmic distribution (Figure 4.8, 2A and 2B). The expression of the mBF-1-ECFP and the mBF-1-EYFP fusion protein also showed the punctate distribution of the fluorescent protein, which indicated that the mBF-1 also directed the fluorescent fusion protein expressed here to the nucleus.

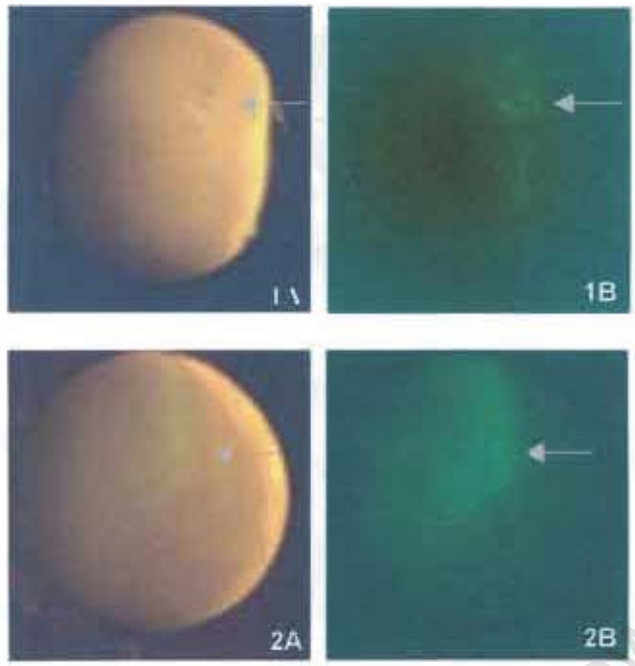

Figure 4.8: Injection of mBF-1-GFP (1A and 1B) and pCSGFP3 (2A and 2B) into *Xenopus* embryos shows that the mBF-1 is able to drive the protein expressed from the mBF-1-GFP construct to the nucleus, giving rise to the punctate distribution of the expressed mBF-1-GFP protein. The GFP fluorescence, of the expressed pCSGFP3 protein exhibits a diffuse distribution, indicating that the signal is cytoplasmic, and that GFP is unable to drive any construct to the nucleus if the construct does not carry a nuclear localisation signal. The grey arrows locate the mBF-1-GFP and GFP proteins under bright field fluorescent microscopy together (A), and under fluorescent microscopy only (B). For both 1 and 2, the same embryo has been visualised in the exact same view for A and B respectively

4.2.3 Analysis of the distribution of the expression of each of the fluorescent fusion proteins in *Xenopus* embryos

Analyses of the fusion constructs were carried out on neurula stage embryos to assess the functionality of the BF-1 when fused to the fluorescent protein. The mBF-1-GFP, mBF-1-ECFP and mBF-1-EYFP fusion DNA constructs were injected into *Xenopus laevis* embryos. The effect of the ectopic expression of the fusion proteins on neuronal development was assayed by examining the distribution of the expressed *N-tubulin* and *XSox3* genes.

In the uninjected control embryos (Figure 4.9 A and B), all the embryos (n=7) showed the purple staining of the *N-tubulin* positive/expressing cells in three punctate (dotted) bilateral stripes distributed symmetrically on either side of the dorsal midline. The three bilateral punctate stripes, the medial, intermediate and lateral stripes, represent the three classes of the

primary neurons, that is the motor neurons, the interneurons and the sensory neurons, in that respective distribution from the dorsal midline (Figure 4.9 A; Hardcastle *et al.*, 2000). Double *in situ* hybridisation of *XSox3* with *N-tubulin* showed the *XSox3*, the light blue colour, in a thin diffuse band distributed between the medial and intermediate stripes of the punctate *N-tubulin* stripes, as well as in the dorsal and lateral marginal zone of the neurula stage embryo (Figure 4.9 B). *XSox3* is an early development transcription factor that acts as a marker for genes expressed early on during development, where it marks out the neural plate and the cranial placodes (Kenyon *et al.*, 2001), as well as genes expressed in the anterior and dorsal region of the early embryo. *XSox3* is also expressed within the medial and intermediate regions of *N-tubulin* expression domains, in the undifferentiated neuroepithelial cells only (Bellefroid *et al.*, 1998).

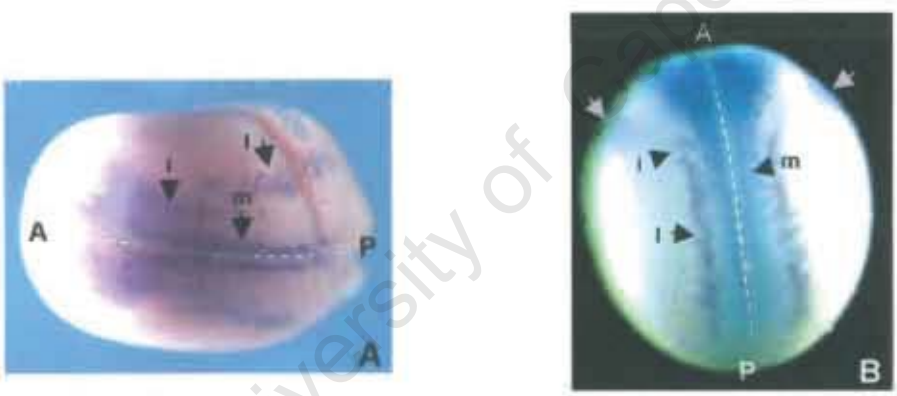

Figure 4.9 (A and B): Uninjected neural stage embryos (A and B) showing single and double in situ hybridisation signals using *N-tubulin* (purple or dark blue punctate distribution) and *N-tubulin* with *XSox3* (blue diffuse distribution) respectively. *N-tubulin* is distributed in three symmetrical bilateral stripes (domains), indicated by the black arrowheads, on either side of the dorsal midline (shown by the dotted white line). The 3 bilateral stripes indicate the medial (m) motorneurons, the intermediate (i) interneurons, and the lateral (l) sensory neurons. The *XSox3* signal is shown along the dorsal and the lateral marginal zone of the embryo, between the medial and intermediate *N-tubulin* stripes. Expression of *XSox3* is an early developmental transcription factor that delineates the anterior neural plate and the cranial placodes (grey arrowheads). A: anterior, P: posterior.

Eight embryos were injected with *lacZ* mRNA only (Figure 4.10 A). Analysis of these *Xenopus* embryos showed a lateral distribution of the *lacZ* tracer in six of these embryos. In two of the embryos (Figure 4.10 A1 and A2), the *lacZ* tracer was distributed along the dorsal midline, between the bilateral medial stripes of *N-tubulin* expressing cells. No visual perturbation of the three *N-tubulin* bilateral domains was observed in any of these embryos.

From these results it was concluded that the injection or expression of the *lacZ* tracer did not interfere with the expression of the *N-tubulin* domains, but only served as a marker to locate the distribution of the expressed injected constructs. As the *lacZ* tracer used in this study carried a nuclear localisation signal (Bourguignon *et al*., 1998), a dotted blue distribution (Figure 4.10 A) was observed.

Analysis of the distribution of *N-tubulin* in the pCSGFP3 injected embryos showed that injection of pCSGFP3 did not result in the perturbation of the distribution of the *N-tubulin* stripes in any of the injected embryos (Figure 4.10 B). The three symmetrical bilateral stripes were the same as those observed in the uninjected controls. Thus it was concluded that injection or expression of pCSGFP3 played no part in directing the fusion constructs to the nucleus, nor caused any visible perturbations in the distribution of the *N-tubulin*.

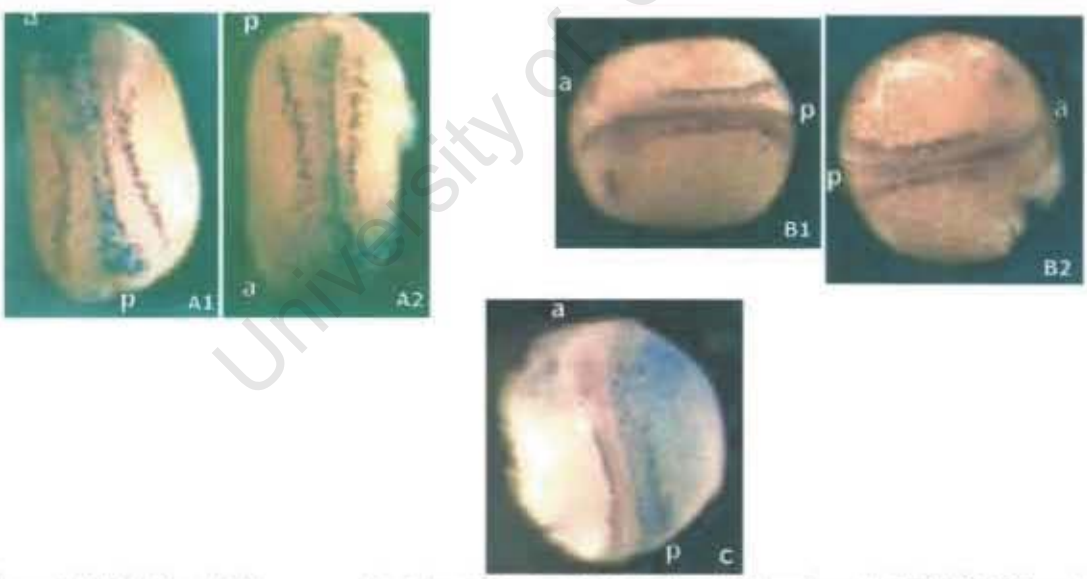

Figure 4.10 (A, B and C): Injection of *lacZ* mRNA (A1 and A2) only and pCSGFP3 (B1 and B2) only does not give rise to perturbations of any of the *N-tubulin* domains. In A the expression of *lacZ* (dotted blue) is distributed within the medial and intermediate domains of *N-tubulin* (punctate purple) expression and throughout the posterior section of the embryo. No GFP fluorescence is visible in B as the embryos were imaged under bright field only to show the effect (or lack thereof as is the case in B) of GFP expression on *N-tubulin* expression. Injection of mBF-1-CS2 antisense (that is with mBF-1 in the incorrect orientation in pCS2) showed that there were no perturbations of the *N-tubulin* domains upon expression of antisense mBF-1 (C). mBF-1-CS2 antisense was co-injected with *lacZ* DNA, to trace the expression of the injected constructs (construct does not have a GFP gene whose expression would have been used to follow the cells that are expression the construct). *lacZ* expression was distributed along the dorsal, medial and anterior-lateral regions of the embryo (C). a: anterior, p: posterior.

Injection of embryos with the mBF-1-CS2 construct, wherein mBF-1 was in the incorrect orientation (Figure 4.10 C), showed that while *lacZ* was distributed in a broad domain across the medial and intermediate region of the *N-tubulin* domains, there were no perturbations of the *N-tubulin* domains. This suggested that the mBF-1 protein expressed from the injected mBF-1-GFP construct, in the correct orientation, was responsible for the perturbation of the *N-tubulin* domains.

In Figure 4.11 A, *Xenopus* embryos were co-injected with the mBF-1-GFP fusion construct and *lacZ* DNA. Visualisation of GFP fluorescence in the embryos after X-gal staining showed that both the GFP fluorescence and the *lacZ* signal were found on the same side of the embryo and in the same region (Figure 4.11 A). Hence *lacZ* can be used a lineage marker to indicate where the injected construct has been distributed within the embryo, on a cell-by-cell basis (Figure 4.11 A and B). Although GFP fluorescence was co-localised with the *lacZ* tracer, they were not visualised within the same cell (Figure 4.11 A). However, as GFP was fused to the DNA construct under study, GFP fluorescence would acts as a more precise lineage marker of the inherited construct (Figure 4.11 and Figure 4.12).

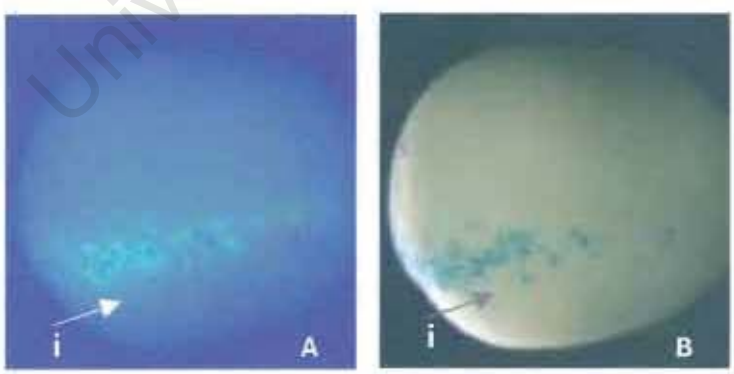

Figure 4.11: Visualisation of a *Xenopus* embryo co-injected with mBF-1-GFP and *lacZ*, after X-gal staining, shows how the expression of *lacZ* can be used to visualise the injected side (i) of the embryo (B) under bright field, as well as to delineate, on a cell by cell basis, where the injected construct has migrated to using fluorescence microscopy (A and B). Visualisation of the same embryo using fluorescence shows that mBF-1 and *lacZ* have been inherited on the same side of the embryo, and within the same area (A). However, *lacZ* and GFP (mBF-1-GFP) are not expressed within the same cell (A). This could be due to the chromogenic quenching of GFP by *lacZ* in *lacZ* positive cells.

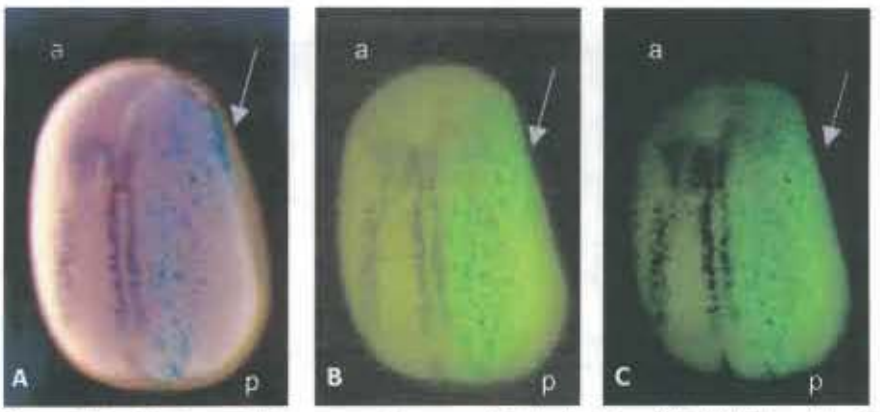

Figure 4.12: Visualisation of *Xenopus* embryos co-injected with mBF-1-GFP and *lacZ*, after in situ hybridisation, to show that the expressed fluorescent protein can be detected within the same region as in which *lacZ* is expressed (B and C). Comparison of the expression of *lacZ* (A) or GFP (B and C) with *N-tubulin* showed that *N-tubulin* is not expressed within the region of GFP or *lacZ* positive cells. Expression of the intermediate *N-tubulin* domain is suppressed and the lateral domain is moved further laterally and/or ventrally, in regions of GFP and *lacZ* negative cells. *LacZ* can be used to delineate the migration and region of expression of the inherited DNA, but the expression and use of the fluorescent gene is a more precise lineage marker. C is a low intensity copy of B to show the expression of GFP in GFP positive cells. a: anterior, p: posterior

In the neurula stage (stage 15/16; Nieuwkoop *et al.*, 1967) of mBF-1-GFP injected embryos, GFP fluorescence and/or *lacZ* were used to locate mBF-1-GFP expression within the embryos. The expressed mBF-1-GFP was found distributed either in a broad band within the intermediate and lateral *N-tubulin* stripes of half the injected embryos, or found in a much broader band within the lateral domain of the embryo in the remaining half of the injected embryos (n=12). This distribution was spread along the anterior-posterior axis and was within the same region as the *lacZ*-positive cells. In these embryos, the lateral *N-tubulin* domain was suppressed, with the ectopic expression of *N-tubulin* on the ventral side of the *lacZ*-expression domain. In three of these embryos, this expansion was found across the entire lateral domain and into the ventral side of the embryo. In three of the embryos, the *lacZ* was found dispersed within the expanded *N-tubulin* domain in the ventral side of the embryos. Although dispersed, the *N-tubulin* and the *lacZ*-positive cells were found grouped into clusters respective of each of the different proteins, rather than interspersed within this region.

The *X*BF-1 DNA samples were not fused to the fluorescent gene (Figure 4.13). In the *X*BF-1 injected embryos, the *lacZ* tracer signal was found distributed between the medial and intermediate *N-tubulin* domains of the embryo, displacing the distribution of *N-tubulin* within this region (Figure 4.13 C). The lateral *N-tubulin* domain was shifted further into the lateral region of the embryo as compared to the uninjected side. For the remaining embryos, the *lacZ* signal was found located towards the posterior region of the embryo, and found interspersed freely within the region of cells where *N-tubulin* has been ectopically expressed. The normal bilateral *N-tubulin* stripes are seemingly unchanged, however, ectopic expression of *N-tubulin* was found across the lateral regions of the embryo, expanding into the ventral side of the embryo (Figure 4.13 E and F).

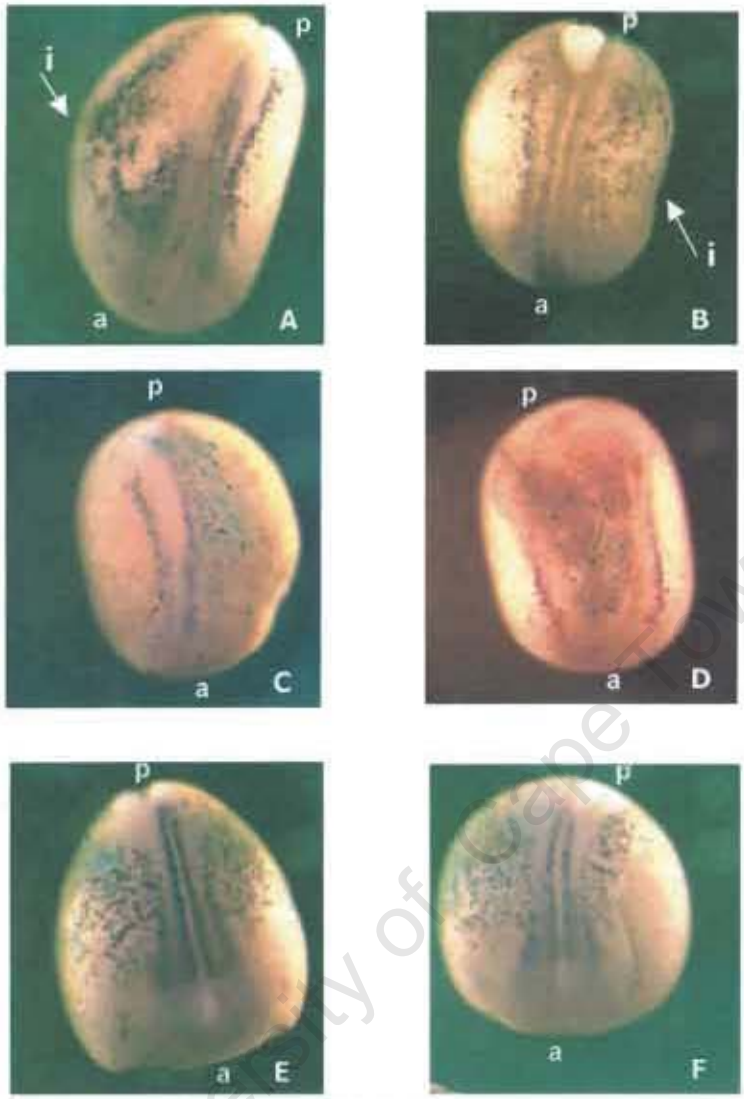

Figure 4.13: Low staining of the injected embryos with X-gal (A and B). As high levels of *lacZ* expression are required for X-gal staining, not all cells expressing *lacZ* will stain blue. Injection of *X*BF-1 DNA, without *lacZ* (A), shows a perturbation in all 3 *N-tubulin* stripes of the injected side (i) of the embryo, resulting in the expansion of the *N-tubulin* domains. This is similar to (B) where mBF-1-GFP has been co-injected with *lacZ*. Injection of the mBF-1-GFP with *lacZ* (B and D) and *X*BF-1 with *lacZ* (C, E and F) shows how *lacZ* can be used to visualise the injected side of the embryo. The expression of BF-1 and *lacZ* are located within the medial domains of *N-tubulin* in, C and D, suppressing the expression of the medial and intermediate *N-tubulin* domains. Visualisation of the distribution of *X*BF-1 DNA co-injected with *lacZ* DNA (E and F) shows that *X*BF-1 and *lacZ* have been inherited on both sides of the embryo (E and F). a: anterior, p: posterior.

One of the embryos injected with mBF-1-GFP and *lacZ* only (Figure 4.13 C), had a similar distribution of the *lacZ* and the mBF-1 protein as that of the *X*BF-1 injected embryo (Figure 4.13 D), that is these signals were located within the medial-midline region of the injected embryo, replacing the medial and intermediate *N-tubulin* domains within this region (Figure 4.13). However, the remaining mBF-1-GFP injected embryos displayed a similar *N*-

tubulin distribution as that of the *X*BF-1 injected embryos, where the lateral *N-tubulin* domain was expanded throughout the lateral region of the injected side of the embryo.

Of the nine mBF-1-EYCP embryos co-injected with *lacZ* mRNA and probed for both *N-tubulin* and *XSox3*, only two of these embryos had clearly visible *lacZ*-positive cells, while the rest had a weak *lacZ* signal. In one of these two embryos, the blue-stained *lacZ*-positive cells were found distributed in the anterior region of the embryo, just beyond the marginal zone demarcated by *XSox3* at the anterior neural fold. In the second *lacZ*-positive embryo, the X-gal stained cells were distributed in a broad band within the intermediate region of the *N-tubulin* domain, replacing the *N-tubulin* domain within this region (Figure 4.14 A). The expression of the lateral *N-tubulin* domain was suppressed within this region. However, in the ventral region, *N-tubulin* was ectopically expressed where *lacZ* positive cells were absent (yellow arrow). While the *XSox3* band of expression remained in a fairly narrow band between the medial and intermediate *N-tubulin* domains in the uninjected side (u) of the embryo, in the injected side, the *XSox3* domain had expanded into the lateral side of the embryo. Part of the expanded *XSox3* region overlapped with the *lacZ* positive region (blue arrow). However, the *lacZ* positive cells appear to occlude the presence of the *XSox3* and the *N-tubulin* domains within the region of where *lacZ* is expressed (Figure 4.14 A).

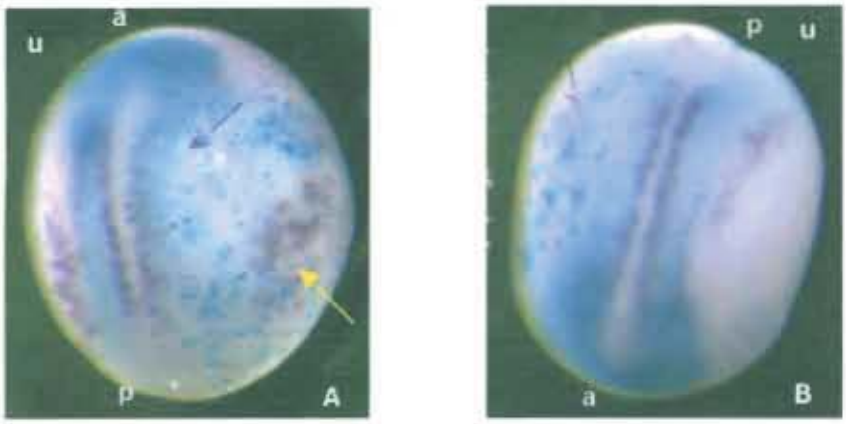

Figure 4.14: Co-injection of mBF-1-EYFP DNA (A) and mBF-1-ECFP DNA (B) each with *lacZ* DNA, followed by double in situ hybridisation using *N-tubulin* (purple dotted cells) and *XSox3* (light blue diffuse *XSox3* expression pattern) as probes. In situ hybridisation shows how the *XSox3* domain (blue arrow), normally expressed within the medial and intermediate domains of *N-tubulin*, has expanded into the intermediate and lateral regions of *N-tubulin* expression domains, and diffusing into the *lacZ* (dotted blue expression) expressing-cell regions. The expansion of the *XSox3* domain has also resulted in the suppression of the expression of the intermediate and lateral *N-tubulin* domains, as well as in the ectopic expression of *N-tubulin* further ventrally, in regions where *lacZ* positive cells are absent (A, yellow arrow). u= uninjected side. a: anterior, p: posterior.

Injection of mBF-1-EYFP (Figure 4.14 A) and mBF-1-ECFP DNA (Figure 4.14 B) into the *Xenopus* embryos gave rise to a similar morphology as that of the high dosage *X*BF-1 injected embryos (Bourguignon *et al.*, 1998). That is the *XSox3* expression domain was expanded, while the lateral *N-tubulin* domains was suppressed, with ectopic expression of *N-tubulin* into the ventral region of the embryo. The expression of the *lacZ* signal was within the intermediate and lateral parts of the embryos.

4.2.4 Transient transfection of OP6 cell line

To study the localisation of mBF-1 *in vitro*, transient transfections, using mBF-1-GFP as the experimental construct and pCSGFP3 as the control plasmid, were carried in the OP cell line. The transfected cells were visualised using a fluorescent microscope.

The pCSGFP3 and mBF-1-GFP constructs were transfected into the OP6 cells using the FuGene6 transfection method. Using pCSGFP3 as the control plasmid, the initial transfections showed that pCSGFP3 was expressed throughout the cytoplasm and the nucleus of the

transfected cells, when the cells were viewed under the bright field and fluorescence microscope (Figure 4.15 B).

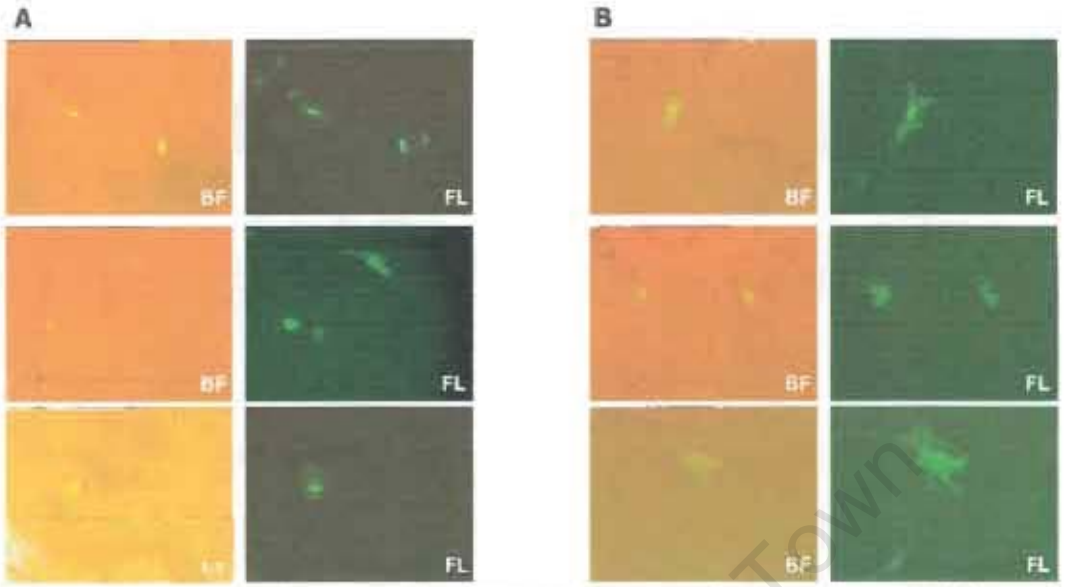

Figure 4.15: mBF-1-GFP (A) and pCSGFP3 (B) were transfected into the OP6 cell line and visualised using bright field (BF) with fluorescence, and under GFP fluorescence (FL) only, to locate the transfected cells in culture, and to show the localisation of the fluorescent proteins with respect to the entire cell. GFP fluorescence of the pCSGFP3-transfected cells was located throughout the cytoplasm and the nucleus (B), whereas the GFP fluorescence of the mBF-1-GFP transfected cells was located within the nucleus only (A). As the constitutively active CMV promoter drove the over-expression of the mBF-1-GFP construct in the transfected OP6 cells, large amounts of the expressed protein was toxic to the cells. This resulted in the packaging of excess expressed protein into cytoplasmic vesicles or bodies, in the mBF-1-GFP transfected cells, giving rise to the seemingly cytoplasmic distribution of the expressed construct (A).

Transfection carried out using the mBF-1-GFP DNA showed that the fluorescence from the expression of the fluorescent fusion construct was localised within the nucleus (Figure 4.15 A). This confirmed the *Xenopus* injection studies where mBF-1-GFP was nuclear located (Figure 4.10 A), unlike the pCSGFP3 control, which was located in a diffuse pattern across the embryo (Figure 4.10 A).

To verify that the mBF-1-GFP protein was nuclear localised, the tranfected cells were fixed and stained with Hoechst, to stain for nucleic acid (Figure 4.16 A). The results showed that that the expressed mBF-1-GFP fusion protein was indeed nuclear localised, as visualisation of the same culture, in the exact same region under fluorescent or UV light, resulted in an overlap of the mBF-1-GFP fluorescence and Hoechst stain dye (Figure 4.16 A).

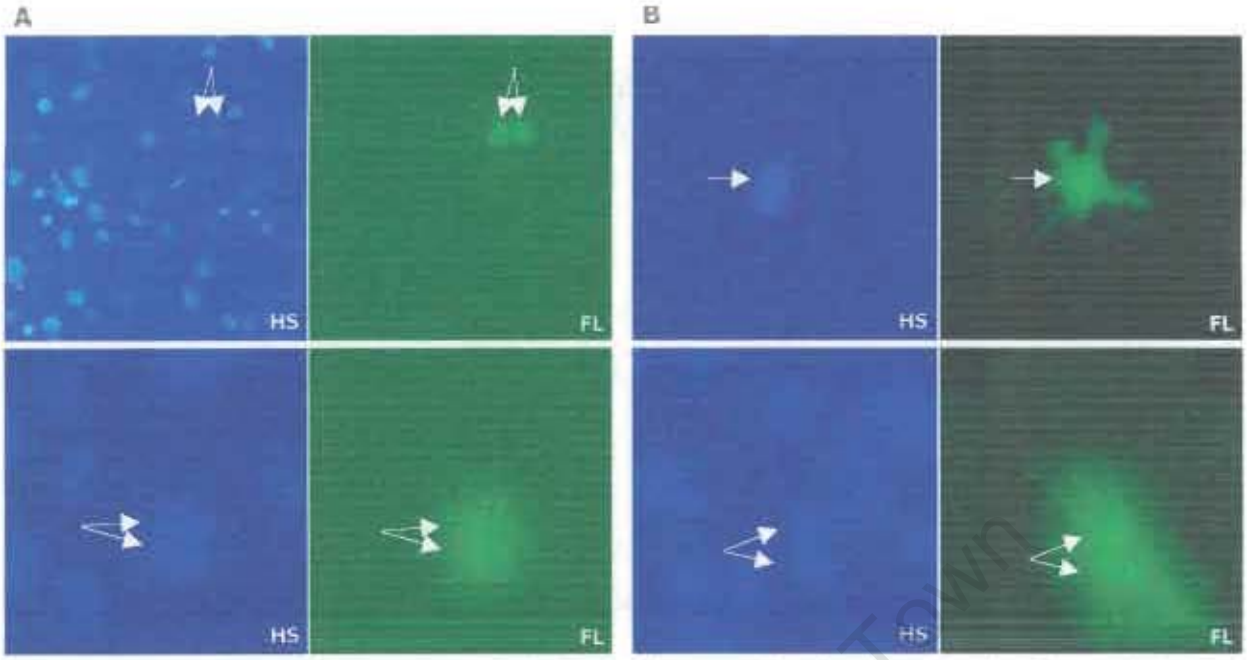

Figure 4.16: Transfected cells were stained with Hoechst to confirm that the expression of the mBF-1-GFP construct was localised within the nucleus (A), whilst the expression of the pCSGFP3 control was distributed throughout the cytoplasm (B). The GFP fluorescing cells (FL) and their corresponding Hoechst stained nuclei (HS) are indicated by the white arrows.

Visual estimation of the GFP fluorescent cells of both the mBF-1-GFP-transfected and the pCSGFP3-transfected cells suggested that the transfection efficiency of the constructs into the OP6 cell line was low. To obtain a more accurate estimate of the transfection efficiency of pCSGFP3 and mBF-1-GFP DNA transfected into the OP6 cells, an independent reporter gene was employed for the calculation of transfection efficiency. The cultured cells were co-transfected with pCSFP3 and pCMVβ-Gal and the expressed reporter gene was analysed by staining the cultured cells with the X-gal histochemical stain. After staining of the fixed cells with the X-gal histochemical stain, the number of X-gal stained cells of three different areas of the plate, under bright field, were enumerated as a percentage of the total number cells per view, and the average transfection efficiency was found to be 10% (Figure 4.17). The pCMVβ-Gal reporter gene was also expressed throughout the entire cell or cytoplasm, and not localised to the nucleus only (Figure 4.17 at 20× magnification).

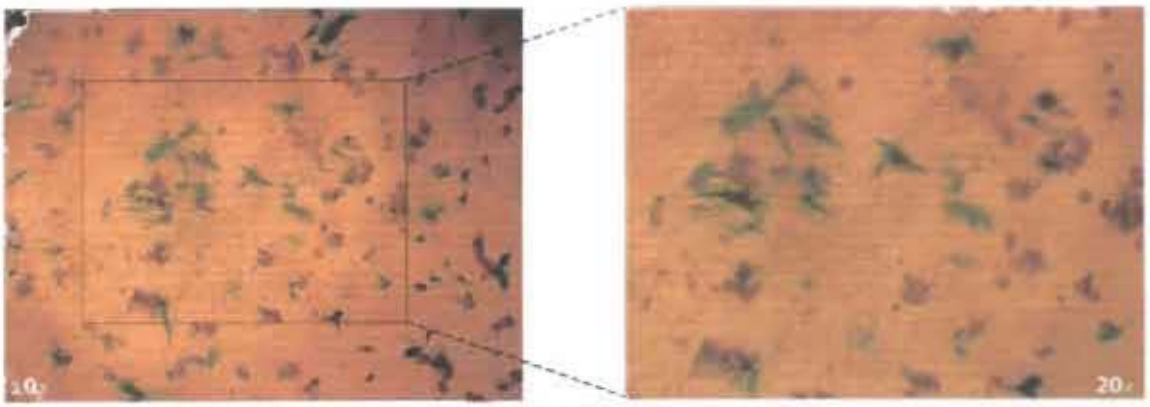

Figure 4.17: OP6 cells co-transfected with pCSGFP3 and pCMVβ-Gal were used to calculate the transfection efficiency. The total number of the X-gal positive cells per view, under bright field, as a percentage of the total number of cells visualised per view showed that the average transfection efficiency was only 10%.

Taking advantage of the low transfection efficiency, specifically identified cells were tracked to determine whether or not morphological changes could be followed on a cell-by-cell basis. Tracking of specific cells undergoing proliferation or differentiation, as well as the localisation of the protein expressed from the mBF-1-GFP construct transfected into the cells, was essential for the precise description and characterisation of the spatial regulation and role of BF-1 during neuronal progenitor cell growth and development. Cells were plated and transfected on the CELLocate (Eppendorf) coverslip, and specifically marked cells were followed, using GFP-positive cells, over three days. The cells could, however, only be monitored for two to three days.

In Figure 4.18 only one of the GFP-positive cells (1) of the pCSGFP3 transfected cells (P) could be followed for three days. (1) was localised at the exact same position for day one and two, but had moved almost two cell widths by day three. (2) had been visible for two days, while (3) had likely been a detached rounded up cell, on day one, which floated away with time and was thus not visible on subsequent days.

In the mBF-1-GFP transfected cells (W), three cells were identified on day two only, that had not been visible on day one at all (data not shown). From the high density of the cells cultured on this coverslip, it is likely that these cells may have been embedded beneath other cells on day one, and due to the migration of cells, were uncovered by day two. However, by day three, the cells located in W (marked by arrowheads) on day two seem to have detached and migrated or floated away from their original location. Thus the tracking of specific cells seemed to be possible for a short time period only.

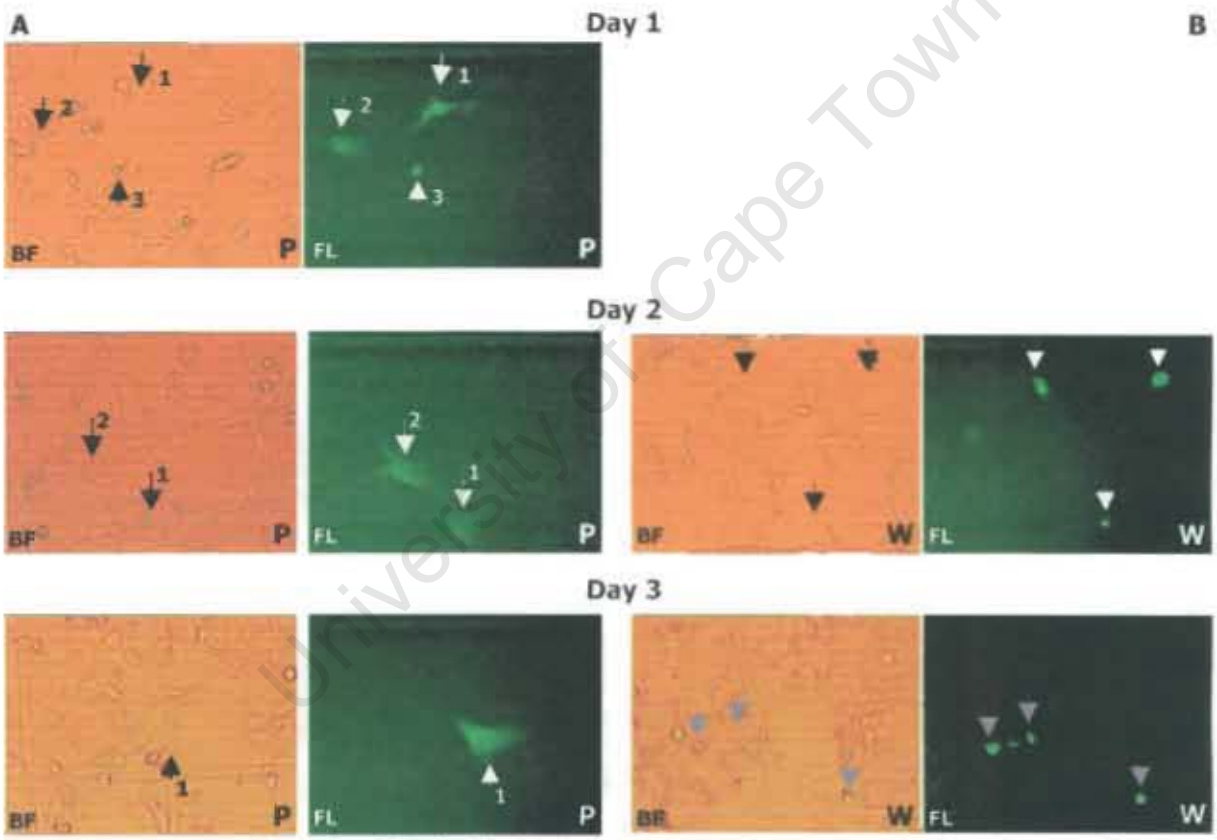

Figure 4.18: Tracking of specifically identified pCSGFP3-transfected (A) and mBF-1-GFP-transfected (B) cells by plating onto CELLocate (Eppendorf) coverslips. In A, cells located at coverslip engraving P, could only be followed for three days (1), as the GFP-positive cells died (3) or migrated elsewhere (1 and 2) on the surface of the coverslip, and were no longer visible in the same location after a few days. In B, the cells located at coverslip engraving W, could only be located from day two onwards, and only for two days. No cells had been GFP positive at this location on day one, suggesting that these cells were may have had been embedded within the dense population of cells on the coverslip, and thus not detected on day one. On day three (in B) all the GFP-positive cells seem to have migrated to a different location within the same view (indicated by the grey arrows).

4.3 Discussion

4.3.1 Construction and verification of the mBF-1 plasmids

This study was set up to investigate the localisation of BF-1 in the OP cell lines. To this end, mBF-1 fluorescent fusions were generated to facilitate the monitoring of the localisation of BF-1 within the cell lines. The constructs were sequenced, the results of which confirmed that no sequence variations, such as frameshifts, had occurred.

4.3.2 Analysis of the distribution and functionality of the expressed mBF-1 fluorescent fusion proteins

Injection of the constructs into *Xenopus* embryos confirmed that there were no sequence rearrangements, as the fluorescent fusions was expressed and could be detected when the embryos were viewed under the fluorescent microscope. Preliminary analysis by comparing fluorescence of the mBF-1-GFP injected embryos versus the pCSGFP3 injected embryos showed that the mBF-1-GFP signal was directed to the nucleus whilst the pCSGFP3 signal was found diffused throughout the embryo. Thus the mBF-1 fluorescent fusion constructs were successfully generated and able to express the fusion protein.

The patterns of expression of the fluorescent fusion protein constructs in *Xenopus* embryos were analysed to assess the functionality of mBF-1 as a fluorescent-fusion construct, and when mBF-1 was not fused to the fluorescent gene. The ultimate *in vitro* experiment to conclude this work would be to compare the localisation of BF-1 in proliferating neuronal progenitor cells to the localisation of BF-1 in cells induced to differentiate by the addition of RA and FGF2 to the cells. This would enable the investigation into whether the spatial localisation of BF-1 played a role in regulation of BF-1 function during neuronal development. Thus it was important to assess the functionality of the mBF-1 fluorescent fusions in *Xenopus*

embryos prior to their transfection into the OP cell lines. This would ensure that the changes resulting from cell culture manipulations (for example addition of RA and FGF2) to the cells was due to the RA and FGF2 rather than to a non-functional mBF-1 fluorescent fusion protein, especially a non-functional mBF-1 protein.

Double *in situ* hybridisation with *N-tubulin* and *XSox3* showed that injection of the pCSGFP3 and *lacZ* DNA, each on their own, enabled the visualisation of the fluorescent gene and the X-gal-positive cells without any perturbation to the normal expression of the tissue-specific markers. This indicated that GFP fluorescence and *lacZ* expression could be utilised as lineage-specific markers without affecting the expression or distribution of the fluorescent fusion constructs injected into the embryos. Injection of the *lacZ* DNA along with the fluorescent fusion constructs enabled visualisation of the localisation of the injected construct without the need for use of a fluorescent microscope.

Injection of the low dosage (100 pg) of the mBF-1-fluorescent fusion construct DNA, and co-injection with the *lacZ* DNA, resulted in the suppression of the endogenous lateral, and, in some of the embryos, the intermediate *N-tubulin* expression domains within the region of GFP and *lacZ* positive cells. However, ectopic expression of *N-tubulin* was observed in the GFP and *lacZ* negative areas of adjacent cells. Comparison of the mBF-1-fluorescent fusions (DNA) with the *X*BF-1 (mRNA) injected embryos at the low concentration of mBF-1-GFP, 100 pg, showed that the mBF-1 fusion constructs displayed a suppression of the intermediate and lateral *N-tubulin*. These results suggest that the CMV driven mBF-1 fusion constructs exhibit phenotypes characteristic of the high dosage *X*BF-1 mRNA injections. That is, even at a low concentration of DNA, the CMV promoter drove the expression of the injected DNA to give rise to phenotypes that were equivalent to the high dosage *X*BF-1 RNA injected phenotypes. Experiments would need to be carried out, however, to determine the phenotypes

of "low" dosage DNA injections. Injection of higher DNA dosage (200 pg or more) had resulted in the expression of ectopic protein levels that led to the toxicity and death of the injected embryos (data not shown). Too low DNA concentrations (40-50 pg) of the injected have also resulted in the absence or the inability of the visualisation of the GFP positive cells, suggesting that DNA injections may not be as stable or as functional as the mRNA injections. It is suggested that future experiments be undertaken utilising the in vitro transcribed mBF-1 fluorescent fusion constructs and the effect of dosage on the growth development of the *Xenopus* neuroepithelium be investigated, as GFP fluorescence provides a useful tool by which to localise ectopic BF-1 expression *in vivo*.

These injection experiments also confirmed that the expression of BF-1 was responsible for the perturbations of the expression of *N-tubulin* and *XSox3*. From these results it was concluded that the mBF-1, when fused to the fluorescent gene, was expressed as a functional protein, and that mBF-1 was able to direct the expressed mBF-1-GFP protein to the nucleus.

We also show that the antisense mBF-1 is unable to drive the ectopic expression of the *N-tubulin* and thus re-confirm our previous findings that our constructs were in frame and functional, and that the resultant protein could be detected by fluorescence. Thus the mBF-1-GFP construct was chosen for use in subsequent cell culture and transient transfection studies to investigate the spatial regulation of BF-1 during neuronal progenitor cell proliferation and upon induction to differentiate

4.3.3 Transfection of the OP6 cell-line

The transfection of mBF-1-GFP had been carried out successfully, albeit at a low transfection efficiency and only for transient expression.

We have shown that mBF-1-GFP is located within the nucleus, while the pCGFP3 was located throughout the cytoplasm. These results correlate with previous observation of the constructs in the *Xenopus* embryos, wherein the mBF-1-GFP injected embryos displayed a punctate fluorescence signal, while the pCSGFP3-injected embryos had a diffused distribution of the fluorescence signal (Figure 4.4 C).

4.3.4 Monitoring of specific cells

Induction of cell differentiation by the addition of RA (see section 2.1.12) had been attempted on synchronised and transfected OP6 cells (none of the results were shown). High cell death of the GFP-positive cells was observed, resulting in the inability to investigate or visualise changes in the cell morphology or in the spatial localisation of the mBF-1GFP in these cells. Also, cells undergoing differentiation versus cells undergoing proliferation or lag phase growth were indistinguishable in culture (data not shown). Thus the tracking of specifically identified cells had been investigated in an attempt to identify morphological changes of specifically marked cells.

Cells could only be monitored for two to three days and this restriction could be attributed to a number of factors that need to be optimised in future cell tracking experiments. The first restriction arose through the cell density, where a reduction in the competence and the number of the cells that took up the DNA construct was observed (Figure 4.6 F (B)). The manufacturer's of the FuGene6 transfection reagent (instruction manual; Roche) recommended that the cells be approximately 50 to 80% confluent at transfection, for the efficient uptake of the DNA. However, too high a cell density could also mask the fluorescence of cells that may have taken up and were expressing the DNA, as these cells were embedded and could not be visualised under the fluorescent microscope at that time (Figure 4.6 F (B)). Another restriction

could be attributed to the constitutively active CMV promoter that drove the expression of the gene of interest. Expression of high levels of the gene of interest may have resulted in high levels of protein becoming toxic to the cells. This toxicity could have resulted in the cell death or in the cells packaging the toxic/excess protein into vesicles and expelling the protein from the nucleus (Figure 4.15 A) or the cell. Migration of cells during culture was advantageous here as it enable the unmasking of the embedded cells, however, for the tracking of specifically marked cells, migration is detrimental to the experiment. Higher transfection efficiencies of more than 80% would overcome many of the problems encountered in this study.

These experiments have, however, provided the basis upon which to optimise transfection efficiencies, as well as to support the need to generate stably transfected cell lines that would enable the observation and investigation of the different experimental effects, such as the induction of the cell line to differentiate, and the study of the localisation of BF-1 over extended periods of time. Different transfections reagents and protocols, such as the calcium phosphate-mediated and the DEAE-dextran methods could also be investigated as alternative methods for the transfection of the OP cell lines. It is also imperative that much optimisation be undertaken to ensure that the cell density is low enough for efficient transfection, but remains high enough for the study to provide valuable information.

5 Conclusion

Little is know of the molecular mechanisms that control BF-1 function. This study aimed to characterise the role of BF-1 during neuronal development by investigating the mechanisms by which BF-1 is regulated during neuronal development.

5.1 Characterisation of BF1-IP$_1$ and BF-1

Two mRNA transcripts of BF1-IP$_1$ and only one BF-1 mRNA transcript were identified by northern blot analysis in total RNA extracted from OP6, OP27 and OP55, but none in OP47 cell lines. These results confirmed that BF1-IP$_1$ and BF-1 were indeed found simultaneously in the same cell line. Semi-quantitative analysis of the expression of both BF1-IP$_1$ and BF-1 during neuronal proliferation and upon induction of the cells to differentiate, would generate valuable data regarding the expression levels and regulation of BF-1 at the transcriptional level, resulting in the further characterisation of BF1-IP$_1$ as a BF-1 interacting protein.

This study was also interested in investigating the level of post-translational regulation of BF-1 by studying endogenous BF-1 protein expression during neuronal cell proliferation and upon induction of the cells to differentiate. Preliminary western blot results have suggested a role for BF-1 at the onset and during the differentiation of the neuronal progenitor cells. The expressed BF-1 protein is proposed to be post-translationally modified upon induction of the cells to differentiate, suggesting that BF-1 may have a direct role in the control of the number of cells that leave the cell cycle to undergo neurogenesis. These results would need to be repeated to generate more conclusive evidence. The regulation of BF-1 during cell proliferation and the post-translational modifications that BF-1 undergoes during neuronal development also need to be investigated. Further experiments could also include the western blot analysis of the ectopic expression of BF-1, using mBF-1-GFP transfected cell lines, to

investigate the levels of ectopic BF-1 expression as compared to the endogenous levels, and to study how these results correlate with the regulation and the role of BF-1 during neuronal development.

5.2 The mapping of the BF-1 domains

Very little is known of BF1-IP$_1$, as BF1-IP$_1$ was isolated as a short C-terminal fragment using the yeast two-hybrid assay. Investigation of the domains of BF-1 required for the interaction with BF1-IP$_1$ would enable the study of how BF-1 interacts with proteins in the cell to carry out its activity, and ultimately clarify how BF-1 is regulated during neuronal development. The construction of the deletion domains was unsuccessful, to varying degrees, for all three of the constructs attempted in this study. Hence, the protocols carried out in this study would need to be optimised, to successfully clone the constructs and to allow for the introduction of these constructs into the yeast two-hybrid system. The subsequent yeast two-hybrid assay for β-galactosidase, to locate the domain involved in these protein-protein interactions, would result in the identification of the BF-1 domain required for protein-protein interactions, with the further characterisation of BF-1 during neuronal development. Additionally, to further characterise BF1-IP$_1$, the isolation of the full-length BF1-IP$_1$ protein would need to be carried out in future experiments. The results obtained from the full-length protein would enable the identification of the BF1-IP$_1$ as well as to elucidate the function of BF1-IP$_1$ during neuronal development.

5.3 Localisation of BF-1 in the OP cell line

To investigate the possible spatial regulation of BF-1, BF-1-fluorescent fusion constructs were successfully generated. Injection of these constructs into *Xenopus* embryos was used to assess the functionality of BF-1, and these injections demonstrated that the BF-1 was functional as a fluorescent fusion, as it is on its own. Transfection of the mBF-1-GFP

construct into the OP6 cell line showed that mBF-1 was able to direct the GFP to the nucleus, whilst transfections carried out using the pCSGFP3 control DNA showed a cytoplasmic distribution of the GFP fluorescence. This confirmed the *Xenopus* injection experiments whereby mBF-1-GFP was nuclear localised whilst pCSGFP3 was located throughout the cytoplasm.

However, to address the question of the visualisation of BF-1 localisation during neuronal progenitor cell proliferation and upon induction of the neuronal cells to differentiate, this study was unsuccessful due to various reasons. The transfection efficiency was low, and future work would require the optimisation of transfection to increase transfection efficiency to 80% or more. The use of alternate transfection reagents could be investigated and optimised in order to increase the number of cells transfected with the DNA of interest. It is also suggested that the generation of a much higher, that is 80 % or more, and more uniformly transfected cell-line could result in transfection efficiencies that would enhance the visualisation of the localisation of BF-1. Moreover, the production of a stably transfected cell line, with the collection of the stable clones, would allow for the establishment of an important population of cells containing the mBF-1-GFP construct inserted into the genome. The expression of mBF-1-GFP using the CMV promoter also resulted in toxic levels of protein expression in the cell-line, due to the constitutively active promoter, whilst the protein expressed using the CMV promoter, in the *Xenopus* embryos, exhibited a "high-dosage" phenotype. These preliminary experiments suggest that the use of an inducible promoter may be more efficient for future studies, in that the amount and the period of induction of mBF-1 in the cell line, to reduce toxicity, can be regulated. Also, the phenotype resultant of a "low-dosage" DNA injection would need to be investigated for comparative analyses.

5.4 Summary

Thus the experiments carried out in this study may provide useful methods by which to investigate the role of BF-1 during neuronal development. Much work remains to be carried out in order to address the questions that this study aimed to investigate. This study has also highlighted the difficulties in the investigation of the regulation of BF-1 function and the role of BF-1 during neuronal development in the olfactory neuroepithelium. However, the olfactory neuroepithelium remains the most important and the simplest of all the regions of the developing anterior neuroectoderm in which to investigate the complex mechanisms by which the developing vertebrate forebrain is co-ordinated.

Appendix 1:

Table 1: List of primers used in this study

Primer Name	Primer Sequence	Function	Source
AS1.5 3' sequencing primer	5' CGTTTTAAAACCTAAGAGTCA 3'	Sequencing of antisense strand of AS1.5 deletion construct across ligation site	UCT Oligo Lab
BF Fs10	5' ACGAGGATCCGGGCAAGGGC 3'	BF-1 sense primer	Boolay (1999)
BF R1474	5' TACGAATTCGGTGGAGAAGGAGTGG 3'	BF-1 antisense primer	Boolay (1999)
Bst-F	5' CTACTGATTTTTCCTCGAGAAGACCTTGACATG 3'	AS1.5$\Delta_{HPQ, DBD, TRD}$ forward primer	UCT Oligo Lab
Bst-mut[F]	5'AGCCACGGTCACTAACCGTCGACCTGC 3'	AS1.5$\Delta_{HPQ, DBD, TRD}$ mutagenesis forward primer	UCT Oligo Lab
Bst-mut[R]	5' GCAGGTCGACGGTTAGTGACCGTGGCT 3'	AS1.5$\Delta_{HPQ, DBD, TRD}$ mutagenesis reverse primer	UCT Oligo Lab
Bst-R	5' GTATTGTTTGTGCACTTGCCGGCATGCC 3'	AS1.5$\Delta_{HPQ, DBD, TRD}$ reverse primer	UCT Oligo lab
EC/EY CMV primer	5' GTAGGCGTGTACGGTGGGAG 3'	Sequencing sense strand of mBF-1-ECFP and mBF-1-EYFP across ligation site	Sigma Genosys
ECFP/EYFP antisense primer	5'CGTCGCCGTCCAGCTCGACCAG 3'	Sequencing antisense strand of mBF-1-ECFP and mBF-1-EYFP constructs across ligation site	Sequence taken from CLONTECH
mBF-1 antisense2	5' GTTGGAAGAAGACCCCTGATTTTGATG 3'	PCR reverse primer	Sigma Genosys
mBF-1 MID primer	5' CAGAACTCCATCCGCCACAAC 3'	Sequencing the middle of mBF-1 insert in sense direction	Sigma Genosys
mBF-1 sense2	5' ACCATGCTGGACATGGGAGATAGG 3'	PCR forward primer,	Sigma Genosys

		adds 5'ACC Kozak sequence to fragment	
Msc-mut[F]	5' TCATCATGATGGTAACCGTCGACCTGC 3'	AS1.5$\Delta_{DBD, TRD}$ mutagenesis forward primer	UCT Oligo Lab
Msc-R	5' GTATTGTTTGTGCACTTGCCGGCATGC 3'	AS1.5$\Delta_{DBD, TRD}$ reverse primer	UCT Oligo Lab
pCSGFP3	5'GTAGGCGTGCCTAATGGGAG 3'	Sequencing sense strand of mBF-1-GFP across ligation site	Sigma Genosys
Primer No. 44	5' CCTGTATAGTTCATCCATGCC 3'	Sequencing antisense strand of mBF-1-GFP across ligation site	Papalopulu N (personal communication)
SP6 promoter primer	5' GATTTAGGTGACACTATAG 3'	Sequencing of mBF-1-CS2	Standard sequencing primers
T3 promoter primer	5' ATTAACCCTCACTAAAGGGA 3'	Sequencing of mBF-1-CS2	Standard sequencing primers
T7 promoter primer	5' GTAATACGACTCACTATAGGGC 3'	Sequencing of mBF-1-CS2	Standard sequencing primers

Appendix 2 A

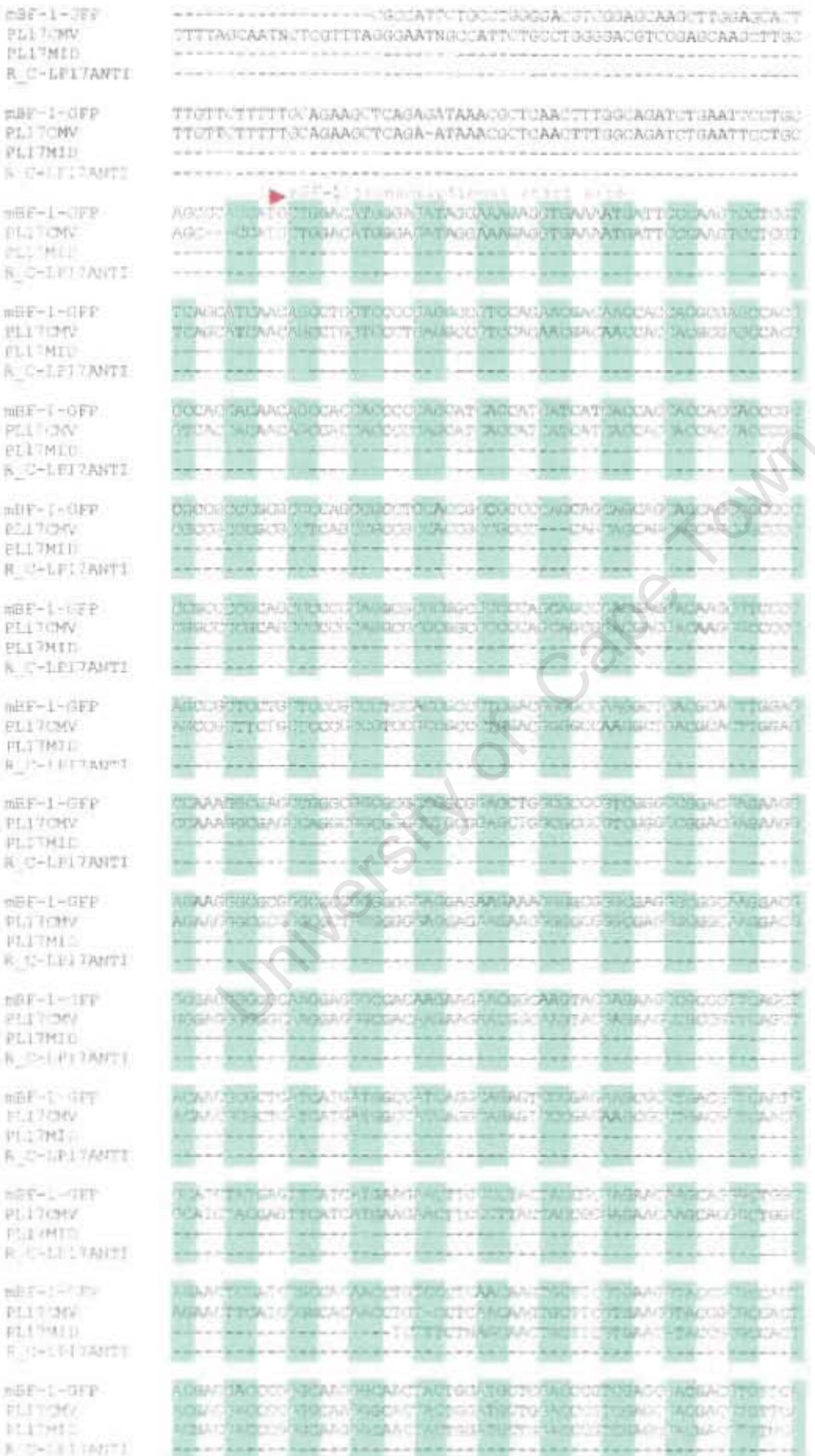

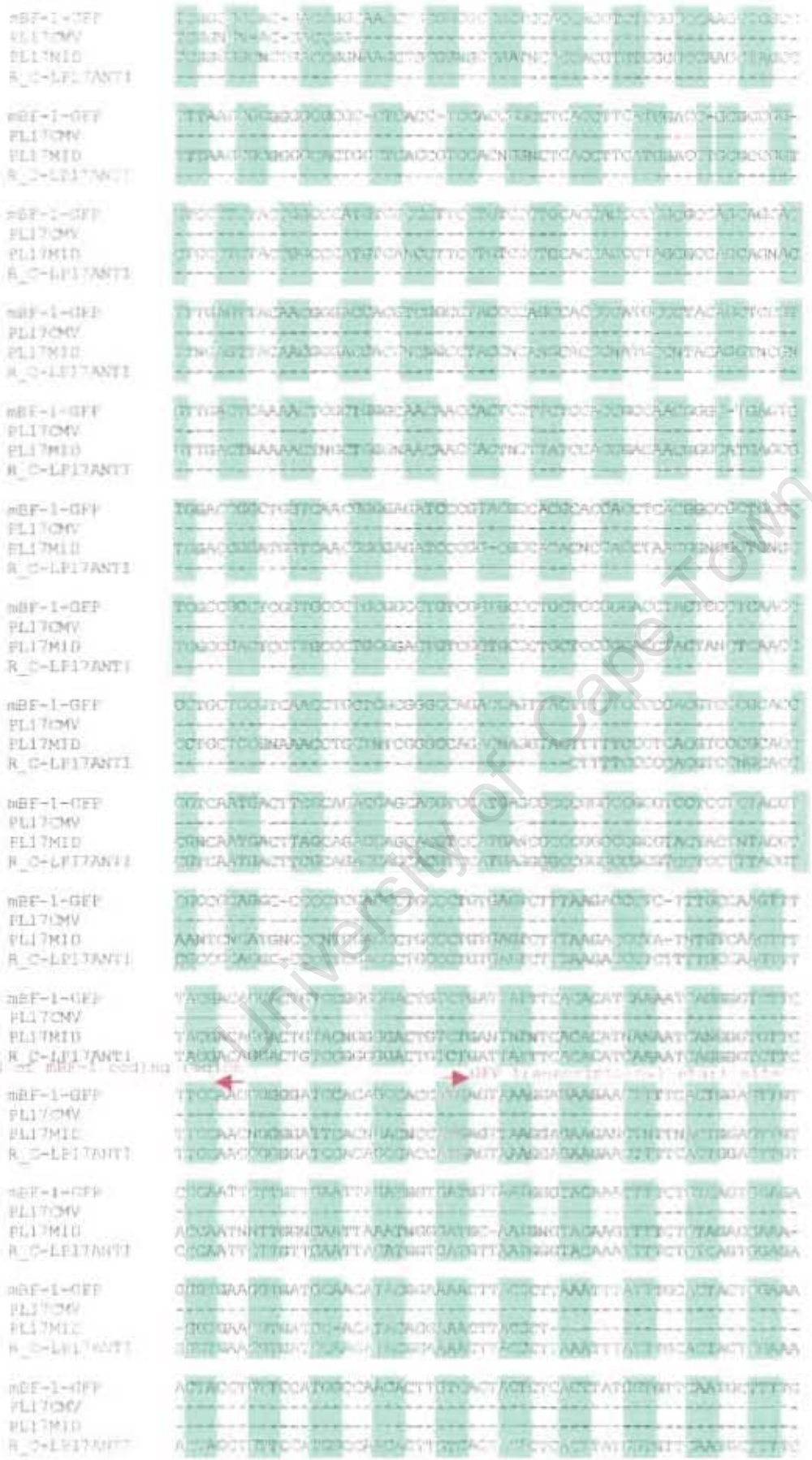

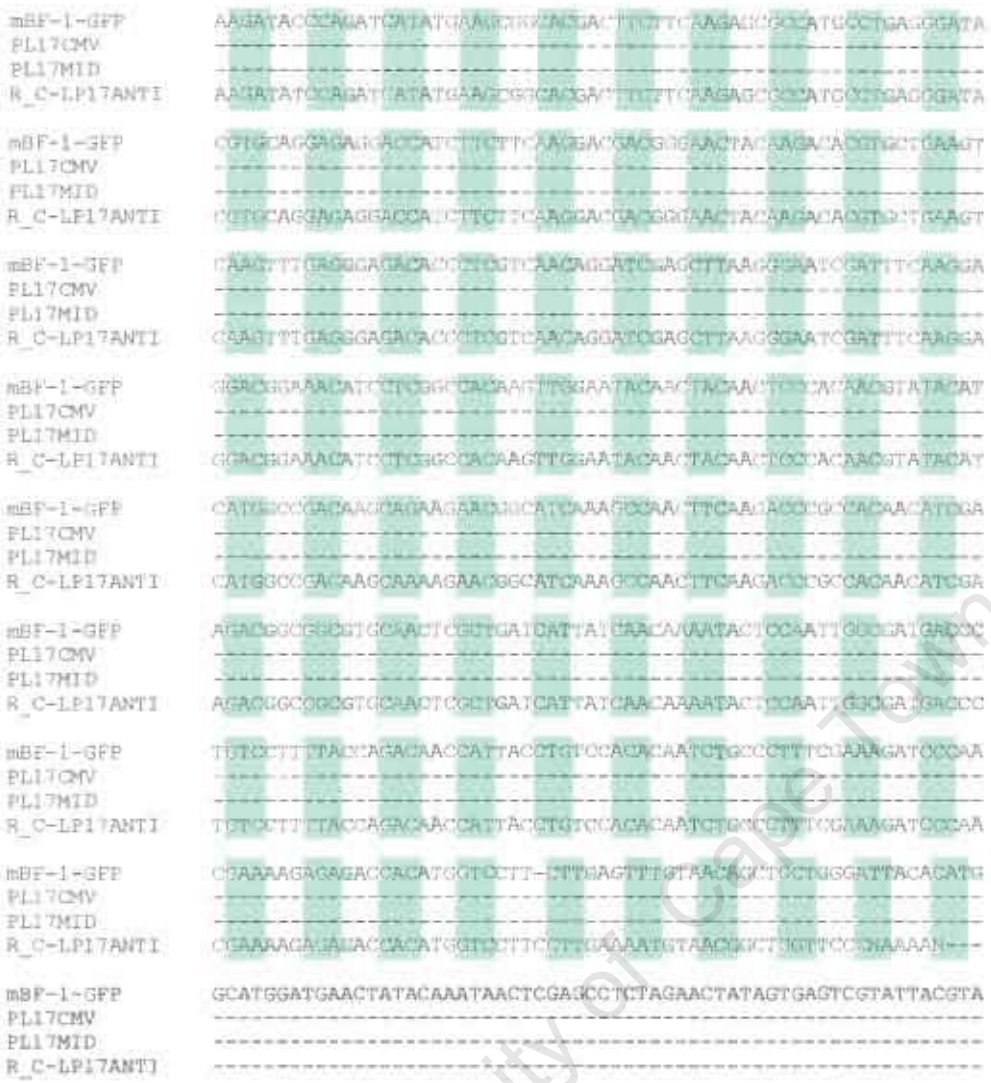

Appendix 2 A: Alignment of the sequencing products obtained using the CMV primer (pCSGFP3 CMV Primer), PL17CMV, the mBF-1 MID primer (mBF-1 MID Primer), PL17MID, and of the antisense primer (Primer No. 44), LP17ANTI, of which the reverse complement sequence is shown (R_C_LP17ANTI), against the theoretical sequence mBF-1-GFP generated in DNAMAN. The correct reading frame is highlighted in green, the Kozak sequence added is in blue, and the transcriptional start codons are indicated in red.

Appendix 2 B

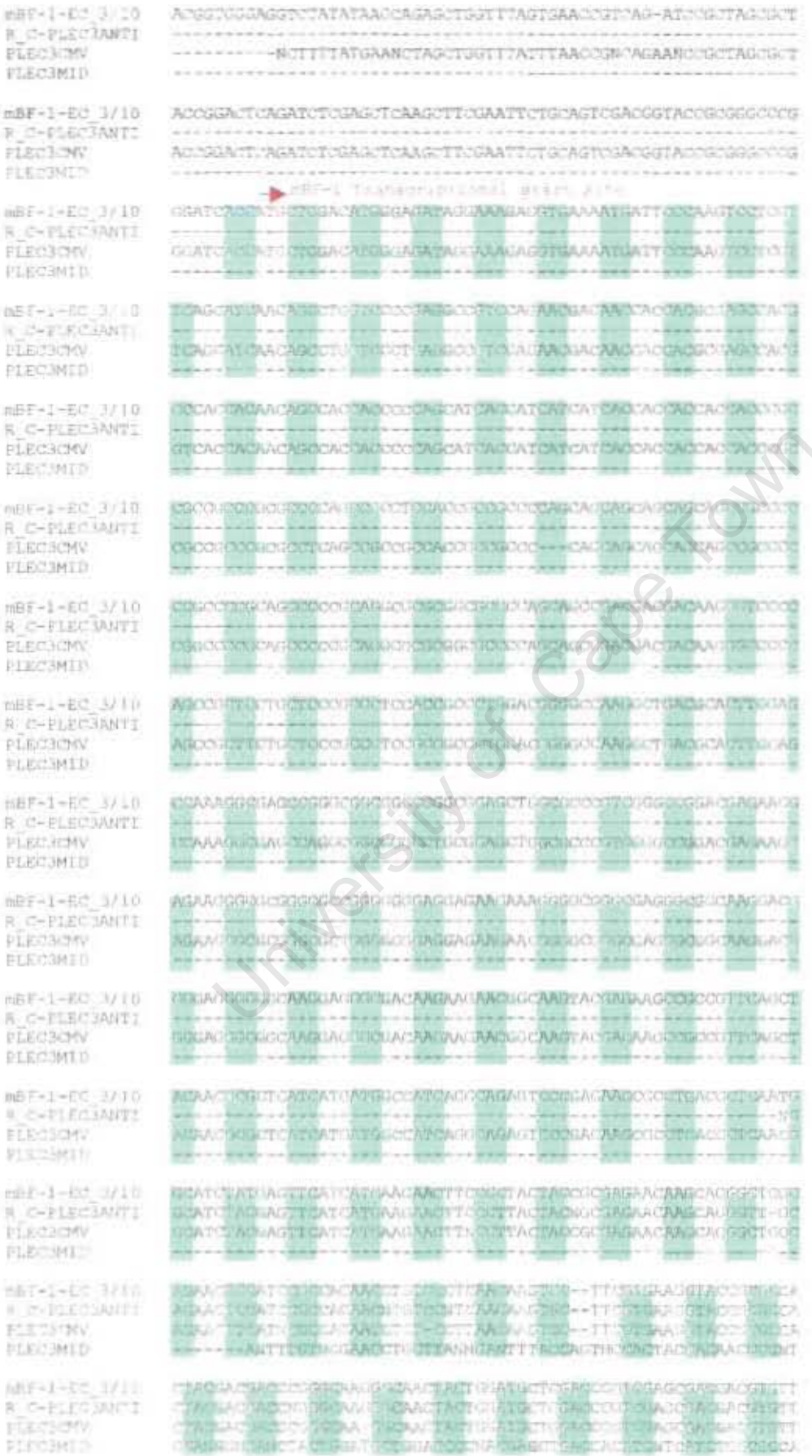

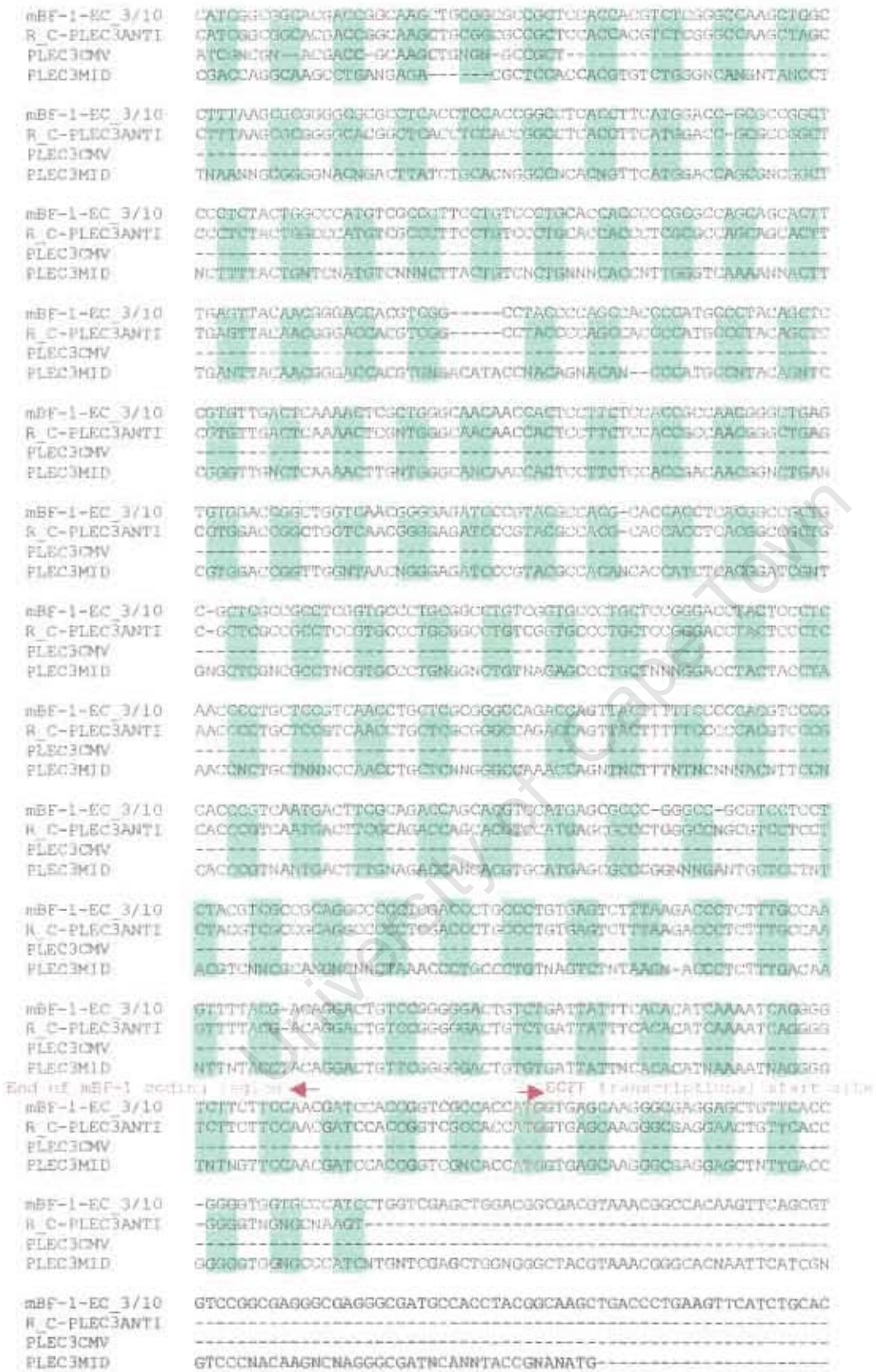

Appendix 2 B: Alignment of the sequencing products obtained using the CMV primer (EC/EY CMV Primer), PLEC3CMV, the mBF-1 MID primer (mBF-1 MID Primer), PLEC3MID, and of the antisense primer (ECFP/EYFP), PLEC3ANTI, of which the reverse complement sequence is shown (R_C_PLEC3ANTI), against the theoretical sequence mBF-1-EC_3/10 generated in DNAMAN. The correct reading frame is highlighted in green, the Kozak sequence added is in blue, and the transcriptional start codons are indicated in red.

Appendix 2 C

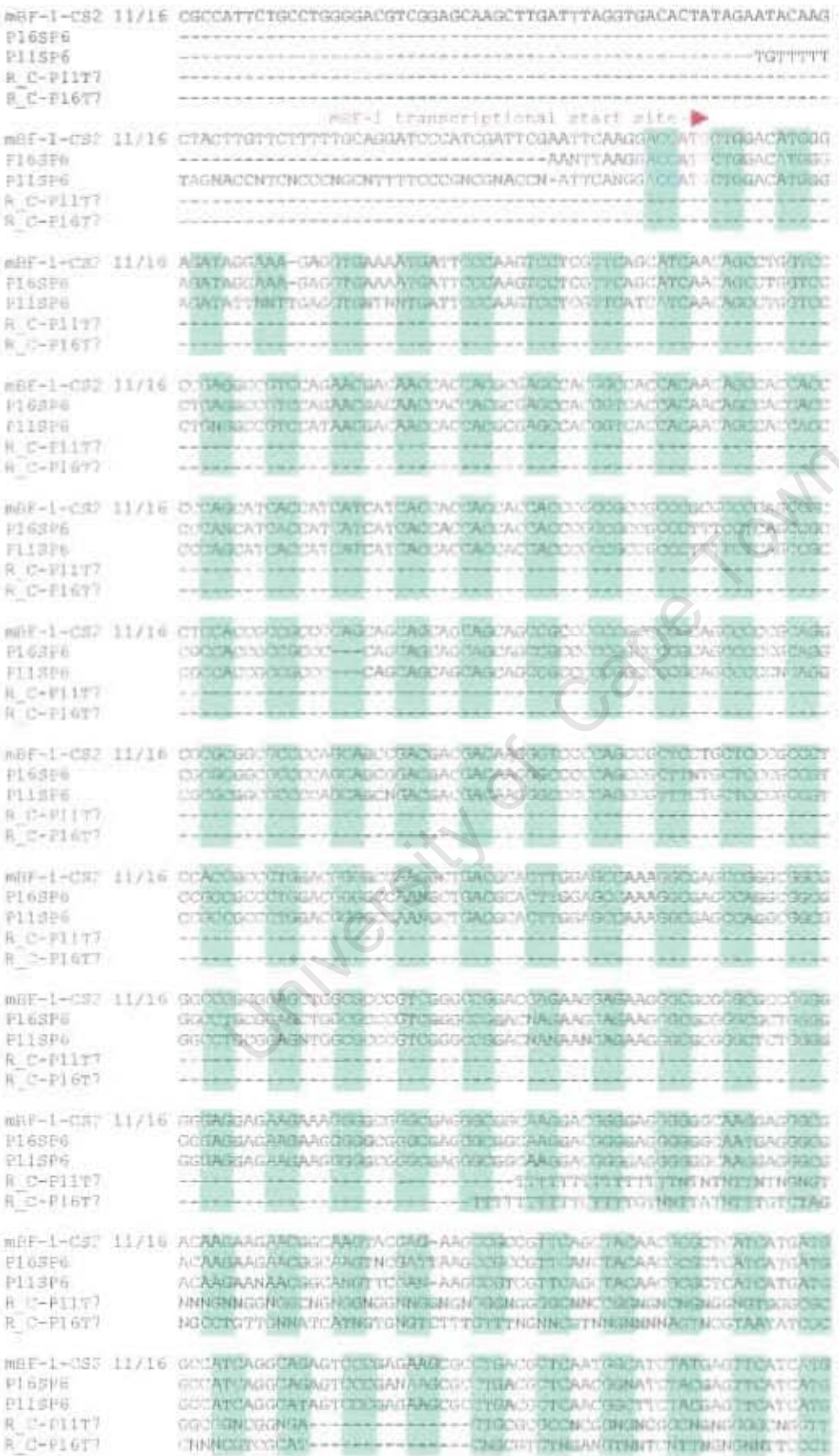

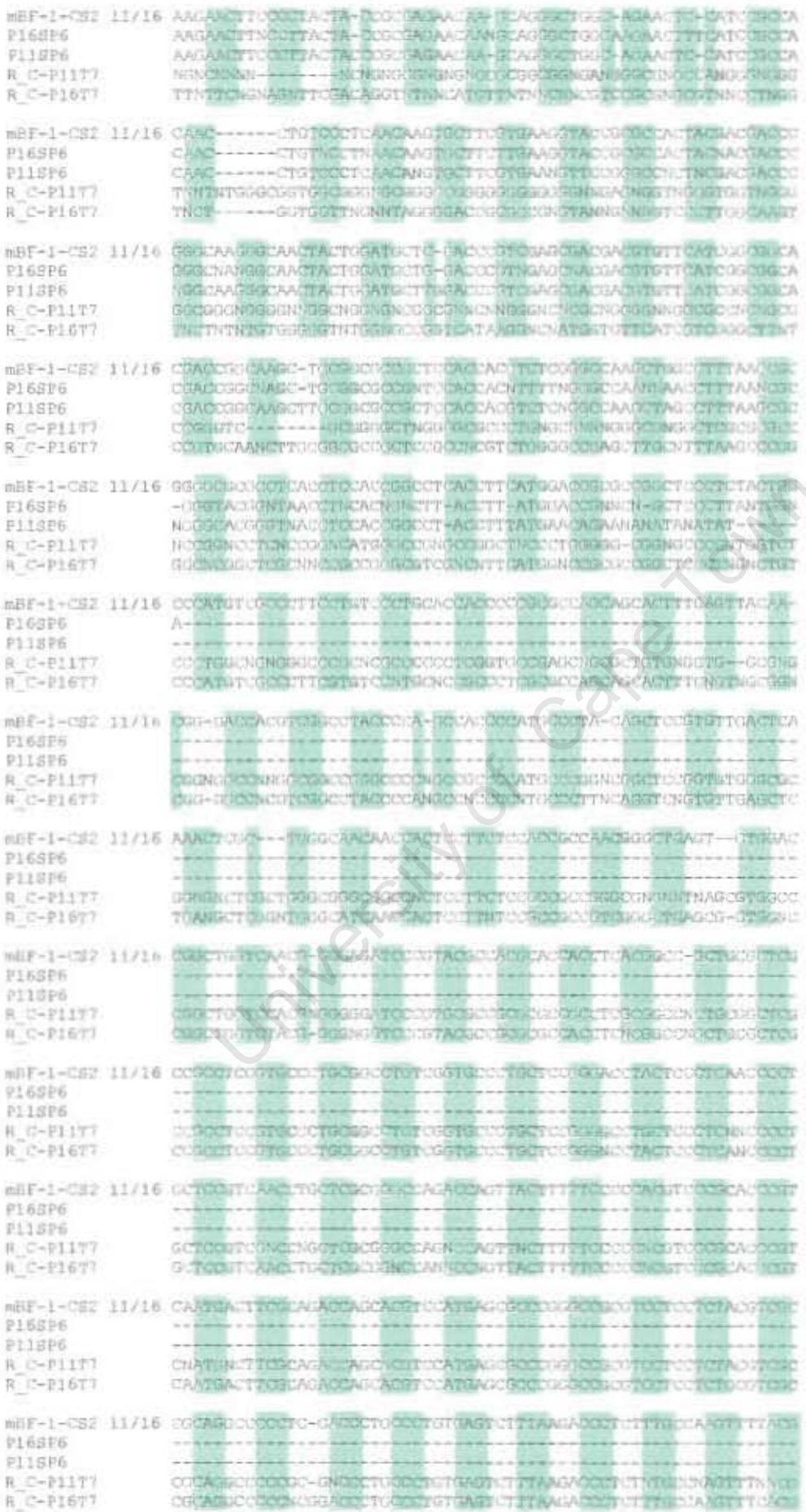

Appendix 2 C: Alignment of the sequencing products, of plasmids mBF-1-CS2 #11 and mBF-1-CS2 #16, obtained using the forward primer (SP6), P11SP6 and P16SP6, and the antisense primer (T7), P11T7 and P16T7, of which the reverse complement sequences are shown (R_C-P11T7 and R_C-P16T7), against the theoretical sequence (mBF-1-CS2 11/16) generated in DNAMAN. The correct reading frame is highlighted in green, the Kozak sequence added is in blue, and the transcriptional start codon is indicated in red.

Appendix 2 D

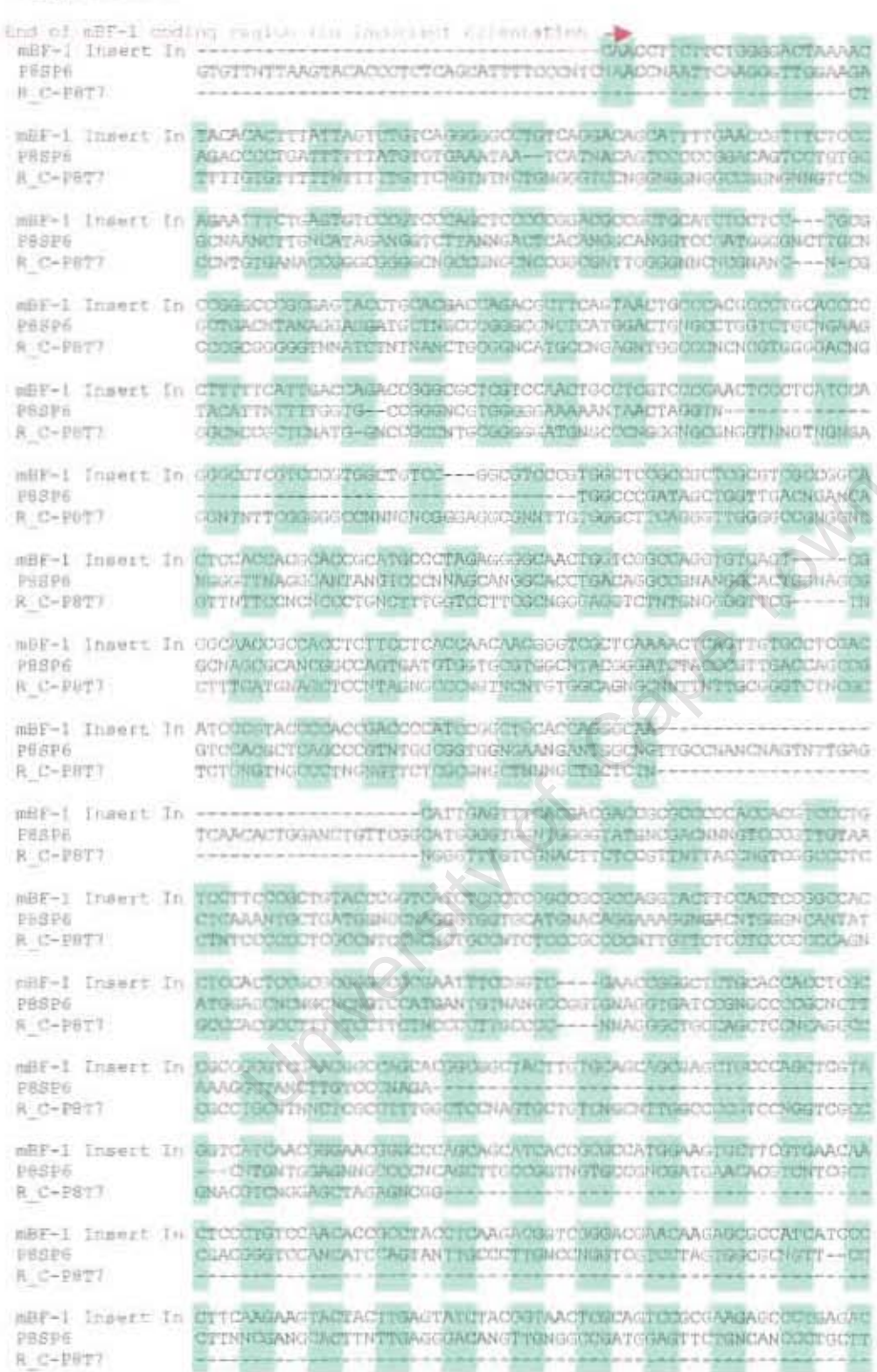

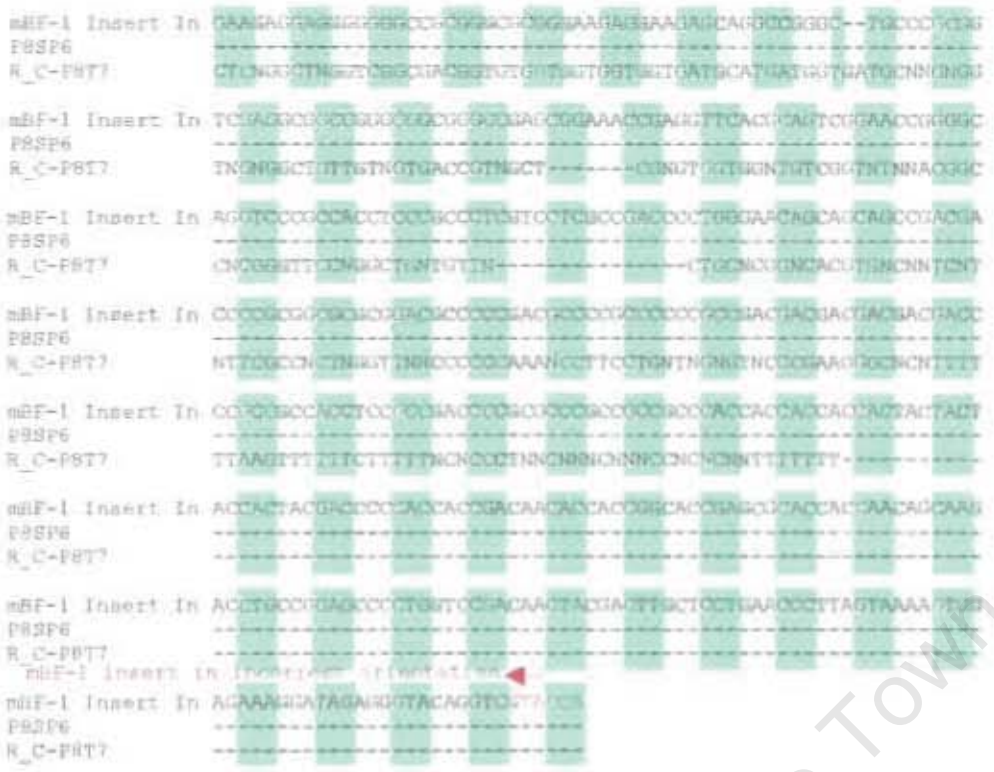

Appendix 2 D: Alignment of the sequencing products, of plasmid mBF-1-CS2 #8, obtained using the forward primer (SP6), P8SP6, and the antisense primer (T7), P8T7, of which the reverse complement sequence is shown (R_C-P8T7), against the theoretical insert sequence in incorrect orientation (mBF-1 Insert In) generated in DNAMAN. The correct reading frame is highlighted in green, the Kozak sequence added is in blue, and the transcriptional start codon is indicated in red.

Appendix 2 E

```
                                                                    score     e
Sequences producing significant alignments:                         (bits)  value

gi|6978844|ref|nm_012560.1|  Rattus Norvegicus Forkhead Box ...      511    e-142
gi|203134|gb|m87634.1|ratbfla  Rat BF-1 mRNA, complete cds           511    e-142
gi|6679842|ref|nm_008241.1|  Mus Musculus Forkhead Box g1 (F...      448    e-123
gi|28422749|gb|bc046958.1|  Mus Musculus, Similar To Forkhea...      448    e-123
gi|1036832|gb|u36760.1|mmu36760  Mus Musculus Brain Factor-1...      448    e-123

>gi|6679842|ref|nm_008241.1|  Mus Musculus Forkhead Box G1 (Foxg1), mRNA
length = 2934

 Score =  448 bits (226), expect = e-123
 Identities = 553/677 (81%), gaps = 9/677 (1%)
 Strand = plus / minus

QUERY: 255  CGGGNCGTGGGGGAAAAANTAACTAGGTNTGGCCCGATAGCTGGTTGACNGANCANGGGT 314
            |||| ||||||||||||| ||||| ||| ||||||| ||| ||||||| |||| ||||
SBJCT: 1807 CGGGACGTGGGGGAAAAAGTAACT-GGTCTGGCCCGCGAGCAGGTTGACGGAGCAGGGGT 1749

QUERY: 315  TNAGGGANTANGTCCCNNAGCANGGCACCTGACAGGCCGNANGGCACTGGNAGCGGCNAG 374
            | ||||| || ||||| |||| |||||| ||||||||| | ||||| |  ||||| ||
SBJCT: 1748 TGAGGGAGTAGGTCCCGGAGCAGGGCACC-GACAGGCCGCAGGGCACCGAG-GCGGCGAG 1691

QUERY: 375  CGCANCGGCCAGTGATGTGGTGCGTGGCNTACGGGATCTACCCGTTGACCAGCCGGTCCA 434
            |||| ||||| |||| |||||||||||| |||||||||| ||||||||||||||||||||
SBJCT: 1690 CGCAGCGGCC-GTGAGGTGGTGCGTGGCGTACGGGATCTCCCCGTTGACCAGCCGGTCCA 1632

QUERY: 435  CGCTCAGCCCGTNTGGCGGTGGNGAANGANTGGCNGTTGCCNANCNAGTNTTGAGTCAAC 494
            | |||||||||| |||||||||| ||| |||| |||||| | | ||| ||||||||||
SBJCT: 1631 CACTCAGCCCGT-TGGCGGTGGAGAAGGAGTGGTTGTTGCCCAGCGAGTTTTGAGTCAAC 1573

QUERY: 495  ACTGGANCTGTTCGGCATGGGGTGGNTGGGGTATGNCGACNNNGTCCCGTTGTAACTCAA 554
            || ||| |||| |||||||||| ||||||| | ||||  ||||||||||||||||||
SBJCT: 1572 AC-GGAGCTGTAGGGCATGGGGTGGCTGGGGTAGGCCGACGTGGTCCCGTTGTAACTCAA 1514

QUERY: 555  ANTGCTGATGGNGCNAGGGTGGTGCATGNACAGGAAAGGNGACNTGGGNCANTATATGGA 614
            | ||||| ||| || |||||||||| | ||||||| || ||| |||| || || | |||
SBJCT: 1513 AGTGCTGCTGGCGCGGGGGTGGTGCAGGGACAGGAAGGGCGACATGGGCCAGTAGAGGGA 1454

QUERY: 615  GCNCNGCNCNGTCCATGANTGTNANGCCGGTGNAGGTGATCCGNGCCCCGCNCTTAAAGG 674
            || | || |||||||| || | ||||||| |||||| || ||||||| ||||||||
SBJCT: 1453 GC-CGGCGCGGTCCATGAAGGTGAGGCCGGTGGAGGTGAGGCGCGCCCCGCGCTTAAAGG 1395

QUERY: 675  CTANCTTGTCCCNAGACNTGNTGGAGNNGCCCCNCAGCTTGCCGGTNGTGCCGNCGATGA 734
            | | |||| ||| |||| || ||||| || || |||||||||||| |||||| ||||||
SBJCT: 1394 CCAGCTTGGCCCGAGACGTGGTGGAGCGGCGCCGCAGCTTGCCGGTCGTGCCGCCGATGA 1335

QUERY: 735  ACACGTCNTCGCTCGACGGGTCCANCATCCAGTANTTGCCCTTGNCCNGGTCGTCCTAGT 794
            ||||||| |||||||||||||| | |||||||| |||||||| || ||||||| ||||
SBJCT: 1334 ACACGTCGTCGCTCGACGGGTCGAGCATCCAGTAGTTGCCCTTGCCCGGGTCGTCGTAGT 1275

QUERY: 795  GGCGCNGTTCCCTTNNCGANGCACTTNTTGAGGGACANGTTGNGGCCGATGGAGTTCTGN 854
            ||||| | | |||| ||| |||||| |||||||||| |||| ||| ||||||||||||
SBJCT: 1274 GGCGCGG-TACCTTCACGAAGCACTTGTTGAGGGACAGGTTGTGGCGGATGGAGTTCTGC 1216

QUERY: 855  CANCCCTGCTTNTTCTNCCGGTACNAANGNTAAGTTCTTCATGNTGAACTCNTAAATGCC 914
            || |||||||| |||| ||||| | | |||||||||||| ||||||| || |||||
SBJCT: 1215 CAGCCCTGCTTGTTCTCGCGGTA-GTAGGGGAAGTTCTTCATGATGAACTCATAGATGCC 1157

QUERY: 915  GNTGAGCNTCAAGCGCT 931
              ||||| ||| |||||
SBJCT: 1156 ATTGAGCGTCAGGCGCT 1140
```

```
 Score =  105 bits (53), expect = 1e-19
 Identities = 101/116 (87%), gaps = 3/116 (2%)
 Strand = plus / minus

QUERY: 48   AAGGGTTGGAAGAAGACCCCTGATTTTTTATGTGTGAAATAATCATNACAGTCCCCCGGA 107
           ||||||||||||||||||||||||| |||| ||||||||||||||||  ||||||||||||
SBJCT: 2000 AAGGGTTGGAAGAAGACCCCTGA-TTTTGATGTGTGAAATAATCA-GACAGTCCCCCGGA 1943

QUERY: 108  CAGTCCTGTGCGCNAANCTTGNCATAGANGGTCTTANNGACTCACANGGCANGGTC 163
           ||||||||| ||  || |||| || ||| |||||||  |||||||| |||| ||||
SBJCT: 1942 CAGTCCTGT-CGTAAAACTTGGCAAAGAGGGTCTTAAAGACTCACAGGGCAGGGTC 1888


>gi|1036832|gb|u36760.1|mmu36760  Mus Musculus Brain Factor-1 (HFHBF1) mRNA,
Class 2, complete cds          Length = 2934

 Score =  448 bits (226), expect = e-123
 Identities = 553/677 (81%), gaps = 9/677 (1%)
 Strand = plus / minus

QUERY: 255  CGGGNCGTGGGGGAAAAANTAACTAGGTNTGGCCCGATAGCTGGTTGACNGANCANGGGT 314
           |||| ||||||||||||| ||||| ||| ||||||| ||| |||||||| || ||||
SBJCT: 1807 CGGGACGTGGGGGAAAAAGTAACT-GGTCTGGCCCGCGAGCAGGTTGACGGAGCAGGGGT 1749

QUERY: 315  TNAGGGANTANGTCCCNNAGCANGGCACCTGACAGGCCGNANGGCACTGGNAGCGGCNAG 374
           | ||||| || |||||  |||| |||||| |||||||| | ||||| |   ||||| ||
SBJCT: 1748 TGAGGGAGTAGGTCCCGGAGCAGGGCACC-GACAGGCCGCAGGGCACCGAG-GCGGCGAG 1691

QUERY: 375  CGCANCGGCCAGTGATGTGGTGCGTGGCNTACGGGATCTACCCGTTGACCAGCCGGTCCA 434
           |||| ||||| |||| |||||||||| |||||||| ||||||||||||||||||||
SBJCT: 1690 CGCAGCGGCC-GTGAGGTGGTGCGTGGCGTACGGGATCTCCCCGTTGACCAGCCGGTCCA 1632

QUERY: 435  CGCTCAGCCCGTNTGGCGGTGGNGAANGANTGGCNGTTGCCNANCNAGTNTTGAGTCAAC 494
           | |||||||||| ||||||||| ||| |||||  |||||| | | ||| ||||||||||
SBJCT: 1631 CACTCAGCCCGT-TGGCGGTGGAGAAGGAGTGGTTGTTGCCCAGCGAGTTTTGAGTCAAC 1573

QUERY: 495  ACTGGANCTGTTCGGCATGGGGTGGNTGGGGTATGNCGACNNNGTCCCGTTGTAACTCAA 554
           || ||| |||| |||||||||| |||||||| | ||||  ||||||||||||||||||
SBJCT: 1572 AC-GGAGCTGTAGGGCATGGGGTGGCTGGGGTAGGCCGACGTGGTCCCGTTGTAACTCAA 1514


QUERY: 555  ANTGCTGATGGNGCNAGGGTGGTGCATGNACAGGAAAGGNGACNTGGGNCANTATATGGA 614
           | ||||| |||| |||||||||| | ||||||| || ||| |||| || || | |||
SBJCT: 1513 AGTGCTGCTGGCGCGGGGGTGGTGCAGGGACAGGAAGGGCGACATGGGCCAGTAGAGGGA 1454

QUERY: 615  GCNCNGCNCNGTCCATGANTGTNANGCCGGTGNAGGTGATCCGNGCCCCGCNCTTAAAGG 674
           || | || | |||||||||  || | ||||||| |||||||  || ||||||| ||||||||
SBJCT: 1453 GC-CGGCGCGGTCCATGAAGGTGAGGCCGGTGGAGGTGAGGCGCGCCCCGCGCTTAAAGG 1395

QUERY: 675  CTANCTTGTCCCNAGACNTGNTGGAGNNGCCCCNCAGCTTGCCGGTNGTGCCGNCGATGA 734
           | | |||| ||| |||| || |||||  || || |||||||||||| |||||| ||||||
SBJCT: 1394 CCAGCTTGGCCCGAGACGTGGTGGAGCGGCGCCGCAGCTTGCCGGTCGTGCCGCCGATGA 1335

QUERY: 735  ACACGTCNTCGCTCGACGGGTCCANCATCCAGTANTTGCCCTTGNCCNGGTCGTCCTAGT 794
           ||||||| |||||||||||||| | |||||||| ||||||||| || ||||||| ||||
SBJCT: 1334 ACACGTCGTCGCTCGACGGGTCGAGCATCCAGTAGTTGCCCTTGCCCGGGTCGTCGTAGT 1275

QUERY: 795  GGCGCNGTTCCCTTNNCGANGCACTTNTTGAGGGACANGTTGNGGCCGATGGAGTTCTGN 854
           ||||| | | ||||  ||| |||||| |||||||||| |||| ||| ||||||||||||
SBJCT: 1274 GGCGCGG-TACCTTCACGAAGCACTTGTTGAGGGACAGGTTGTGGCGGATGGAGTTCTGC 1216

QUERY: 855  CANCCCTGCTTNTTCTNCCGGTACNAANGNTAAGTTCTTCATGNTGAACTCNTAAATGCC 914
           || |||||||| |||| |||||   | |  |||||||||||| ||||||| || |||||
SBJCT: 1215 CAGCCCTGCTTGTTCTCGCGGTA-GTAGGGGAAGTTCTTCATGATGAACTCATAGATGCC 1157
```

```
QUERY: 915  GNTGAGCNTCAAGCGCT 931
            ||||| ||| |||||
SBJCT: 1156 ATTGAGCGTCAGGCGCT 1140

 Score =  105 bits (53), expect = 1e-19
 Identities = 101/116 (87%), gaps = 3/116 (2%)
 Strand = plus / minus

QUERY: 48   AAGGGTTGGAAGAAGACCCCTGATTTTTTATGTGTGAAATAATCATNACAGTCCCCCGGA 107
            ||||||||||||||||||||||| |||| ||||||||||||||||  ||||||||||||
SBJCT: 2000 AAGGGTTGGAAGAAGACCCCTGA-TTTTGATGTGTGAAATAATCA-GACAGTCCCCCGGA 1943

QUERY: 108  CAGTCCTGTGCGCNAANCTTGNCATAGANGGTCTTANNGACTCACANGGCANGGTC 163
            ||||||||| ||  || |||| || ||| |||||||  |||||||| |||| ||||
SBJCT: 1942 CAGTCCTGT-CGTAAAACTTGGCAAAGAGGGTCTTAAAGACTCACAGGGCAGGGTC 1888
```

Appendix 2 E: BLAST search results using the sequencing product P8SP6, obtained with the SP6 primer of the plasmid mBF-1-CS2 # 8. The reading frame alignment, as in Appendix 2 D is not shown, as the entire mBF-1-CS2 or mBF-1 sequence is not represented. However, the sequencing results identified mouse BF-1 (SBJCT) as indicated above.

Appendix 2 F

```
                                                                  score    e
Sequences producing significant alignments:                       (bits) value

gi|6978844|ref|nm_012560.1|  Rattus Norvegicus Forkhead Box ...    90   9E-15
gi|203134|gb|m87634.1|ratbf1a  Rat BF-1 mRNA, complete cds         90   9E-15
gi|6679842|ref|nm_008241.1|  Mus Musculus Forkhead Box G1 (F...    84   6E-13
gi|28422749|gb|bc046958.1|  Mus Musculus, Similar To Forkhea...    84   6E-13
gi|1036832|gb|u36760.1|mmu36760  Mus Musculus Brain Factor-1...    84   6E-13

>gi|6679842|ref|nm_008241.1|  Mus Musculus Forkhead Box G1 (FoxG1),
mRNA          Length = 2934

 Score = 83.8 bits (42), expect = 6e-13
 Identities = 81/97 (83%), gaps = 1/97 (1%)
 Strand = plus / plus

QUERY: 149 CCCGNGGCCGTNNANACCGACANCCACCACNCGAGCNACGGTCACNACAACAGCCNCNAC 208
           |||| ||||||  | | ||||| ||||||| ||||| |||| ||| |||||||||| | ||
SBJCT: 638 CCCGAGGCCGTCCAGAACGACAACCACCACGCGAGCCACGGCCACCACAACAGCCACCAC 697

QUERY: 209 CNCNNGCATCACCATCATGCATCACCACCACCACCAC 245
           | |  |||||||||||||| ||||||||||||||||||
SBJCT: 698 CCCCAGCATCACCATCAT-CATCACCACCACCACCAC 733

 Score = 48.1 bits (24), expect = 0.031
 Identities = 37/41 (90%), gaps = 1/41 (2%)
 Strand = plus / plus

QUERY: 402 GGACGGGGCCAANGCNGACAGCACTNGGAGCCAAAGGCGAG 442
           |||||||||||| || ||| ||||| ||||||||||||||||
SBJCT: 889 GGACGGGGCCAAGGCTGAC-GCACTTGGAGCCAAAGGCGAG 928

>gi|1036832|gb|u36760.1|mmu36760  Mus Musculus Brain Factor-1
(HFHBF1) mRNA, class 2, complete cds          Length = 2934

 Score = 83.8 bits (42), expect = 6e-13
 Identities = 81/97 (83%), gaps = 1/97 (1%)
 Strand = plus / plus

QUERY: 149 CCCGNGGCCGTNNANACCGACANCCACCACNCGAGCNACGGTCACNACAACAGCCNCNAC 208
           |||| ||||||  | | ||||| ||||||| ||||| |||| ||| |||||||||| | ||
SBJCT: 638 CCCGAGGCCGTCCAGAACGACAACCACCACGCGAGCCACGGCCACCACAACAGCCACCAC 697

QUERY: 209 CNCNNGCATCACCATCATGCATCACCACCACCACCAC 245
           | |  |||||||||||||| ||||||||||||||||||
SBJCT: 698 CCCCAGCATCACCATCAT-CATCACCACCACCACCAC 733

 Score = 48.1 bits (24), expect = 0.031
 Identities = 37/41 (90%), gaps = 1/41 (2%)
 Strand = plus / plus

QUERY: 402 GGACGGGGCCAANGCNGACAGCACTNGGAGCCAAAGGCGAG 442
           |||||||||||| || ||| ||||| ||||||||||||||||
SBJCT: 889 GGACGGGGCCAAGGCTGAC-GCACTTGGAGCCAAAGGCGAG 928
```

Appendix 2 F: BLAST search results using the sequencing product P8T7, obtained with the T7 primer of the plasmid mBF-1-CS2 # 8. The reading frame alignment, as in Appendix 2 d is not shown, as the entire mBF-1-CS2 or mBF-1 sequence is not represented. However, the sequencing results identified mouse BF-1 (SBJCT) as indicated above.

References

Alberts, B., D. Bray, J. Lewis, M. Raff, K. Roberts, and J. D. Watson. 1994. Molecular biology of the cell.

Allman, J. M., 2000. Evolving Brains. Scientific American Library. W. H. Freeman and Co., USA. Chapter 3 and Chapter 4.

Altschul, S. F., W. Gish, W. Miller, E. W. Myers, D. J. Lipman. 1990. Basic local alignment search tool. J Mol Biol **215**:403-10.

Artavanis-Tsakonas, S., M. D. Rand, and R. J. Lake. 1999. Notch signaling: cell fate control and signal integration in development. Science **284**:770-6.

Ausubel, F. M., R. Brent, R. E. Kingston, D. D. Moore, J. G. Sedman, J. A. Smith, and K. Struhl. Eds. (1995). Current Protocols in Molecular Biology. New York: John Wiley and Sons.

Bellefroid, E. J., A. Kobbe, P. Gruss, T. Pieler, J. B. Gurdon, and N. Papalopulu. 1998. Xiro3 encodes a *Xenopus* homolog of the *Drosophila* Iroquois genes and functions in neural specification. EMBO J. **17**:191-203.

Blumberg B., J. Bolado Jr, T. A. Moreno, C. Kintner, R. M. Evans, and N. Papalopulu. 1997. An essential role for retinoid signaling in anteroposterior neural patterning. Development **124**:373-9.

Boolay, S., (1999). Immortalisation, Characterisation and Differentiation of Temperature Sensitive Cell Lines from the Olfactory Neuroepithelium. Department of Biochemistry, University of Cape Town, South Africa.

Bourguignon, C., J. Li, and N. Papalopulu. 1998. XBF-1, a winged helix transcription factor with dual activity, has a role in positioning neurogenesis in *Xenopus* competent ectoderm. Development **125**:4889-4900.

Butler, A. B. and W. Hodos. 1996. Comparative Vertebrate Neuroanaotmy: Evolution and Adaptation. John Wiley and Sons, Inc., Wiley-Liss, USA. Chapter 29.

Chang, H. W., J. Li, D. Kretzschmar, and P. K. Vogt. 1995. Avian cellular homolog of the *Qin* oncogene. Proc.Natl.Acad.Sci.U.S.A **92**:447-451.

Chitnis, A., D. Henrique, J. Lewis, D. Ish-Horowicz, and C Kintner. 1995. Primary neurogenesis in *Xenopus* embryos regulated by a homologue of the *Drosophila* neurogenic gene Delta. Nature **375**:761-6.

Chomczynski, P., and N. Sacchi. 1987. Single-step method of RNA isolation by acid guanidinium thiocyanate-phenol-chloroform extraction. Anal Biochem **162**:156-9.

Clark, D., P. Mitra, and S. Wang. 2001. Scalable architecture in mammalian brains. Nature **411**:189-193.

Clevidence D. E., D. G. Overdier, W. Tao, X. Qian, L. Pani, E. Lai, and R. H. Costa. 1993. Identification of nine tissue-specific transcription factors of the hepatocyte nuclear factor 3/forkhead DNA-binding-domain family. Proc Natl Acad Sci **90**:3948-52.

Coffman, C. R., P. Skoglund, W. A. Harris, and C. R. Kintner. 1993. Expression of an extracellular deletion of Xotch diverts cell fate in *Xenopus* embryos. Cell **73**:659-671.

Coffman, C., W. Harris, and C. Kintner, C. 1990. Xotch, the Xenopus homolog of *Drosophila* notch. Science **249**(4975):1438-41.

Darnell, J., H. Lodish, and D. Baltimore. 1990. Molecular Cell Biology. Second Edition. Chapter 8. Scientific American Books, W. H. Freeman and Co., U.S.A.

Doniach, T. 1993. Planar and vertical induction of anteroposterior pattern during the development of the amphibian central nervous system. J. Neurobiol. **24**:1256-1275.

Dou, C. L., S. Li, and E. Lai. 1999. Dual role of brain factor-1 in regulating growth and patterning of the cerebral hemispheres. Cereb.Cortex **9**:543-550.

Dou, C., J. Lee, B. Liu, F. Liu, J. Massague, S. Xuan, and E. Lai. 2000. BF-1 interferes with transforming growth factor beta signaling by associating with Smad partners. Mol.Cell Biol. **20**:6201-6211.

Filosa, S., J. A. Rivera-Perez, A. P. Gomez, A. Gansmuller, H. Sasaki, R. R. Behringer, and S. L. Ang. 1997. Goosecoid and HNF-3beta genetically interact to regulate neural tube patterning during mouse embryogenesis. Development **124**:2843-54.

Furuta, Y., D. W. Piston, and B. L. Hogan. 1997. Bone morphogenetic proteins (BMPs) as regulators of dorsal forebrain development. Development **124**:2203-2212.

Gilbert, S. F. 2000. Part 1. Principles of development in biology in Developmental biology, 6th Ed. Sinauer Associates, Inc., Sunderland, MA, USA.

Gomez-Skarmeta, J. L., E. Calle-Mustienes, J. Modolell, and R. Mayor. 1999. *Xenopus* brain factor-2 controls mesoderm, forebrain and neural crest development. Mech.Dev. **80**:15-27.

Guillemot, F., and A. L. Joyner. 1993. Dynamic expression of the murine *Achaete-Scute* homologue *Mash-1* in the developing nervous system. Mechs Dev. **42**:171-185.

Hacker, U., H. Grossniklaus, W. J. Gehring, and H. Jackle. 1992. Developmentally regulated *Drosophila* gene family encoding the fork head domain. Proc Natl Acad Sci **89**:8754-8.

Hanashima, C., L. Shen, S. C. Li, and E. Lai. 2002. Brain factor-1 controls the proliferation and differentiation of neocortical progenitor cells through independent mechanisms. J.Neurosci. **22**:6526-6536.

Hardcastle, Z. and N. Papalopulu. 2000. Distinct effects of XBF-1 in regulating the cell cycle inhibitor p27(XIC1) and imparting a neural fate. Development **127**:1303-1314.

Harland, R. M. 1991. In situ hybridization: an improved whole-mount method for *Xenopus* embryos. Methods Cell Biol. **36**:685-95.

Hatini, V., W. Tao, and E. Lai . 1994. Expression of winged helix genes, BF-1 and BF-2, define adjacent domains within the developing forebrain and retina. J.Neurobiol. **25**:1293-1309.

Hatini, V.; X. Ye, G. Balas, and E. Lai. 1999. Dynamics of placodal lineage development revealed by targeted transgene expression. Dev. Dyn. **215**:332-343.

Hentges, K., K. Thompson, and A. Peterson. 1999. The flat-top gene is required for the expansion and regionalization of the telencephalic primordium. Development **126**:1601-1609.

Hiemisch, H., A. P. Monaghan, G. Schutz, and K. H. Kaestner. 1998. Expression of the mouse Fkh1/Mf1 and Mfh1 genes in late gestation embryos is restricted to mesoderm derivatives. Mech.Dev. **73**:129-132.

Huh, S., V. Hatini, R. C. Marcus, S. C. Li, and E. Lai. 1999. Dorsal-ventral patterning defects in the eye of BF-1-deficient mice associated with a restricted loss of shh expression. Dev.Biol. **211**:53-63.

Hulander, M., W. Wurst, P. Carlsson, and S. Enerback. 1998. The winged helix transcription factor Fkh10 is required for normal development of the inner ear. Nat.Genet. **20**:374-376.

Illing, N., S. Boolay, J. S. Siwoski, D. Casper, M. T. Lucero, and A. J. Roskams. 2002. Conditionally immortalized clonal cell lines from the mouse olfactory placode differentiate into olfactory receptor neurons. Mol.Cell Neurosci. **20**:225-243.

Kageyama, R., M. Ishibashi, K. Takebayashi, and K. Tomita. bHLH transcription factors and mammalian neuronal differentiation. Int. J. Biochem. Cell. Biol. **29**(12):1389-1399.

Kaufmann E, and W. Knochel. 1996. Five years on the wings of fork head. Mech Dev **57**:3-20.

Kenyon, K. L., N. Zaghloul, and S. A. Moody. 2001. Transcription factors of the anterior neural plate alter cell movements of epidermal progenitors to specify a retinal fate. Dev.Biol. **240**:77-91.

Keynes, R., and A. Lumsden. 1990. Segmentation and the origin of regional diversity in the vertebrate central nervous system. Neuron **4**:1-9.

Knecht, A. K., P. J. Good, I. B. Dawid, and R. M. Harland. 1995. Dorsal-ventral patterning and differentiation of noggin-induced neural tissue in the absence of mesoderm. Development **121**:1927-1935.

Kozak M. 1991. An analysis of vertebrate mRNA sequences: intimations of translational control. J Cell Biol **115**:887-903.

Kume, T., K. Deng, and B. L. Hogan. 2000. Murine forkhead/winged helix genes Foxc1 (Mf1) and Foxc2 (Mfh1) are required for the early organogenesis of the kidney and urinary tract. Development **127**:1387-1395.

Lee, J. E., S. M. Hollenberg, L, Snider, D. L. Turner, N. Lipnick, and H. Weintraub. Conversion of *Xenopus* ectoderm into neurons by NeuroD, a basic helix-loop-helix protein. Science **268**(5212):836-844.

Li, H., W. Tao, and E. Lai. 1996. Characterization of the structure and function of the gene for transcription factor BF-1, an essential regulator of forebrain development. Brain Res.Mol.Brain Res. **37**:96-104.

Li, J. and P. K. Vogt. 1993. The retroviral oncogene *Qin* belongs to the transcription factor family that includes the homeotic gene fork head. Proc.Natl.Acad.Sci.U.S.A **90**:4490-4494.

Li, J., H. W. Chang, E. Lai, E. J. Parker, and P. K. Vogt. 1995. The oncogene *Qin* codes for a transcriptional repressor. Cancer Res. **55**:5540-5544.

Lodish, H., A. Berk, L. S. Zipursky, P. Matsudaira, D. Baltimore, and J. Darnell. 2000. Molecular Cell Biology. W. H. Freeman and Co. New York.

Maniatis, T., E. F. Fritsch, and J. Sambrook. Eds (1982). Molecular Cloning: A Laboratory Manual, Cold Spring Harbor Laboratory, USA.

Mariani, F. V. and R. M. Harland. 1998. XBF-2 is a transcriptional repressor that converts ectoderm into neural tissue. Development **125**:5019-5031.

McCaughern-Carucci, J.1997. The "Neverfail" Northern Blot Hybridization. Molecular Biology Protocols: http://www.nwfsc.noaa.gov/protocols/northernblot.html (September 2002).

Newport, J, M. Kirschner. 1982. A major developmental transition in early *Xenopus* embryos: II. Control of the onset of transcription. Cell **30**:687-96.

Nieuwkoop, P. D. and J. Faber. 1967. Normal Table of *Xenopus* laevis (Daudin). Hubrecht Lab., Utrecht; North-Holland Publishing Co., Amsterdam. 2nd. Ed.

Papalopulu, N., and C. Kintner. 1996. A posteriorising factor, retinoic acid, reveals that anteroposterior patterning controls the timing of neuronal differentiation in *Xenopus* neuroectoderm. Development **122**:3409-18.

Puelles L., and J. L. Rubenstein. 1993. Expression patterns of homeobox and other putative regulatory genes in the embryonic mouse forebrain suggest a neuromeric organization. Trends Neurosci. **16**(11):472-9.

Rodriguez, C., L. J. Huang, J. K. Son, A. McKee, Z. Xiao, and H. F. Lodish. 2001. Functional cloning of the proto-oncogene brain factor-1 (BF-1) as a Smad-binding antagonist of transforming growth factor-beta signaling. J.Biol.Chem. **276**:30224-30230.

Rubenstein, J. L. and P. A. Beachy. 1998. Patterning of the embryonic forebrain. Curr.Opin.Neurobiol. **8**:18-26.

Rupp, R. A., L. Snider, H. Weintraub. 1994. *Xenopus* embryos regulate the nuclear localization of XMyoD. Genes Dev **8**:1311-23.

Sanes, D. H., T. A. Harris, and A. William. 2000. Development of the Nervous System. Academic Press, USA. Chapter 1 to Chapter 5.

Sanger, F., S. Nicklen, and A. R. Coulson. 1977. DNA sequencing with chain-terminating inhibitors. Proc Natl Acad Sci **74**:5463-7.

Schuurmans, C., and F. Guillemot. 2002. Molecular mechanisms underlying cell fate specification in the developing telencephalon. Curr. Opin. Neurobiol. **12**:26-34.

Schwegmann, A. 2000. Identification of Proteins that Interact with Brain Factor-1 and Characterisation of these Interactions. Department of Biochemistry, University of Cape Town, South Africa.

Shimamura, K. and J. L. Rubenstein. 1997. Inductive interactions direct early regionalization of the mouse forebrain. Development **124**:2709-2718.

Shimamura, K., D. J. Hartigan, S. Martinez, L. Puelles, and J. L. Rubenstein. 1995. Longitudinal organization of the anterior neural plate and neural tube. Development **121**:3923-3933.

Tanabe Y, and T. M. Jessell. 1996. Diversity and pattern in the developing spinal cord. Science **274**:1115-23.

Tao, W. and E. Lai. 1992. Telencephalon-restricted expression of BF-1, a new member of the HNF-3/fork head gene family, in the developing rat brain. Neuron **8**:957-966.

Treier, M., A. S. Gleiberman, S. M. O'Connell, D. P. Szeto, J. A. McMahon, A. P. McMahon, and M. G. Rosenfeld. 1998. Multistep signaling requirements for pituitary organogenesis in vivo. Genes Dev. **12**:1691-1704.

Turner, D. L., and H. Weintraub. 1994. Expression of achaete-scute homolog 3 in *Xenopus* embryos converts ectodermal cells to a neural fate. Genes Dev **8**:1434-47.

Wiese, S., D. B. Murphy, A. Schlung, P. Burfeind, D. Schmundt, V. Schnulle, M. G. Mattei, and U. Thies. 1995. The genes for human brain factor 1 and 2, members of the fork head gene family, are clustered on chromosome 14q. Biochim Biophys Acta **1262**:105-12.

Wilson, S. T., and J. L. R. Rubenstein. 2000. Induction and dorsoventral patterning of the telencephalon. Neuron **28**:641-651.

Wolpert L. 1998. Principles of Development. Current Biology Press, London.

Xuan, S., C. A. Baptista, G. Balas, W. Tao, V. C. Soares, and E. Lai. 1995. Winged helix transcription factor BF-1 is essential for the development of the cerebral hemispheres. Neuron **14**:1141-1152.

Yao, J., E. Lai, and S. Stifani. 2001. The winged-helix protein brain factor 1 interacts with groucho and hes proteins to repress transcription. Mol.Cell Biol. **21**:1962-1972.

Zernicka-Goetz, M., J. Pines, K. Ryan, K. R. Siemering, J. Haseloff, M. J. Evans, and J. B. Gurdon. 1996. An indelible lineage marker for *Xenopus* using a mutated green fluorescent protein. Development **122**:3719-24.